



AFRL-RX-WP-TM-2010-4114

**COLLABORATIVE RESEARCH AND DEVELOPMENT
CONTRACT**

Delivery Order 0038: Microbial Biotechnology and Biocatalysis

Matthew Eby and Heather R. Luckarift

Universal Technology Corporation

**APRIL 2010
Final Report**

Approved for public release; distribution unlimited.

See additional restrictions described on inside pages

STINFO COPY

**AIR FORCE RESEARCH LABORATORY
MATERIALS AND MANUFACTURING DIRECTORATE
WRIGHT-PATTERSON AIR FORCE BASE, OH 45433-7750
AIR FORCE MATERIEL COMMAND
UNITED STATES AIR FORCE**

NOTICE AND SIGNATURE PAGE

Using Government drawings, specifications, or other data included in this document for any purpose other than Government procurement does not in any way obligate the U.S. Government. The fact that the Government formulated or supplied the drawings, specifications, or other data does not license the holder or any other person or corporation; or convey any rights or permission to manufacture, use, or sell any patented invention that may relate to them.

This report was cleared for public release by the Wright-Patterson Public Affairs Office and is available to the general public, including foreign nationals. Copies may be obtained from the Defense Technical Information Center (DTIC) (<http://www.dtic.mil>).

AFRL-RX-WP-TM-2010-4114 HAS BEEN REVIEWED AND IS APPROVED FOR PUBLICATION IN ACCORDANCE WITH ASSIGNED DISTRIBUTION STATEMENT.

*//Signature//

MARK N. GROFF
Program Manager
Business Operations Branch
Materials and Manufacturing Directorate

//Signature//

KENNETH A. FEESER
Branch Chief
Business Operations Branch
Materials and Manufacturing Directorate

This report is published in the interest of scientific and technical information exchange, and its publication does not constitute the Government's approval or disapproval of its ideas or findings.

*Disseminated copies will show “//Signature//” stamped or typed above the signature blocks.

REPORT DOCUMENTATION PAGE				<i>Form Approved</i> <i>OMB No. 0704-0188</i>				
The public reporting burden for this collection of information is estimated to average 1 hour per response, including the time for reviewing instructions, existing data sources, gathering and maintaining the data needed, and completing and reviewing the collection of information. Send comments regarding this burden estimate or any other aspect of this collection of information, including suggestions for reducing this burden, to Department of Defense, Washington Headquarters Services, Directorate for Information Operations and Reports (0704-0188), 1215 Jefferson Davis Highway, Suite 1204, Arlington, VA 22202-4302. Respondents should be aware that notwithstanding any other provision of law, no person shall be subject to any penalty for failing to comply with a collection of information if it does not display a currently valid OMB control number. PLEASE DO NOT RETURN YOUR FORM TO THE ABOVE ADDRESS.								
1. REPORT DATE (DD-MM-YY) April 2010		2. REPORT TYPE Final		3. DATES COVERED (From - To) 05 December 2005 – 31 March 2008				
4. TITLE AND SUBTITLE COLLABORATIVE RESEARCH AND DEVELOPMENT CONTRACT Delivery Order 0038: Microbial Biotechnology and Biocatalysis				5a. CONTRACT NUMBER F33615-03-D-5801-0038				
				5b. GRANT NUMBER				
				5c. PROGRAM ELEMENT NUMBER 62102F				
6. AUTHOR(S) Matthew Eby and Heather R. Luckarift				5d. PROJECT NUMBER 4349				
				5e. TASK NUMBER L0				
				5f. WORK UNIT NUMBER 4349LOVT				
7. PERFORMING ORGANIZATION NAME(S) AND ADDRESS(ES) Universal Technology Corporation 1270 North Fairfield Road Dayton, OH 45432-2600				8. PERFORMING ORGANIZATION REPORT NUMBER S-531-038				
9. SPONSORING/MONITORING AGENCY NAME(S) AND ADDRESS(ES) Air Force Research Laboratory Materials and Manufacturing Directorate Wright-Patterson Air Force Base, OH 45433-7750 Air Force Materiel Command United States Air Force				10. SPONSORING/MONITORING AGENCY ACRONYM(S) AFRL/RXOB				
				11. SPONSORING/MONITORING AGENCY REPORT NUMBER(S) AFRL-RX-WP-TM-2010-4114				
12. DISTRIBUTION/AVAILABILITY STATEMENT Approved for public release; distribution unlimited.								
13. SUPPLEMENTARY NOTES PAO case number 88ABW-2010-0715, cleared 22 February 2010. Research completed March 2008. Report contains color.								
14. ABSTRACT This research in support of the Air Force Research Laboratory Materials and Manufacturing Directorate was conducted at Tyndall AFB, Florida from 5 December 2005 through 31 March 2008. This task performed fundamental and developmental research support the RXQL program in microbial biotechnology. This effort involved research in four primary areas: Chemical synthesis, Chemical/biological threat neutralization, Diagnostic/detection sensors, and Antimicrobial Bionanocomposites. These research areas are discussed in this report.								
15. SUBJECT TERMS chemical/biological threat neutralization, diagnostic/detection sensors								
16. SECURITY CLASSIFICATION OF: <table border="1" style="width: 100%; border-collapse: collapse;"> <tr> <td style="padding: 2px;">a. REPORT Unclassified</td> <td style="padding: 2px;">b. ABSTRACT Unclassified</td> <td style="padding: 2px;">c. THIS PAGE Unclassified</td> </tr> </table>			a. REPORT Unclassified	b. ABSTRACT Unclassified	c. THIS PAGE Unclassified	17. LIMITATION OF ABSTRACT: SAR		18. NUMBER OF PAGES 104
a. REPORT Unclassified	b. ABSTRACT Unclassified	c. THIS PAGE Unclassified						
			19a. NAME OF RESPONSIBLE PERSON (Monitor) Mark N. Groff 19b. TELEPHONE NUMBER (Include Area Code) N/A					

1.0 CHEMICAL SYNTHESIS

Enzymes are remarkable biocatalysts and catalyze a wide variety of processes that can be utilized for the production of novel compounds or pharmaceutical intermediates. In addition, biocatalysis can often produce chemical synthons that are otherwise unachievable by conventional chemical synthesis. Enzyme immobilization, however, is often essential to provide a stable biocatalyst that facilitates the use of enzymes in potential applications. Biomimetic mineralization reactions, developed in-house were used to generate silica nanoparticles that provide a suitable support for enzyme immobilization. The versatility of the silica-immobilization technique was demonstrated for the synthesis of substituted aminophenols. The resulting chemical products were designed for use in high performance military applications, such as structural polymers for potential application to bullet proof vests and protective coatings. In an extension to the project, a microfluidic system was developed for the multi-step synthesis of complex antibiotics. The microfluidic system is widely applicable to medical diagnostics, biosensing and biosynthesis. Single unit reactors containing enzyme or metal catalysts were integrated to make a chemo-enzymatic microfluidic reactor for the synthesis of potential high value phenoxazinone products from readily available and simple substrates. The reaction sequence involves three separate synthetic steps to form amino-phenoxazinone, a precursor in antibiotic synthesis. The technique is versatile in that the order of the chips can be changed to create a modular flow-through system amenable to a wide range of microfluidic devices. One of the limitations of biocatalytic systems is the need to provide a cofactor during a reaction mechanism. We developed a system that overcame this limitation by co-immobilization of two enzymes in tandem that catalyze cofactor regeneration *in situ*.

The results of this research task resulted in three peer-reviewed publications and a patent submission (Appendix B).

Publications

1. Luckarift, H.R., Ku, B., Dordick, J.S*, and Spain, J.C.*, “*Silica-Immobilized Enzymes for Multi-Step Synthesis in Microfluidic Devices*,” Biotechnology and Bioengineering 2007, 98 (3), 701-705.
2. Luckarift, H.R. and Spain, J.C.*, “Continuous-Flow Applications of Silica Encapsulated Enzymes,” (Invited Book Chapter). In: ACS symposium series, ‘Nano-scale Science and Technology in Biomolecular Catalysis.’ In press.
3. Betancor, L., Berne, C., Luckarift, H.R. and Spain, J.C.*, “*Coimmobilization of a redox enzyme and a cofactor regeneration system*,” Chemical Communications 2006, 3640-3642.

Patent application

Biocatalytic process for the production of ortho-aminophenols from chloramphenicol and analogs. Provisional Application Serial No. 60/735,643

2.0 CHEMICAL/BIOLOGICAL THREAT NEUTRALIZATION

Biologically-derived silica creates an immobilization matrix with high loading capacities that provides advantageous recovery, reuse and reproducibility. The integration of immobilized enzymes into continuous flow-through systems provides an added advantage to many applications, as the immobilized biocatalyst is stabilized and can be recycled. The resulting immobilized enzyme reactors (IMERs) can also be integrated directly to further analytical methods such as liquid chromatography or mass spectrometry. Immobilized enzyme reactors (IMER) were investigated for chemical warfare agent monitoring and detection by integration into a flow through system to create a biosensor for continuous sampling of chemical agent aerosols.

To deal with biological threats, methods to develop antimicrobial coatings were established in house. The antimicrobial enzyme, lysozyme, was found to precipitate silica and retain its antimicrobial activity. The resulting silica/lysozyme composite exhibited antimicrobial activity against a number of bacterial species. Lysozyme also catalyzes the reduction of metals (i.e. silver) to produce a silver/lysozyme composite that could be electroplated to surgical steel blades and demonstrated exceptional antimicrobial activity against a wide variety of bacterial strains. The self-sanitizing surfaces may find application in field hospitals and combat environments to reduce surgical and implant associated infections

The results of this research task resulted in three peer-reviewed publications (Appendix C).

Publications

1. Luckarift, H.R.*, Johnson, G.R. and Spain, J.C., "*Silica-Immobilized Enzyme Reactors; Application to Cholinesterase-Inhibition Studies*," Journal of Chromatography B: Biomedical Sciences and applications 2006, 843, 310-316.
2. Luckarift, H.R.*, "*Silica-Immobilized Enzyme Reactors (Invited Review)*," Journal of Industrial Chromatography and Related Technologies. Status: In Press.
3. Luckarift, H.R., Dickerson, M.B., Sandhage, K.H., and Spain, J.C.*, "*Rapid, Room Temperature Synthesis of Anti-Bacterial Bio-Nano-Composites of Lysozyme with Amorphous Silica or Titania*," (Selected for front cover). Small, 2006; 2(5), 640-643.

3.0 DIAGNOSTIC/DETECTION SENSORS

The IMER methodology developed in house was extended to the development of diagnostic systems and biosensors. An IMER containing biosilica-immobilized butyrylcholinesterase was demonstrated for screening the activity of cholinesterase inhibitors and was also integrated with an aerosol collection system to develop a biosensor for the detection of organophosphate nerve agents in air. The system was tested with model organophosphates including paraoxon, demeton-S and malathion. The substrates are all potent nerve agents and the system proved suitable for detection of organophosphates in air at practical detection limits.

In addition, methods were developed to attach silica-encapsulated enzymes to the surface of a plasmon resonance transducer demonstrated for the detection of organophosphate contaminants in liquid samples. We also developed a method for attachment of silica-immobilized enzymes to silicon wafers. These techniques are versatile and widely applicable to a wide range of diagnostic and detection systems.

A microfluidic IMER for diagnostic evaluation of prodrug activation was also demonstrated. A prodrug is administered in an inactive form and is metabolized in vivo into an active metabolite. The ability to screen this activation is an essential step in the development of drug therapies.

The results of this research task resulted in four peer-reviewed publications (Appendix D).

Publications

1. Luckarift, H.R.*, Greenwald, R., Bergin, M., Spain, J.C., and Johnson, G.R., “*Biosensor for Continuous Monitoring of Organophosphate Aerosols*,” *Biosensors and Bioelectronics* 2007, 23, 400 – 406.
2. Luckarift, H.R., Balasubramanian, S., Paliwal, S., Johnson, G.R., and Simonian, A.L.*, “*Enzyme-Encapsulated Silica Monolayers for Rapid Functionalization of A Gold Waveguide Surface*,” (Invited Publication). *Colloids and Surfaces B: Biointerfaces* 2007, 58(1), 28-33.
3. Betancor, L., Luckarift, H.R., Seo, J.H., Brand, O., and Spain, J.C.*, “*Three Dimensional Immobilization of B-Galactosidase On A Silicon Surface*” *Biotechnology and Bioengineering* 2007, 99 (2), 261-267.

Application of a microfluidic reactor for screening cancer prodrug activation using silica-immobilized nitrobenzene nitroreductase. Berne, C., Betancor, L., Luckarift, H.R., and Spain, J.C.*. *Biomacromolecules* 2006; 7, 2631-2636.

4.0 ANTIMICROBIAL BIONANOCOMPOSITES

Design of antimicrobial composites spans a wide range of product development fields, from food preparation and medical devices to fuel systems and latex paints. In the fabrication of surfaces which inhibit microbial growth, a significant challenge is integrating the bioactive properties of organic antimicrobial molecules with the inorganic surfaces of many instruments and devices. One approach is protein-mediated self-assembly of inorganic macromolecular structures, which incorporates biological molecules into abiotic matrices.

The antimicrobial enzyme lysozyme was used to precipitate silver to form hybrid organic-inorganic nanocomposites that exhibit antimicrobial properties. Enzymatic activity of lysozyme-silver nanoparticles was confirmed through hydrolysis assays using natural and synthetic substrates. In addition, electrophoretic deposition was completed in efforts to generate antimicrobial coatings for medical devices and anti-fouling applications. Antimicrobial coatings were electrochemically deposited onto surfaces of stainless steel surgical blades and syringe needles. Under our experimental conditions, antimicrobial films did not form when either lysozyme or silver was absent from electrodeposition solutions, or when a direct current was not applied to solutions. Electrodeposited films were firmly adhered to stainless steel surfaces, even after extensive washing, and retained antimicrobial activity. In addition, the efficacy of coatings was tested by subjecting blades and needles to an *in vitro* lytic assay designed to mimic the normal application of the tools. Coated blades and needles were used to make incisions and stabs, respectively, into agarose infused with *M. lysodeikticus* cells. Cell lysis was seen at the site of the incisions and stabs, demonstrating that antimicrobial activity is transferred into the media, as well as retained on the surface of the blades and needles. Results show that a one-step electrochemical deposition can be used to prepare antimicrobial biocomposite coatings.

Also completed was the self-immobilization and retention of an antimicrobial peptide within various inorganic matrices. The resulting nanoparticles retain biocidal activity, protect the antibiotic from proteolytic degradation and provide a continuous release of the antimicrobial agent over time. Antimicrobial peptides constitute the next generation of antibiotics, where they provide a different biocidal mechanism to current mainstream antibiotics. The current overuse of conventional antibiotics has become ineffective against several multi-drug resistant pathogens. This study demonstrates the potential of a new class of self-synthesizing antimicrobial biomaterials.

Manuscripts in progress for publication

1. Eby, D.M., Farrington, K.E., and Johnson, G.R., “*Self-Mediated Synthesis of Antimicrobial Biomaterials by A Cationic Peptide.*”
2. Eby, D.M., Farrington, K.E., and Johnson, G.R., “*Lysozyme Catalyzes the Formation of Antimicrobial Silver Nanoparticles.*”
3. Eby, D.M., Luckarift, G.R., and Johnson, G.R., “*Electrochemical Deposition of Lysozyme and Antimicrobial Silver. Bionanocomposites on Medical Instruments.*”

Appendix A: Presentations During Reporting Period

2007 Scientific Conference on Chemical and Biological Defense Research, Timonium, Maryland. November 13-15, 2007. Immobilization of Antimicrobial Activities in Inorganic Nanomaterials. Johnson, G.R.*, Luckarift, H.R., Eby, D.M., and Nadeau, L.J.

Topical Session: Nano-scale Science and Engineering in Biomolecular Catalysis. American Institute of Chemical Engineers, Annual Meeting, Salt Lake City, UT, November 5-9, 2007. Enzyme Encapsulation in Oxide Matrices. Luckarift, H.R.*, Eby, D.M., Nadeau, L.J., and Johnson, G.R.

Topical Session: Nanostructured Biomimetic and Biohybrid Materials and Devices. American Institute of Chemical Engineers, Annual Meeting, Salt Lake City, UT, November 5-9, 2007. Bio-Derived Antimicrobial Materials and Coatings. Eby, D.M., Luckarift, H.R., and Johnson, G.R.*

12th Topical Conference on Quantitative Surface Analysis, Bellevue, WA, 12-13 Oct 2007. Application of XPS for Estimating Efficiency of Enzyme Immobilization. Artyushkova, K.*, Ivnitshi, D., Rincon, R.A., Atanassov, P., Luckarift, H.R., and Johnson, G.R.

Air Force Office of Scientific Research Biophysical Mechanisms Program Review, Arlington, VA, August 15-17, 2007. Synthesis of Reactive Nanocoats: Insights into Bacillus Spore Coat Assembly. Eby, D.M., and Johnson, G.R.

Air Force Research Laboratory Materials Directorate, Biotechnology Group First Annual Review, Dayton, OH, August 14, 2007. Protein/Silver Nanocomposites. Eby, D.M. and Johnson, G.R.

Air Force Office of Scientific Research SAB Review, Arlington, VA August 1, 2007. Nanoscale Biomimetic Protection for the Air Force Warfighter. Eby, D.M., Luckarift, H.R., and Johnson, G.R.

Seeing at the Nanoscale Conference V, Santa Barbara, CA. June 24-27, 2007. Atomic Force Microscopy Study of the Effect of Antimicrobial Lysozyme-Silver Nanoparticles on Bacterial Cells. Eby, D.M. and Johnson, G.R.

5th Annual Nano-Materials for Defense Applications Symposium: Accelerating the Transition, San Diego, CA, 23 - 26 April 2007. Bio-Derived Antimicrobial Materials and Coatings. Johnson, G.R.*, Luckarift, H.R., and Eby, D.M.

58th Southeast Regional Meeting, American Chemical Society, Augusta, GA, November 1-4, 2006. Gold-Surface Modified with Enzyme-Encapsulated Silica Monolayers for Biosensor Applications. Balasubramanian, S.*, Luckarift, H.R., Paliwal, S., Johnson, G.R., and Simonian, A.L. Session: Biocomposites.

American Institute of Chemical Engineers, Annual Meeting, San Francisco, CA, November 12-17, 2006. Electrodeposition of Lysozyme-Silver Antimicrobial Bionanocomposites onto Stainless Steel Medical Instruments. Eby, D.M.*, Luckarift, H.R., and Johnson, G.R.

Topical Session: Nano-scale Science and Engineering in Biomolecular Catalysis. American Institute of Chemical Engineers, Annual Meeting, San Francisco, CA, November 12-17, 2006. Biomimetic silica encapsulation: An Efficient and Versatile Enzyme-Immobilization Technique. Luckarift, H.R.*, Johnson, G.R., Tomczak, M.M., Naik, R.R., and Spain, J.C.

Topical Session: Nano-scale Science and Technology in Biomolecular Catalysis. 232nd American Chemical Society National meeting, San Francisco, CA, September 10-14, 2006. Biomimetic Methods for Enzyme Encapsulation. Tomczak, M.M.*, Luckarift, H.R., Smith, H., Brott, L.L., Johnson, G.R., and Naik, R.R.

BioNanoFluidic MEMS Workshop, Georgia Institute of Technology, June 26-29th, 2006. Enzyme Immobilization by Silicification Reactions. Luckarift, H.R. and Spain, J.C.*

International Symposium in Biologically Inspired Design, Georgia Institute of Technology, May 10-12, 2006. Enzyme Immobilization by Silicification Reactions. Betancor, L., Luckarift, H.R.*, Berne, C., and Spain, J.C.

Georgia Institute of Technology, Environmental Systems Microbiology Symposium, Atlanta, GA. March 31-31, 2006. Enzyme Immobilization by Silicification Reactions. Betancor, L.,* Luckarift, H.R., Berne, C., and Spain, J.C.

Silica-Immobilized Enzymes for Multi-Step Synthesis in Microfluidic Devices

Heather R. Luckarift,¹ Bosung S. Ku,² Jonathan S. Dordick,² Jim C. Spain³

¹Air Force Research Laboratory, 139 Barnes Drive, Tyndall AFB, Florida 32403

²Department of Chemical and Biological Engineering, Rensselaer Polytechnic Institute, Troy, New York 12180; telephone: 518-276-2899; fax: 518-276-2207; e-mail: dordick@rpi.edu

³School of Civil and Environmental Engineering, 311 Ferst Drive, Georgia Institute of Technology, Atlanta, Georgia 30332-051; telephone: 404-894-0628; fax: 404-894-2278; e-mail: jspain@ce.gatech.edu

Received 5 January 2007; accepted 20 March 2007

Published online 5 April 2007 in Wiley InterScience (www.interscience.wiley.com). DOI 10.1002/bit.21447

ABSTRACT: The combinatorial synthesis of 2-aminophenoxazin-3-one (APO) in a microfluidic device is reported. Individual microfluidic chips containing metallic zinc, silica-immobilized hydroxylaminobenzene mutase and silica-immobilized soybean peroxidase are connected in series to create a chemo-enzymatic system for synthesis. Zinc catalyzes the initial reduction of nitrobenzene to hydroxylaminobenzene which undergoes a biocatalytic conversion to 2-aminophenol, followed by enzymatic polymerization to APO. Silica-immobilization of enzymes allows the rapid stabilization and integration of the biocatalyst within a microfluidic device with minimal preparation. The system proved suitable for synthesis of a complex natural product (APO) from a simple substrate (nitrobenzene) under continuous flow conditions.

Biotechnol. Bioeng. 2007;98: 701–705.

© 2007 Wiley Periodicals, Inc.

KEYWORDS: microfluidics; immobilized enzyme; aminophenoxazinone; chips; sequential catalysis

Introduction

The use of microfluidics and ‘lab-on-a-chip’ devices for efficiently miniaturizing biochemical assays and chemical synthesis is now well recognized (Barry and Ivanov, 2004; Figeys and Pinto, 2000; Haswell et al., 2001; Mitchell, 2001; Polson and Hayes, 2001; Urban et al., 2006). The dramatically increased surface to volume ratios lead to rapid mass transfer and greatly reduced analysis time and sample consumption. There is increasing interest in the integration of enzymes into microfluidic systems for applications in medical diagnostics, biosensing and natural product and

organic synthesis (Hadd et al., 1997; Jones et al., 2004; Krenkova and Foret, 2004; Ku et al., 2006; Lee et al., 2003; Srinivasan et al., 2003, 2004). Such biocatalytic systems are typically enabled by covalent attachment of the biocatalysts to channel walls, physical absorption onto solid matrices, or copolymerization (Holden et al., 2004, 2005; Honda et al., 2005; Mao et al., 2002; Sakia-Kato et al., 2004). Biocatalysts encapsulated in sol-gels and hydrogels can be subject to leaching, which reduces the active enzyme concentrations (Sakai-Kato et al., 2003). We recently reported a method of enzyme immobilization in biomimetic silica that increases the mechanical stability of the immobilized enzyme and facilitates application to flow-through reaction systems (Berne et al., 2006; Luckarift et al., 2004, 2006). The silica immobilization method is simple, rapid, and applicable to a wide variety of enzymes. The strategy precludes the need to modify the surface to allow enzyme attachment, greatly reducing preparation time and enhancing the loading capacity of the reaction system.

In this study we investigated the applicability of silica-immobilized enzymes for entraining biomolecules in microfluidic devices, and in the process developed a functional chemoenzymatic microfluidic platform. Specifically, with nitrobenzene (NB) (1) as a model substrate we demonstrate a three-step continuous reaction system for the production of 2-aminophenoxazin-3-one (APO) (4) (Fig. 1). In the first step, metallic zinc reduces NB (1) to hydroxylaminobenzene (HAB) (2) (Furniss et al., 1989), which then undergoes an enzymatic intramolecular rearrangement catalyzed by HAB-mutase to form 2-aminophenol (2-AP) (3) (Davis et al., 2000; Luckarift et al., 2005; Nadeau et al., 2003). In the final stage, soybean peroxidase

Correspondence to: J.S. Dordick and J. C. Spain
Contract grant sponsor: Air Force Office of Scientific Research
Contract grant sponsor: NIH
Contract grant number: GM66712

 **WILEY**
InterScience®
DISCOVER SOMETHING GREAT

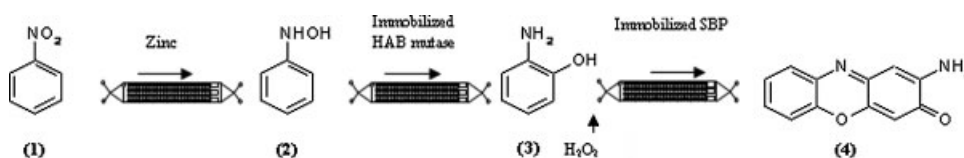


Figure 1. Schematic of a multi-step microfluidic process for the conversion of nitrobenzene to 2-aminophenoxazin-3-one.

(SBP) catalyzes the oxidation of 2-AP to form APO (4) (Fomsgaard et al., 2004; Hishida et al., 1974; Horvath et al., 2004; Lee et al., 2003; Reihmann and Ritter, 2002; Simandi et al., 2004; Srinivasan et al., 2003; Toussaint and Lerch, 1987) APO is an intermediate in the synthesis of actinomycins; an important group of antibiotics with anti-fungal and anti-tumor properties (Barry et al., 1989; Shimizu et al., 2004; Veselkov et al., 2003).

Materials and Methods

Materials

Hydroxylaminobenzene was synthesized as described previously (Furniss et al., 1989). Partially purified HAB mutase A was prepared and immobilized as described previously (Luckarift et al., 2005). All other chemicals were of analytical grade and obtained from Sigma–Aldrich (St. Louis, MO).

Fabrication of Microfluidic Chips

Standard photolithographic and molding techniques were used to fabricate a microfluidic channel (40 mm long \times 1.5 mm wide \times 0.1 mm deep; volume of 6 μ L) in polydimethylsiloxane as described previously (Ku et al., 2006; Srinivasan et al., 2004). The resulting chip is fabricated with three 50 μ m channels to form an exit network to retain the immobilized catalysts. Silica-immobilized biocatalysts were loaded into the channel by applying a vacuum to the product reservoir. HAB-mutase enzyme activity was determined as described previously (Davis et al., 2000). SBP enzyme activity was determined with ABTS (2, 2'-Azino-bis(3-ethylbenzthiazoline-6-sulfonic acid)) and hydrogen peroxide as described previously (Amisha Kamal and Behere, 2003).

Chip-Based Synthesis

All substrates were dissolved in water containing NH_4Cl (40 mM). Substrates were pumped at fixed flow rates and the eluate collected in an equal volume of acetonitrile for HPLC analysis. Reactants and products of all conversions

were monitored by reverse-phase HPLC on a Supelco ABZ column with an acetonitrile/water gradient as described previously (Luckarift et al., 2005).

Synthesis of 2-Aminophenoxazin-3-One Product Standard

2-Aminophenol (100 mg in 1L of potassium phosphate buffer, pH 7.4) was incubated with 0.01 U/mL SBP enzyme and 0.6 mM H_2O_2 . A deep red product characteristic of APO formed rapidly and precipitated from solution. The product was purified by solid phase extraction and was characterized and identified by NMR as 2-aminophenoxazin-3-one by comparison to proposed chemical shifts and previous literature reports (Gabriele et al., 2003). The yield of the reaction was approximately 83% and the product was used as a standard for future reactions. NMR spectra were recorded on a Varian Inova spectrometer equipped with a 5 mm indirect detection probe, operating at 500 MHz for ^1H and at 125 MHz for ^{13}C .

Results and Discussion

Biosynthesis of APO in a Microfluidic Chip

Silica-immobilized SBP was prepared and demonstrated good retention of enzyme activity (65–85%) relative to the soluble enzyme. The silica-immobilized SBP was packed into a microfluidic channel with an equal volume of agarose beads (1:1 vol/vol), to give a final enzyme loading of approximately 0.5 U. The presence of agarose beads prevents the silica particles from packing and reduces the void volume of the microfluidic reactor (effective volume \sim 3 μ L). 2-AP (0.5 mM) was pumped through the SBP chip at a range of flow rates and the conversion efficiency of the enzyme was determined by measuring production of APO. Hydrogen peroxide (0.5–2.5 mM in 10% DMF) was added continuously as a second reactant for the oxidation reaction. A molar ratio of 2.5:1 H_2O_2 :2-AP was optimal for conversion of 2-AP to APO (Fig. 2). The initial reaction velocity of immobilized SBP was 83 and 98 $\mu\text{M}/\text{min}$ at 1.0 and 2.5 mM H_2O_2 , respectively.

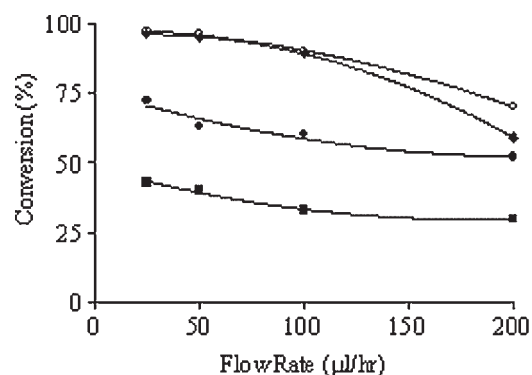


Figure 2. Effect of H_2O_2 concentration on conversion of 2-AP to APO in a silica-immobilized SBP chip. Conversion efficiency of 2-AP catalyzed by SBP with 2.5 mM (○), 1 mM (◆), 0.5 mM (●) and 0.1 mM (■) H_2O_2 .

Biosynthesis of 2-Aminophenol in a Microfluidic Chip

Immobilized HAB-mutase demonstrated good retention of enzyme activity relative to soluble enzyme, with little variability among replicate preparations (45–65%). Silica-immobilized HAB-mutase was mixed with an equal volume of agarose beads and packed into the channel as described above to give a final enzyme loading of approximately 1 unit (U). HAB (1 mM) was pumped through the HAB-mutase chip at a range of flow rates and the conversion efficiency determined. Conversion efficiency decreased with increasing flow rate as expected due to the decreased residence time (Fig. 3). The maximum 2-AP product concentration obtained from 1 mM HAB was 0.61 mM (± 0.09) at a flow rate of 50 $\mu\text{L}/\text{h}$. The reusability of the silica-immobilized HAB-mutase within the microfluidic chip was also determined to verify the retention of the biocatalyst within the channel during continuous flow. The

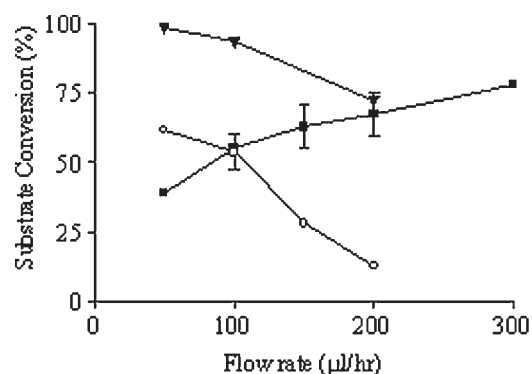


Figure 3. Substrate conversion efficiency as a function of flow rate. Conversion efficiency of 1 mM NB by Zn (■), 1 mM HAB by HAB-mutase (○) and 1 mM 2-AP by SBP and 1 mM H_2O_2 (▼).

enzyme chips were washed and stored repeatedly at 4°C and retained >50% of the original enzyme activity over a number of subsequent cycles (Fig. 4).

Biosynthesis of APO From HAB

The two immobilized-enzyme chips (HAB-mutase and SBP) were connected in series and an aqueous solution of HAB (1 mM) was introduced at a flow rate of 100 $\mu\text{L}/\text{h}$. This resulted in the production of APO (0.13 mM ± 0.025) continuously for over 4 h (conversion efficiency of $\sim 52\%$) (Table I). The addition of H_2O_2 to the system diluted the substrate concentration and reduced the theoretical product concentration by 50%. The flow rate could be increased to 150 $\mu\text{L}/\text{h}$, however, with no loss in conversion efficiency.

Chemoenzymatic Synthesis of APO

To complete the chemoenzymatic microfluidic platform, a metallic zinc chip was prepared (1 mg zinc dust, mixed 1:1 with agarose beads) and attached prior to the two enzyme reactors to demonstrate a combinatorial chemoenzymatic conversion of nitrobenzene to the resultant phenoxazinone. The zinc chip gave approximately 25% conversion of NB to HAB at low flow rates. In contrast to the chips containing biocatalysts, the metal zinc chip showed increased conversion efficiency with increasing flow rate (Fig. 3). At low flow rates, aniline was formed as a byproduct of the zinc reduction in preference to HAB. As a consequence, when the zinc chip was added in series with the two enzyme chips and NB pumped at a flow rate of 150 $\mu\text{L}/\text{h}$, the overall conversion efficiency was reduced to 19% due to the reduction in the corresponding efficiency of the zinc conversion step (Table I). Reduced conversion efficiency was also attributed to absorption and volatility

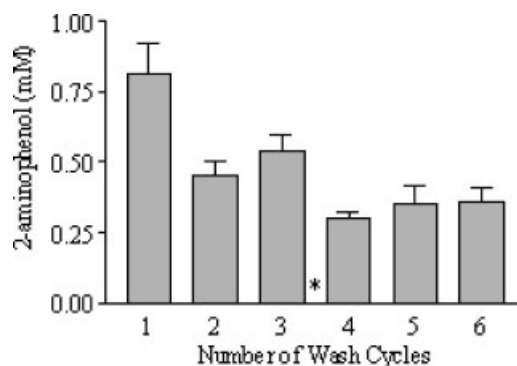


Figure 4. Reusability of HAB-mutase chips over several wash cycles. HAB (100 mL, 1 mM) was pumped through the HAB-mutase chips at a flow rate of 150 $\mu\text{L}/\text{h}$ and the formation of 2-aminophenol was determined. The chips were washed with 20 volumes of buffer between each subsequent cycle. Data shown is the mean and standard deviation of three independent HAB-mutase chips. Chips were stored overnight at 4°C at the point indicated (*).

Table I. Conversion efficiency of multi-step microfluidic synthesis.

Substrate	Chip combination	Conversion efficiency (%)	
		100 μ L/h	150 μ L/h
1 mM NB	Zinc/HAB mutase	16.7 \pm 3.5	28.2 \pm 2.7
1 mM HAB	HAB mutase/SBP	53.2 \pm 8.8	51.7 \pm 10.2
1 mM NB	Zinc/HAB mutase/SBP	ND	18.9 \pm 10.14

ND, not determined.

of the substrate. In an empty chip, observed NB concentrations were reduced in the eluate relative to the starting concentration but the percentage overall loss decreased with increasing flow rate. The conversion of the chemoenzymatic system was, therefore, determined at flow rates considered optimal for the biocatalytic steps. Clearly the step involving conversion of the nitro compound to the corresponding hydroxylamino compound will require optimization for future applications. Despite the low overall yields of the chemoenzymatic steps in series, the system provides a rapid and versatile method for screening the conversion of nitroarenes.

In this work, we demonstrated the first chemoenzymatic microfluidic reactor for the synthesis of a natural product from a readily available and simple substrate, nitrobenzene. The facile silica-immobilization method provides stable heterogeneous catalysts, which can be easily incorporated into microfluidic chips. The flow-through system described could be applied to the transformation of a wide variety of nitroarene substrates into their corresponding phenoxazinone products, and provides an attractive alternative to conventional chemical synthesis. The versatility of the immobilization method makes the system amenable to a wide range of microfluidic devices incorporating biomacromolecules and coupled to chemical synthesis. Single unit reactors containing enzyme or metal catalysts can be integrated to create a variety of synthetic pathways for rapid synthesis and screening.

HRL was supported by Oak Ridge Institute for Science and Education and funding by Air Force Office of Scientific Research. JSD acknowledges funding from the National Science Foundation and NIH (GM66712). The authors acknowledge Lloyd Nadeau for helpful discussions and synthesis of HAB. NMR spectroscopy was performed by Ion Ghiviriga, University of Florida.

References

- Amisha Kamal JK, Behere DV. 2003. Activity, stability and conformational flexibility of seed coat soybean peroxidase. *J Inorg Biochem* 94:236–242.
- Barry R, Ivanov DJ. 2004. Microfluidics in biotechnology. *Nanobiotechnology* 2(2):1–5.
- Barry CE, Nayar PG, Begley TP. 1989. Phenoxazinone Synthase: Mechanism for the formation of the phenoxazinone chromophore of actinomycin. *Biochemistry* 28:6323–6333.
- Berne C, Betancor L, Luckarift HR, Spain JC. 2006. Application of a microfluidic reactor for screening cancer prodrug activation using

- silica-immobilized nitrobenzene nitroreductase. *Biomacromolecules* 7:2631–2636.
- Davis JK, Paoli GC, He Z, Nadeau LJ, Somerville CC, Spain JC. 2000. Sequence analysis and initial characterization of two isozymes of hydroxylaminobenzene mutase from *Pseudomonas pseudoalcaligenes* JS45. *Appl Environ Micro* 66:2965–2971.
- Figey D, Pinto D. 2000. Lab-on-a-chip: A revolution in biological and medical sciences. *Anal Chem* 72(9):330A–335A.
- Fomsgaard IS, Mortensen AG, Carlsen SCK. 2004. Microbial transformation products of benzoxazoline and benzoxazinone allelochemicals—A review. *Chemosphere* 54:1025–1038.
- Furniss BS, Hannaford AJ, Smith PWG, Tatchell AR. 1989. Vogel's Textbook of practical organic chemistry, Longman Scientific and Technical. New York: John Wiley & Sons.
- Gabriele B, Mancuso R, Salerno G, Costa MJ. 2003. An improved procedure for the palladium-catalyzed oxidative carbonylation of β -amino acids to oxazolidin-2-ones. *Org Chem* 68:601–604.
- Hadd AG, Raymond DE, Halliwell JW, Jacobson SC, Ramsey JM. 1997. Microchip device for performing enzyme assays. *Anal Chem* 69:3407–3412.
- Haswell SJ, Middleton RJ, O'Sullivan B, Skelton V, Watts P, Styring P. 2001. The application of micro reactors to synthetic chemistry. *Chem Comm* 391–398.
- Hishida T, Nogami T, Shirota Y, Mikawa H. 1974. Reaction of o-Benzoquinone mono imine with o-aminophenol. *Chem Lett* 3(3):293–296.
- Holden MA, Jung S-Y, Cremer PS. 2004. Patterning enzymes inside microfluidic channels via photo-attachment chemistry. *Anal Chem* 76:1838–1843.
- Honda T, Miyazaki M, Nakamura H, Maeda H. 2005. Immobilization of enzymes on a microchannel surface through cross-linking polymerization. *Chem Comm* 5062–5064.
- Horvath T, Kaizer J, Speier G. 2004. Functional phenoxazinone synthases models. Kinetic studies on the copper-catalyzed oxygenation of 2-aminophenol. *J Mol Catalysis A Chem* 215:9–15.
- Jones F, Forrest S, Palmer J, Lu Z, Elmore J, Elmore BB. 2004. Immobilized enzyme studies in a microscale bioreactor. *Appl Biochem Biotech* 113–116:261–272.
- Krenkova J, Foret F. 2004. Immobilized microfluidic enzymatic reactors. *Electrophoresis* 25:3550–3563.
- Ku B, Cha J, Srinivasan A, Kwon SJ, Jeong J-C, Sherman DH, Dordick JS. 2006. Chip-based polyketide biosynthesis and functionalization. *Biotechnol Prog* 22:1102–1107.
- Lee M-Y, Srinivasan A, Ku B, Dordick JS. 2003. Multienzyme catalysis in microfluidic biochips. *Biotech Bioeng* 83:20–28.
- Luckarift HR, Naik RR, Stone MO, Spain JC. 2004. Enzyme immobilization in a biomimetic silica support. *Nat Biotech* 22:211–213.
- Luckarift HR, Nadeau LJ, Spain JC. 2005. Continuous synthesis of aminophenols from nitroaromatic compounds by combination of metal and biocatalyst. *Chem Comm* 383–384.
- Luckarift HR, Johnson GR, Spain JC. 2006. Silica-immobilized enzyme reactors: Application to cholinesterase-inhibition studies. *J Chrom B* 843:310–316.
- Mao H, Yang T, Cremer PS. 2002. Design and characterization of immobilized enzyme in microfluidic systems. *Anal Chem* 74:379–385.
- Mitchell P. 2001. Microfluidics-downsizing large-scale biology. *Nat Biotech* 19:717–721.
- Nadeau LJ, He Z, Spain JC. 2003. Bacterial conversion of hydroxylamino aromatic compounds by both lyase and mutase enzymes involves intramolecular transfer of hydroxyl groups. *Appl Environ Micro* 69(5):2786–2793.
- Polson NA, Hayes MA. 2001. Microfluidics controlling fluids in small places. *Anal Chem* 73(11):312A–319A.
- Reihmann MH, Ritter H. 2002. Regioselective HRP-catalyzed polymerization of 4-amino-phenol. *J Macromol Sci Pure Appl Chem A39(12):* 1369–1382.
- Sakai-Kato K, Kato M, Toyooka T. 2003. Creation of an on-chip enzyme reactor by encapsulating trypsin in sol-gel on a plastic microchip. *Anal Chem* 75:388–393.

- Sakia-Kato K, Kato M, Ishihara K, Toyóoka T. 2004. An enzyme-immobilization method for integration of biofunctions on a microchip using a water-soluble amphiphilic phospholipid polymer having a reacting group. *Lab Chip* 4:4–6.
- Shimizu S, Suzuki M, Tomoda A, Arai S, Taguchi H, Hanawa T, Kamiya S. 2004. Phenoxazine compounds produced by the reactions with bovine hemoglobin show antimicrobial activity against non-tuberculosis mycobacteria. *Tohoku J Exp Med* 203(1): 47–52.
- Simandi TM, Simandi LI, Gyor M, Rockenbauer A, Gomory A. 2004. Kinetics and mechanism of the ferroxime (II)-catalysed biomimetic oxidation of 2-aminophenol by dioxygen. A functional phenoxazinone synthase model. *Dalton Trans* 7(7):1056–1060.
- Srinivasan A, Wu X, Lee M-Y, Dordick JS. 2003. Microfluidic peroxidase biochip for polyphenol synthesis. *Biotech Bioeng* 81:563–569.
- Srinivasan A, Bach H, Sherman DH, Dordick JS. 2004. Bacterial P450-catalyzed polyketide hydroxylation on a microfluidic platform. *Biotech Bioeng* 88:528–535.
- Toussaint O, Lerch K. 1987. Catalytic oxidation of 2-aminophenols and ortho hydroxylation of aromatic amines by tyrosinase. *Biochem* 26: 8567–8571.
- Urban PL, Goodall DM, Bruce NC. 2006. Enzymatic microreactors in chemical analysis and kinetic studies. *Biotech Adv* 24(1):42–57.
- Veselkov AN, Maleev VY, Glibin EN, Karawajew L, Davies DB. 2003. Structure-activity relation for synthetic phenoxazone drugs. *Eur J Biochem* 270:4200–4207.

Coimmobilization of a redox enzyme and a cofactor regeneration system†

Lorena Betancor,^{‡ab} Cécile Berne,^{‡ab} Heather R. Luckarift^a and Jim C. Spain^{*b}

Received (in Cambridge, MA, USA) 31st March 2006, Accepted 27th June 2006

First published as an Advance Article on the web 28th July 2006

DOI: 10.1039/b604689d

The coimmobilization of nitrobenzene nitroreductase and glucose-6-phosphate dehydrogenase in silica particles enables the continuous conversion of nitrobenzene to hydroxylaminobenzene with NADPH recycling.

Cofactor dependent oxidoreductases catalyze a wide range of enantio- and regio-selective reactions.¹ In intact cells, redox cofactors such as NADPH are continuously regenerated by cellular metabolism. Therefore, whole-cell biocatalysis is widely used for redox reactions including asymmetric hydroxylations and epoxidations.^{2a} Unfortunately, whole-cell systems are often limited by product toxicity, byproduct formation, poor substrate uptake rates and difficulty with product recovery following catalysis.^{2b} The widespread use of purified redox enzymes in biocatalysis is limited by the cost of supplying stoichiometric amounts of cofactors for catalysis. An increasing interest in preparative pure enzyme applications necessitates a search for efficient and robust strategies for *in situ* cofactor recycling.^{2c} Several cofactor regeneration systems have been demonstrated using dehydrogenase enzymes.³ Current systems for NADPH regeneration, however, have not been successfully applied to large scale synthesis, primarily due to the low total turnover number of the recycling enzymes.^{2b} A high specific activity and a strategy for removal of the enzymes during product recovery are goals of an efficient recycling system, but the stability of the enzyme under reaction conditions must be optimized.

The NADPH-dependent nitrobenzene nitroreductase (NBNR) from *Pseudomonas pseudoalcaligenes* JS45 catalyzes a four-electron reduction of nitrobenzene to hydroxylaminobenzene (HAB) and has been successfully employed for whole-cell biocatalysis in *o*-aminophenol synthesis.⁴ However, intact cells have a relatively low specific activity and both substrate and product can be toxic to the cells.^{4b} The applicability of the purified enzymes as biocatalysts is also limited by the requirement for two moles of NADPH per mole of substrate.

The encapsulation of enzymes in silica nanoparticles imparts exceptional stability and high loading capacities for the resulting biocatalysts.⁵ We recently reported the preparation of immobilized-NBNR by encapsulation within silica particles using

polyethyleneimine (PEI) to direct silica formation.⁶ Immobilized NBNR provides a stable and reusable catalyst, but is still limited by a requirement for a stoichiometric amount of NADPH.^{5c} The high loading capacity and versatility of the immobilization system however, led us to investigate the potential for coimmobilization of two enzymes working in tandem. The immobilization of sequentially acting enzymes within a confined space increases the catalytic efficiency of the conversion due to a dramatic reduction in the diffusion time of the substrate. Moreover, the *in situ* formation of substrates generates high local concentrations that lead to kinetic enhancements that can equate to substantial cost savings.⁷ We report here the coimmobilization of NBNR and glucose-6-phosphate dehydrogenase (G6PDH) in a multi-enzyme system for the continuous reduction of nitroaromatic compounds. In this model system NADP⁺ dependent-G6PDH catalyzes the recycling of NADPH *in situ* providing a constant source of reducing equivalents to NBNR for the reduction of nitrobenzene to HAB (Fig. 1A).

NBNR and G6PDH were efficiently coimmobilized in PEI-directed silica particles with negligible loss in activity (Table 1). Kinetic analysis of G6PDH and NBNR activities in the coimmobilized suspension revealed that the apparent K_m of the PEI silica-encapsulated G6PDH for exogenously added NADP⁺ was comparable to that of the soluble enzyme (150.8 ± 12.5 and $156.5 \pm 8.8 \mu\text{M}$ respectively). The apparent K_m value of PEI silica-encapsulated NBNR for exogenously added NADPH was about 3 times higher than that of the soluble enzyme (344.6 ± 28.3 and $116.5 \pm 11.7 \mu\text{M}$ respectively). Modifications of K_m values for immobilized enzyme preparations can be attributed to substrate diffusion limitations and steric hindrances compared to the soluble forms.⁸ The kinetic measurements above were all made with exogenously added cofactors. The actual K_m for NADPH recycled *in situ* may be substantially lower because the NADPH is formed near the site of the reaction and therefore much less limited by diffusion. Despite the differences in the kinetic parameters of the immobilized and soluble enzymes, the dramatic operational and thermal stabilization achieved by silica precipitation⁶ would balance any negative effect of these parameters on the reaction.

The amount of G6PDH required to achieve maximum HAB formation was optimized by adjusting the ratio of NBNR : G6PDH in the coimmobilized preparation. The conversion of nitrobenzene to HAB requires two molecules of NADPH for each molecule of nitrobenzene, indicating a theoretical optimum ratio of enzyme units (U) of 1 U NBNR : 2 U G6PDH. Maximal nitrobenzene conversion was achieved however, by using an excess of G6PDH, with an optimum of 1 U NBNR : 5 U G6PDH. With a starting concentration of 100 μM nitrobenzene, the initial activity

^aAir Force Research Laboratory, 139 Barnes Drive, Suite #2, Tyndall AFB, FL 32403-5323, USA

^bSchool of Civil and Environmental Engineering, 311 Ferst Drive, Georgia Institute of Technology, Atlanta, GA 30332-0512.

E-mail: jcspain@ce.gatech.edu; Fax: +1 404 894 2265; Tel: +1 404 894 0628

† Electronic supplementary information (ESI) available: Experimental section and supporting data. See DOI: 10.1039/b604689d

‡ Both authors contributed equally to this work

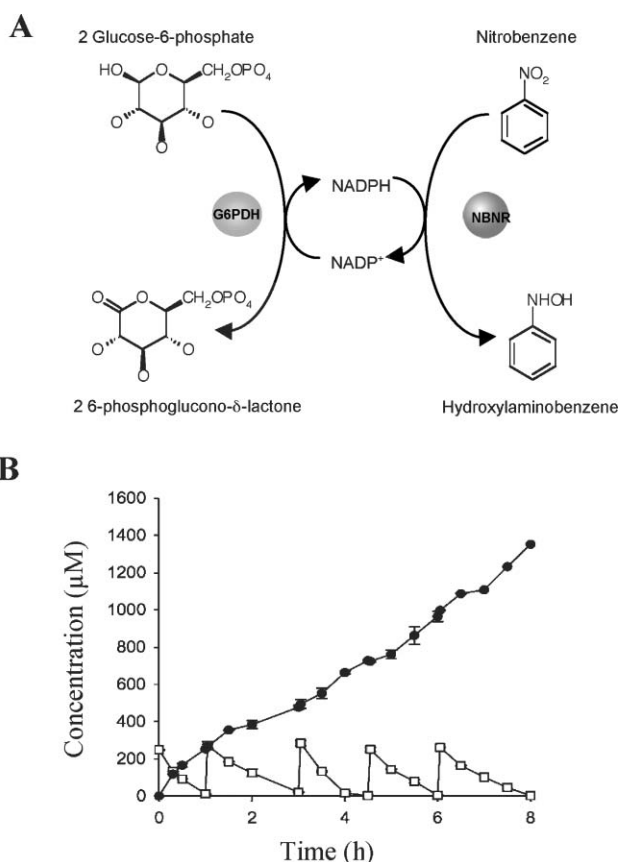


Fig. 1 A. Schematic and B. observations of the continuous conversion of nitrobenzene (100 μM) to HAB and NADPH recycling by a 1 U NBNR : 5 U G6PDH system. Nitrobenzene (□), HAB (●), 240 μM NADPH and 3 mM glucose-6-phosphate added at 0 h. An additional 3 mM glucose-6-phosphate was added after 3 h.

Table 1 Immobilization data

Enzyme preparation	Immobilization yield (%) ^a	Immobilized activity yield (%) ^b
NBNR	99.5 (±0.7)	58.7 (±4.6)
G6PDH	99.6 (±0.6)	33.3 (±0.4)
Coimmobilized NBNR	100 (±0)	52.5 (±0.2)
Coimmobilized G6PDH	98.4 (±0.6)	33.0 (±0.3)

^a Yield (%) = (initial activity – activity in the supernatant) × 100/initial activity. ^b Immobilized activity yield (%) = measured activity in the immobilized enzyme × 100/(initial activity – activity in the supernatant).

of coimmobilized NBNR–G6PDH increased linearly with increasing NADPH concentrations up to 240 μM. The optimized formulation (1 U NBNR : 5 U G6PDH and 240 μM NADPH) was used to test the recycling system in the continuous conversion of nitrobenzene (Fig. 1B). Nitrobenzene was supplied to the system in 250 μM increments to a total of 1.5 mM. NADPH was supplied to initiate the reaction and coupling of NBNR and G6PDH activities was evidenced by the continuous formation of HAB for 8 h without further addition of the cofactor. The conversion efficiency of the reaction was 90% with a final yield of 1.35 mM HAB. The conversion of nitrobenzene to HAB over an 8 h period of sustained activity was reproducible for initial concentrations of nitrobenzene up to 10 mM with no loss in the capacity to

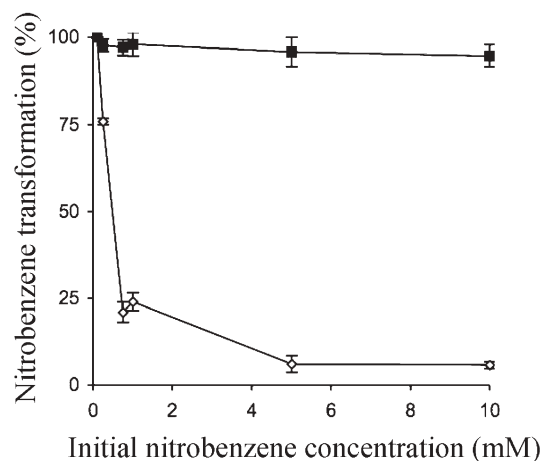


Fig. 2 Transformation of nitrobenzene. Reaction time: 8 h, 240 μM NADPH. 1 U NBNR : 0 U G6PDH (◇), 1 U NBNR : 5 U G6PDH (■).

transform nitrobenzene (Fig. 2). Control reactions containing immobilized-NBNR alone lost activity rapidly as the supply of NADPH became exhausted, leading to incomplete conversion of nitrobenzene (Fig. 2). Control reactions containing immobilized-G6PDH alone did not transform nitrobenzene (data not shown). When nitrobenzene was added in 10 mM increments, transformation was reproducible up to 30 mM (Fig. 3, ESI†). Estimation of HAB concentration became problematic for concentrations higher than 15 mM, probably due to instability or precipitation of the product. Activity of the biocatalyst, however, was undiminished after conversion of 30 mM nitrobenzene as shown by the full recovery of the enzyme activity after washing the coimmobilized system by centrifugation (Fig. 4, ESI†).

The use of immobilized enzymes for cofactor regeneration is receiving increasing attention,⁹ however, there are few literature reports demonstrating coimmobilization as a strategy for biocatalysis with cofactor recycling systems¹⁰ and such studies typically do not report a total turn-over number (moles of product formed/moles of cofactor present in the reaction) for NADPH. The system described herein significantly enhanced product formation (up to 125 fold with respect to the non coupled system) with a total turn-over number for NADPH of 62 under the tested conditions. We did not attempt to optimize the system to maximize the total turnover number but it is clear that our estimate is conservative.

Enzyme entrapment in silica allows the preparation of active and stable composites. Coimmobilizing a catalytic enzyme with a cofactor-regenerating enzyme provides a variety of potential advantages including: continuous operation, catalyst reuse, cost reduction and simplified product isolation. The mild immobilization reaction is widely applicable to a range of biomolecules for application to a variety of potentially interchangeable multienzyme configurations.

This work was funded by the Air Force Office of Scientific Research. CB, LB and HRL were supported by postdoctoral fellowships from Oak Ridge Institute for Science and Education (US Department of Energy).

Notes and references

- 1 S. W. May, *Curr. Opin. Biotechnol.*, 1999, **10**, 370; V. B. Urlacher and R. D. Schmid, *Curr. Opin. Chem. Biol.*, 2006, **10**, 1–6.

- 2 (a) T. Ishige, K. Honda and S. Shimizu, *Curr. Opin. Chem. Biol.*, 2005, **9**, 174–178; (b) W. A. Duetz, J. B. van Beilen and B. Witholt, *Curr. Opin. Biotechnol.*, 2001, **12**, 419–425; (c) W. A. Van der Donk and H. Zhao, *Curr. Opin. Biotechnol.*, 2003, **14**, 421–426; (d) H. Zhao and W. A. van der Donk, *Curr. Opin. Biotechnol.*, 2003, **14**, 583–589; (e) F. Hollman, K. Hofstetter and A. Schmid, *Trends Biotechnol.*, 2006, **24**, 163–171.
- 3 B. R. Riebel, P. R. Gibbs, W. B. Wellborn and A. S. Bommarius, *Adv. Synth. Catal.*, 2003, **345**, 707–712; R. B. Iyer and L. G. Bachas, *J. Mol. Catal. B: Enzym.*, 2004, **28**, 1–9; R. Verho, J. Londeborough, M. Penttila and P. Richard, *Appl. Environ. Microbiol.*, 2003, **69**, 5892–5897; T. W. Johannes, R. D. Woodyer and H. Zhao, *Appl. Environ. Microbiol.*, 2005, **71**, 5728–5734; H. Ichinose, N. Kamiya and M. Goto, *Biotechnol. Prog.*, 2005, **21**, 1192–1197; A. Schmid, I. Vereyken, M. Held and B. Witholt, *J. Mol. Catal. B: Enzym.*, 2001, **11**, 455–462.
- 4 (a) C. C. Somerville, S. F. Nishino and J. C. Spain, *J. Bacteriol.*, 1995, **177**, 3837–3842; L. J. Nadeau, Z. He and J. C. Spain, *J. Ind. Microbiol. Biotechnol.*, 2000, **24**, 301–305; L. J. Nadeau, J. C. Spain, R. Kannan and L. S. Tan, *Chem. Commun.*, 2006, 564–565; (b) V. Kadiyala, L. J. Nadeau and J. C. Spain, *Appl. Environ. Microbiol.*, 2003, **69**, 6520–6526.
- 5 (a) H. R. Luckarift, J. C. Spain, R. R. Naik and M. O. Stone, *Nat. Biotechnol.*, 2004, **22**, 211–213; (b) R. R. Naik, M. M. Tomczak, H. R. Luckarift, J. C. Spain and M. O. Stone, *Chem. Commun.*, 2004, 1684–1685; (c) H. R. Luckarift, L. J. Nadeau and J. C. Spain, *Chem. Commun.*, 2005, 383–384.
- 6 C. Berne, L. Betancor, H. R. Luckarift and J. C. Spain, *Biomacromolecules*, 2006, in press.
- 7 F. van de Velde, N. D. Lourenço, M. Bakker, F. van Rantwijk and R. A. Sheldon, *Biotechnol. Bioeng.*, 2000, **69**, 286–291.
- 8 G. Ozyilmaz, S. S. Tukel and O. Alptekin, *J. Mol. Catal. B: Enzym.*, 2005, **35**, 154–160.
- 9 M. Taylor, D. C. Lamb, R. J. P. Cannell, M. J. Dawson and S. L. Kelly, *Biochem. Biophys. Res. Commun.*, 2000, **279**, 708; N. St. Clair, Y. N. Wang and A. L. Margolin, *Angew. Chem., Int. Ed.*, 2000, **39**, 380–383.
- 10 K. S. Atia, *Radiat. Phys. Chem.*, 2005, 91–99; S. C. Mauer, H. Schulze, R. D. Schmid and V. Urlacher, *Adv. Synth. Catal.*, 2003, **345**, 802–810.

Find a SOLUTION

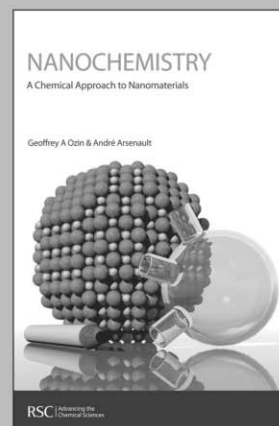
... with books from the RSC

Choose from exciting textbooks, research level books or reference books in a wide range of subject areas, including:

- Biological science
- Food and nutrition
- Materials and nanoscience
- Analytical and environmental sciences
- Organic, inorganic and physical chemistry

Look out for 3 new series coming soon ...

- RSC Nanoscience & Nanotechnology Series
- Issues in Toxicology
- RSC Biomolecular Sciences Series



RSCPublishing

www.rsc.org/books

RESERVE THIS SPACE

Continuous-flow applications of silica-encapsulated enzymes

Heather R. Luckarift¹ and Jim C. Spain^{2*}

**¹Air Force Research Laboratory, 139 Barnes Drive, Suite # 2, Tyndall AFB,
FL 32403, ²School of Civil and Environmental Engineering, Georgia
Institute of Technology, 311 Ferst Drive, Atlanta GA 30332**

Recent studies have demonstrated the applicability of biomineralization reactions to create an inorganic support matrix suitable to enzyme immobilization. The enzyme/inorganic nanocomposites exhibit excellent mechanical stability and provide an effective method for developing immobilized enzyme reactors, applicable to biocatalysis, biosensors and drug discovery.

Enzymes are remarkably versatile catalysts, but in their native soluble form are often labile in the absence of stabilizing agents and are difficult to recover from reaction mixtures. Immobilization of enzymes is therefore frequently employed in an attempt to stabilize enzyme activity and allow reuse of the catalyst. Enzyme immobilization methods primarily involve adsorption, attachment or encapsulation of biomolecules onto or into a solid phase (1-7). A range of silicates have been investigated for enzyme immobilization, either by attachment to functionalized mesoporous silica or encapsulation within sol-gel composites, but processing limitations have restricted widespread applicability (2,4,6,7).

RESERVE THIS SPACE

Silicification for enzyme immobilization

Silaffin polypeptides in diatoms catalyze the biomineralization of silica to form the exoskeleton (8,9). The biosilicification reaction can be mimicked *in vitro* by utilizing synthetic peptides (e.g. R5) based on the native silaffin sequence or from silica-binding peptides identified from combinatorial peptide libraries (8-13). Silica formation is also observed in the presence of simple cationic polymers such as polyethyleneimine and by proteins such as lysozyme and silicateins, producing silica nanospheres with a range of morphologies (Figure 1) (14-18).

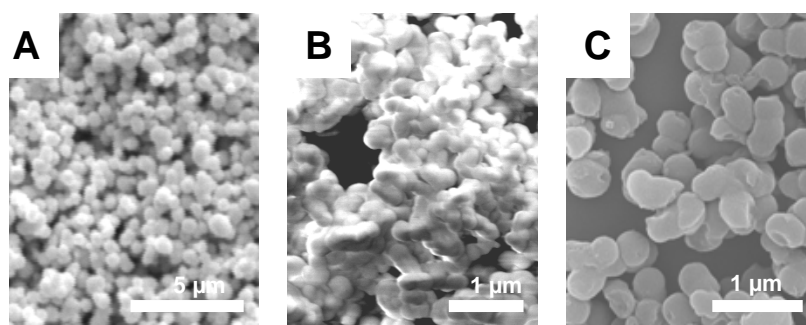


Figure 1. Synthesis of silica nanospheres catalyzed by tetramethylorthosilicate and (a) polyethyleneimine, (b) R5 peptide and (c) lysozyme, as viewed by SEM analysis. (From references 15, 18, 19).

The silica-precipitating species becomes entrapped during the generation of the silica matrix suggesting the potential of the silicification reaction to also encapsulate additional enzymes inside the silica matrix. In practice, the mild encapsulation chemistry and high biocompatibility of the reaction provide a rapid and highly efficient method for immobilizing a wide range of biomolecules (Table I). The biomimetic silicification reaction yields a network of fused silica nanospheres, providing a high surface area for encapsulation and permitting high enzyme loading capacities of up to 20% w/w (19).

Table I. Immobilization efficiency of a range of enzymes in silica nanoparticles

<i>Enzyme</i>	<i>Immobilization efficiency (expressed enzyme activity)</i>	<i>Data from Reference</i>
Butyrylcholinesterase	> 90%	(19)
Catalase	100%	(20)
Soybean peroxidase	65 - 85%	
Horseradish peroxidase	> 90%	(20)
Bromoperoxidase	35 - 48%	
Hydroxylaminobenzene mutase	44 - 67%	(21)
Organophosphate hydrolase	25 - 35%	
Nitrobenzene nitroreductase	~ 80% ^a	(15)

^a Immobilized in silica formed from polyethyleneimine and tetramethylorthosilicate (TMOS). All other enzymes are immobilized in silica formed from R5 peptide and TMOS.

The exceptional stability of the silica-immobilized enzymes under operational conditions, dramatically increases the versatility of the biocatalysts. Silica-immobilized butyrylcholinesterase (BuChE), for example, could be stored in aqueous solution at room temperature with no loss of initial enzyme activity, whereas free enzyme under identical conditions lost activity rapidly. The thermostability of the immobilized enzyme was also significantly enhanced. Silica-immobilized BuChE for example retained enzyme activity after heat-treatment of up to 65°C; conditions which caused rapid denaturation of soluble-BuChE. The enhanced enzyme stability can be attributed to the stabilizing effect of the silica support matrix, which prevents the conformational changes typical of enzyme denaturation (19).

Biotechnological application to continuous flow systems

A stable immobilized-enzyme preparation is attractive for a wide range of applications, particularly facilitating application to continuous flow-systems. Enzymes catalyze a wide variety of processes that can be exploited for example, in biocatalysis; for the production of novel synthons or drug intermediates. Enzymes also possess a wide range of pharmacological activities and are often investigated for therapeutic effects in drug discovery. Inhibitors of cholinesterase enzymes for example, can be used for the treatment of disorders such as Alzheimer's disease (22,23) and nitroreductase enzymes are key activators of prodrugs for cancer therapy (24,25). The applicability of silica-encapsulated enzymes was, therefore, further evaluated with respect to the

specific systems described above to provide insight into the versatility of the method.

Immobilized Enzyme Reactors for Cholinesterase Inhibition Studies

Immobilization of enzymes in packed columns specifically designed for continuous flow systems are often referred to as immobilized enzyme reactors (IMERs) (26-30). IMERs consisting of immobilized cholinesterase for example have been investigated in drug screening to identify inhibitors for treatment of disorders of the central nervous system, such as Alzheimer's disease. Current IMER configurations however, often exhibit specific drawbacks such as low loading capacity and long preparation times (31-34).

An IMER consisting of silica-immobilized BuChE was investigated in an attempt to circumvent some of the current limitations of IMER preparations. Silica-immobilized BuChE was prepared in two alternate column configurations; 1) a fluidized bed and 2) a packed-bed. For the fluidized bed system, substrate conversion was complete for over 12 hours of continuous flow with no loss in enzyme activity or conversion efficiency. The fluidized-bed system could also be operated at higher flow rates with no loss in activity, but with comparably lower conversion efficiency due to a reduced contact time within the column. In the packed-bed system, however, the conversion rate decreased with time. The silica particles became packed under continuous flow conditions, leading to compression and eventual channeling of the silica particles (19). Thus, the mechanical stability of the silica-immobilized enzyme was well suited to flow-through systems but the configuration of the column packing required optimization.

In order to avoid the above mechanical limitations, the silica-immobilization technique was modified such that the silica particles form and attach simultaneously to a commercial pre-packed column via affinity binding of a histidine-tag on the silica-precipitating peptide (35) (Figure 2). The modified method was used to prepare a butyrylcholinesterase immobilized enzyme reactor (BuChE-IMER). A metal ion affinity chromatography column charged with cobalt ions selectively binds histidine residues on proteins or peptides. A (His)₆-homologue of the R5 peptide therefore selectively binds to the cobalt coated surface. The silicification reaction occurs and integrates with the peptide bound to the column, resulting in formation of silica nanospheres attached to the surface of the agarose beads and the concurrent immobilization of the enzyme (Figure 2). The location of the histidine-tag on the silica-nucleating peptide rather than on the protein eliminates any need for recombinant modification of the protein of interest.

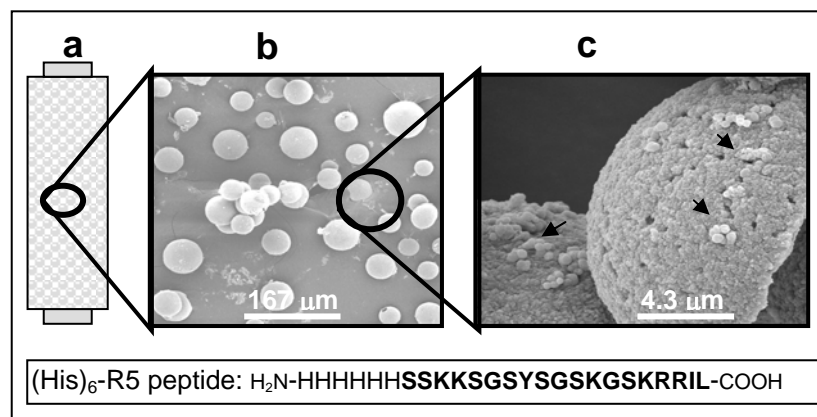


Figure 2. Immobilization of silica beads to agarose beads via affinity binding. A pre-packed affinity chromatography column (a) containing agarose beads (b) is coated with silica (c) by incubation of a histidine tagged-synthetic R5 peptide and TMOS (as viewed by SEM analysis). The (His)₆-R5 peptide sequence is shown. Data from reference 35.

The addition of histidine residues at either the carboxyl-terminus or amino-terminus of the silica-precipitating peptide did not affect the silicification reaction. The resulting BuChE-IMER exhibited high loading capacities and an immobilization efficiency approaching 100%. When connected to a liquid chromatography system, the columns could be operated at a wide range of flow rates (up to 3 ml/min) with low back pressure (Figure 3). Multiple substrate injections by means of an auto sampler provided rapid and reproducible analysis, with no significant loss in enzyme activity or conversion efficiency during continuous flow.

The hydrolysis of substrate by cholinesterases is decreased by the presence of inhibitors from which inhibition constant (IC₅₀) values can be derived. The BuChE-IMER can thus be utilized for rapid analysis of inhibition characteristics. A range of cholinesterase inhibitors were investigated and exhibited a concentration-dependent response, from which inhibition constants could be determined (shown in Figure 3b for the inhibitor, Tacrine). The IMER was stable for more than 50 hours of continuous use. In addition, the reusability of the IMER significantly reduces the amount of enzyme required for analysis.

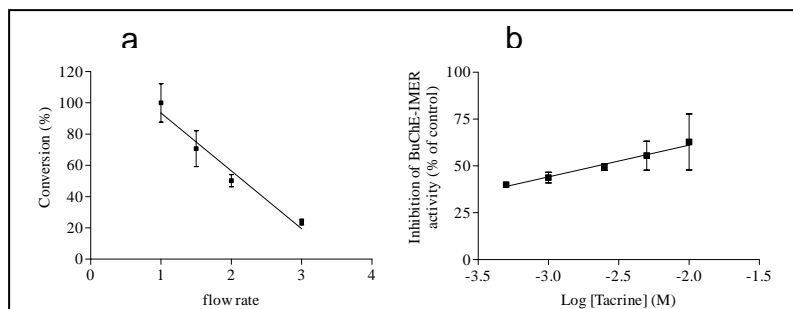


Figure 3 BuChE-IMER activities during continuous flow. Panel (a): Effect of flow rate on the conversion efficiency; (b) Determination of IC_{50} for tacrine using the BuChE-IMER. Data from reference 35

The bioencapsulation strategy described above provides a rapid route for synthesizing IMER systems and provides a model system applicable to a range of formats. The method is also scalable to applications ranging from a microfluidic format for biosensors to large-scale for biocatalysis. Two further examples of silica-immobilized enzymes in packed columns for 1) drug discovery and 2) biocatalysis for drug synthesis will be discussed in more detail below.

Microfluidic Immobilized Enzyme Reactors for Drug Discovery

Nitroreductase enzymes are used to activate prodrugs to a cytotoxic derivative specific to tumor cells (24,25). Nitroreductase enzymes catalyze the reduction of a nitro group (strongly electron-withdrawing) to the corresponding hydroxylamine (electron-donating), which results in a large electronic change and provides an effective enzyme-mediated electronic ‘trigger’. Nitroreductase enzymes are also known to activate nitrofurans antibiotics by reduction to the corresponding hydroxylamine intermediate, which causes the fragmentation of DNA (36,37). Despite the pharmacological relevance of nitroreductases, there are few reports documenting immobilization of such enzymes for drug discovery.

Nitroreductase enzymes were encapsulated in silica formed by a simple cationic polymer; polyethyleneimine (PEI). PEI precipitates silica in a reaction homologous to biogenic systems but with a significant reduction in cost (15). The resulting silica particles proved suitable for encapsulation of nitrobenzene

nitroreductase (NbzA) from *P. pseudoalcaligenes* JS45 with immobilization yields of greater than 80% and high retention of enzyme activity (45 – 55 %) (15).

The main selection criteria for prodrug formulations are a high affinity for substrate and a differential toxicity between the active species and the prodrug. The affinity of the immobilized-NbzA was therefore determined for nitrobenzene, an anticancer prodrug (CB1954) and a proantibiotic (nitrofurazone). The kinetic properties of the immobilized NbzA were comparable to those of the soluble enzyme, indicating that immobilization was not detrimental to enzyme activity. Nitrofurazone was a poor substrate for NbzA (high K_m value) whereas the K_m value for CB1954 was very low, indicating a high affinity for substrate activation of CB1954 in comparison to other bacterial nitroreductases (Table II).

Table II. Kinetic characteristics of nitroreductase enzymes

	<i>E. coli</i> (NTR)	<i>P. pseudoalcaligenes</i> JS45 (NbzA)	
		Soluble	Silica-Immobilized
Nitrobenzene	ND	2.3 (\pm 0.35)	2.0 (\pm 0.23)
CB1954	862	11.7 (\pm 1.0)	33.7 (\pm 4.5)
Nitrofurazone	64	1763 (\pm 572)	5123 (\pm 687)

Data from reference 15. All data represent K_m values in μM

As demonstrated previously for encapsulation of BuChE, the silica-immobilization method conferred enhanced stability to NbzA. Immobilized NbzA retained enzyme activity when stored at 4°C for several weeks and exhibited dramatically higher thermostability than the soluble enzyme (15). The enhanced stability in this system is thought to be a consequence not only of the physical support provided by the silica matrix but also the protective nature of PEI itself (38-40).

The small size (< 1 μm diameter) of the silica-encapsulated NbzA particles provides a high surface to volume ratio considered suitable for microfluidic flow-through systems (41). Silica-encapsulated NbzA was therefore packed into a microfluidic device and demonstrated high conversion efficiencies under continuous flow conditions and at a range of flow rates. At 1 $\mu l/min^{-1}$, for example nitrobenzene, CB1954 and nitrofurazone were all converted stoichiometrically and conversion of nitrobenzene (>90%) could be maintained for more than 3 days of continuous operation.

Immobilized Enzyme Reactors in Biocatalysis

In whole cells of *Pseudomonas pseudoalcaligenes* JS45, the NbzA described above reduces nitrobenzene to hydroxylaminobenzene (HAB), which undergoes further transformation by HAB mutase to form *ortho*-aminophenol (Figure 4). The activity of NbzA and HAB mutase in concert catalyze the conversion of a range of nitroarenes to yield novel *ortho*-aminophenols (42,43), but the use of NbzA for biocatalysis is limited by its requirement for NADPH. The NADPH-dependent reduction of nitroarenes can be replaced however, by a zinc-catalyzed chemical reduction. HAB can then be enzymatically rearranged to *ortho*-aminophenol by HAB mutase, an enzyme with no cofactor requirements.

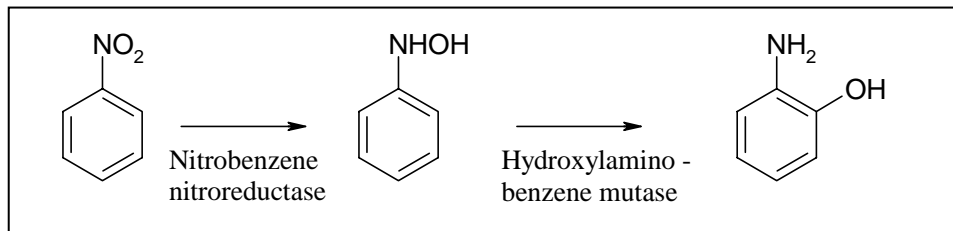


Figure 4. Enzymatic synthesis of *ortho*-aminophenol

To demonstrate the applicability of the approach, HAB mutase was immobilized and packed into a column and connected in series to a second column containing zinc. Nitrobenzene (1 mM) was pumped through the two columns and *ortho*-aminophenol was produced continuously for over 5 hours with a conversion efficiency approaching 90%. The flow-through system could be operated at higher flow rates and substrate concentration (5 mM at 0.5 ml/min) with a conversion efficiency of approximately 70%, which could be maintained for over 8 hours (21).

The use of the zinc/mutase flow-through columns was applied to the formation of a novel antibiotic. The biosynthesis of antibiotics using bacterial cells is limited due to the biocidal properties of the product, for which the immobilized enzyme system provides an attractive alternative. Chloramphenicol contains an active nitro substituent which was converted stoichiometrically to the corresponding aminophenol analog by passage through the zinc and immobilized mutase column in series. At a flow rate of 0.25 ml/min, continuous synthesis of the novel product was maintained for a period of 24 hours (21).

Conclusion

Enzyme immobilization methods have been widely investigated for many years, but recent developments in stabilizing enzymes within biomimetic inorganic matrices substantially extends the range of operational stabilities. Nano-sized materials offer a number of intrinsic advantages such as high surface areas which lead to high loading capacities. Silica-encapsulation has proven to be a versatile method for immobilizing biocatalytic activity and is applicable to a wide range of biomolecules. In addition, the morphology of the particles can be controlled by modifying the reaction conditions during silica formation (13, 44-46). The primary limitation to broad application is the cost of synthesizing peptides required for silica formation. The use of synthetic polyamines for the silica precipitation reaction however, provides a significant reduction in cost and a realistic opportunity to develop the method for large-scale synthesis of immobilized enzyme preparations. The use of lysozyme to catalyze the silica precipitation (18) also imparts the additional benefit of antimicrobial activity to the resulting silica nanoparticles. Lysozyme/silica composites therefore provide antifouling properties to the encapsulated catalysts, for potential use as antibacterial coatings. We anticipate that the resulting silica-encapsulated catalysts will find significant and widespread application in the design of biosensors and for biocatalysis and drug discovery.

References

1. Cao, L. *Curr. Opin. Chem. Biol.* **2005**, 9, 217-226.
2. Gill, I.; Ballesteros, A. *Trends. Biotech.* **2000**, 18, 282-296.
3. Gill, I.; Ballesteros, A. *Trends. Biotech.* **2000**, 18, 469-479.
4. Kim, Y.D.; Dordick, J.S.; Clark, D.S. *Biotechnol. Bioeng.* **2001**, 72, 475-482.
5. Lei, C.; Shin, Y.; Liu, J.; Ackerman, E.J. *J. Am. Chem. Soc.* **2002**, 124, 11242-11243.
6. Avnir, D.; Braun, S.; Lev, O.; Ottolenghi, M. *Chem. Mater.* **1994**, 6, 1605-1614.
7. Gill, I.; Ballesteros, A. *J. Am. Chem. Soc.* **1998**, 120, 8587-8598.
8. Kroger, N.; Duetzmann, R.; Sumper, M. *Science* **1999**, 286, 1129-1132.
9. Kroger, N.; Lorenz, S.; Brunner, E.; Sumper, M. *Science* **2002**, 298, 584-586.
10. Naik, R.R.; Brott, L.L.; Clarson, S.J.; Stone, M.O. *J. Nanosci. Nanotech.* **2002**, 2 (1), 95-100.

11. Cha, J.N.; Stucky, G.D.; Morse, D.E.; Deming, T.J. *Nature* **2000**, *403*, 289-292.
12. Cha, J.N.; Shimizu K.; Zhou Y.; Christiansen S.C.; Chmelka B.F.; Stucky G.D.; Morse D.E. *Proc. Natl. Acad. Sci. U S A*. **1999**, *96*(2), 361-5.
13. Tomczak, M.M.; Stone, M.O.; Naik, R.R. In *Nano-scale science and Technology in Biomolecular Catalysis*. Wang, P.; Kim, J. ACS symposium series; American Chemical Society, Washington DC.
14. Belton, D.J.; Patwardhan, S.V.; Perry, C.C. *J. Mater. Chem.* **2005**, *15*, 4629-4638.
15. Berne, C.; Betancor, L.; Luckarift, H.R.; Spain, J.C. *Biomacromol.* **2006**, *In Press*.
16. Roth, K.M.; Zhou, Y.; Yang, W.; Morse, D.E. *J. Am. Chem. Soc.* **2005**, *127* (1), 325-330.
17. Shimizu, K.; Cha, J.; Stucky, G.D.; Morse, D.E. *Proc. Nat. Acad. Sci. USA* **1998**, *95*, 6234-6238.
18. Luckarift, H.R.; Dickerson, M.B.; Sandhage, K.H.; Spain, J.C. *Small* **2006**, *2* (5), 640-643.
19. Luckarift, H.R.; Spain, J.C.; Naik, R.R.; Stone, M.O. *Nat. Biotech.* **2004**, *22* (2), 211-213.
20. Naik, R.R.; Tomczak, M.M.; Luckarift, H.R.; Spain, J.C.; Stone, M.O. *Chem. Commun. (Cambridge)* **2004**, 1684 -1685.
21. Luckarift, H.R.; Nadeau, L.J.; Spain, J.C. *Chem. Commun. (Cambridge)* **2005**, 383-384.
22. Holden, M.; Kelly, C. *Adv. Psychiatr. Treat.* **2002**, *8*, 89-96.
23. Liston, D.R.; Nielsen, J.A.; Villalobos, A.; Chapin, D.; Jones, S.B.; Hubbard, S.T.; Shalaby, I.A.; Ramirez, A.; Nason, D.; Frost White, W. *Eur. J. Pharmacol.* **2004**, *486*, 9-17.
24. Denny, W.A. *Curr. Pharm. Des.* **2002**, *8*, 1349-1361.
25. Anlezark, G.M.; Melton, R.G.; Sherwood, R.F.; Coles, B.; Friedlos, F.; Knox, R.J. *Biochem. Pharmacol.* **1992**, *44*, 2289-2295.
26. Urban, P.L.; Goodall, D.M.; Bruce, N.C. *Biotech. Adv.* **2006**, *24* (1), 42-57.
27. Krenkova, J.; Foret, F. *Electrophoresis.* **2004**, *25*, 3550-3563.
28. Calleri, E.; Temporini, C.; Furlanetto, S.; Loidice, F.; Fracchiolla, G. ; Massolini, G. *J. Pharma. Biomed. Analysis* **2003**, *32*, 715-724.
29. Girelli, A.M.; Mattei, E.J. *J. Chromatogr. B* **2005**, *819*, 3.
30. Markoglou, N.; Wainer, I.W. *J Chromatogr A.* **2002**, *948*(1-2), 249-56.
31. Bartolini, M.; Cavrini, V.; Andrisano, V. *J. Chromatogr. A.* **2004**, *1031*, 27-34.
32. Bartolini, M.; Cavrini, V.; Andrisano, V. *J. Chromatogr. A.* **2005**, *1065*, 135-144.
33. Andrisano, V.; Bartolini, M.; Gotti, R.; Cavrini, V.; Felix, G. *J. Chromatogr. B.* **2001**, *753*, 375-383

34. Dong, Y.; Wang, L.; Shangguan, D.; Zhao, R.; Liu, G. *J. Chromatogr. B.* **2003**, 788, 193-198.
35. Luckarift, H.R.; Johnson, G.R.; Spain, J.C. *J. Chromatogr. B.* **2006**, *In Press*. doi: 10.1016/j.jchromb.2006.06.036
36. Whiteway, J.; Koziarz, P.; Veall, J.; Sandhu, N.; Kumar, P.; Hoecher, B.; Lambert, I.B. *J. Bacteriol.* **1998**, 180, 5529-5539.
37. Jenks, P.J.; Ferrero, R.L.; Tankovic, J.; Thiberge, J.M.; Labigne, A. *Antimicrob. Agents. Chemother.* **2000**, 44, 2623-2629.
38. Jin, R-H.; Yuan, J-J. *Macromol. Chem. Phys.* **2005**, 206, 2160-2170.
39. Andersson, M.M.; Hatti-Kaul, R. *J. Biotechnol.* **1999**, 72, 21-25.
40. Lopez-Gallego F.; Betancor L.; Hidalgo A.; Alonso N.; Fernandez-Lafuente R.; Guisan J.M. *Biomacromol.* **2005**, 6, 1839-1842.
41. Srinivasan, A.; Wu, X.; Lee, M-Y.; Dordick, J.S. *Biotech. Bioeng.* **2003**, 81 (5), 563-569.0020
42. Nadeau, L.J.; He, Z.; Spain, J.C. *J. Ind. Micro. Biotech.* **2000**, 24, 301-305.
43. Kadiyala, V.; Nadeau, L.J.; Spain, J.C. *Appl. Environ. Micro.* **2003**, 69, 6520-6526.
44. Naik, R.R.; Whitlock, P.W.; Rodriguez, F.; Brott, L.L.; Glawe, D.D.; Clarson, S.J.; Stone, M.O. *Chem. Commun. (Cambridge)* **2003**, 238-239.
45. Tomczak, M.M.; Glawe, D.D.; Drummy, L.F.; Lawrence, C.G.; Stone, M.O.; Perry, C.C.; Pochan, D.J. *J. Am. Chem. Soc.* **2005**, 127 (36), 12577-12582
46. Dickerson, M.B.; Naik, R.R.; Sarosi, P.M.; Agarwal, G.; Stone, M.O.; Sandhage, K.H. *J. Nanosci. Nanotechnol.* **2005**, 5(1), 63-67.

DOI: 10.1002/sml.200500376

Rapid, Room-Temperature Synthesis of Antibacterial Bionanocomposites of Lysozyme with Amorphous Silica or Titania**

Heather R. Luckarift, Matthew B. Dickerson,
Kenneth H. Sandhage, and Jim C. Spain*

The majority of natural biomineralized structures are composed of calcium carbonate or silica, which are not always well suited for biotechnological applications. While many natural silica-forming proteins have been identified,^[1] only the silicatein of marine sponges has been reported to catalyze the formation of titania *in vitro*.^[2] Lysozyme is a ubiquitous antibacterial enzyme that is capable of lysing Gram-positive bacterial cells by hydrolyzing specific peptidoglycan linkages in the cell wall.^[3] Recent reports indicate the involvement of lysozyme in the biomineralization of silica and calcium carbonate,^[4] and heat-denatured lysozyme has also been implicated in the synthesis of bismuth sulfide, although the mechanism is unclear.^[5] Here, a rapid, economical, room-temperature method for encapsulating lysozyme within silica or titania nanoparticles, with appreciable retention of antimicrobial activity, is reported for the first time. The development of a simple, low-cost processing route to lysozyme/inorganic nanocomposites and the evaluation of the antimicrobial activity of such composites provides an opportunity to create bionanocomposite materials that resist bacterial activity for use as broad-spectrum antifouling materials. Lysozyme directs the formation of nanoparticles of silica or titania under ambient conditions, so as to simultaneously entrap the lysozyme in an active form. Amorphous

titania-based materials can possess diverse optical, electronic, biomedical, and chemical properties.^[6] Hence, lysozyme/titania nanocomposites could be attractive multifunctional materials for a variety of applications (for example, for cosmetics with both antimicrobial and sunscreen properties).^[7]

In the present work, lysozyme catalyzed the precipitation of silica within seconds when added to a solution of prehydrolyzed tetramethoxysilane (TMOS). Lysozyme also catalyzed the rapid precipitation of titania when added to a solution of either potassium hexafluorotitanate (PHF-Ti) or titanium(IV) bis(ammonium lactato)dihydroxide (Ti-BALDH). Scanning electron microscopy (SEM) and transmission electron microscopy (TEM) revealed that the silica consisted of interconnected nanospheres with sizes on the range of 300–650 nm, with an average diameter of 570 nm (Figure 1). The silica morphology was similar to that previously observed for the interaction of lysozyme with water glass.^[4a] Energy dispersive spectroscopy (EDS) analysis conducted during SEM characterization indicated that the silica spheres were enriched in carbon and sulfur, as well as oxygen and silicon (Figure 2). The presence of carbon in the EDS spectrum was consistent with a precipitate consisting of an organic/inorganic composite of protein within a silica matrix. The cysteine residues in the lysozyme provided a source of sulfur. Selected-area electron diffraction (SAED) analysis (inset of Figure 1c) and X-ray diffraction (XRD) analysis (not shown) indicated that the precipitated silica was amorphous. The entrapment of lysozyme within the silica-bearing precipitate was confirmed by dissolving the silica in sodium hydroxide to release the entrapped protein. The recovered organic component was analyzed (and compared to soluble lysozyme) by using denaturing sodium dodecylsulfate polyacrylamide gel electrophoresis (SDS-PAGE), which revealed the presence of a protein band with a molecular weight of approximately 14 kDa (the molecular weight of lysozyme; not shown). The presence of a large proportion of organic matter within the precipitate was further confirmed by thermogravimetric (TG) analysis, which resulted in a 61.8% loss of dry mass upon pyrolysis in air at 700 °C. The surface areas of the siliceous material before and after heat treatment (1000 °C) were determined by multipoint nitrogen adsorption Brunauer–Emmett–Teller (BET) analysis to be 6.28 and 7.42 m² g⁻¹, respectively. The observed increase of specific surface area after pyrolysis is consistent with the presence of lysozyme, because the removal of the organic constituent would be expected to create voids and increase the surface area of the sample. SEM characterization of the pyrolyzed material indicates that the overall morphology of the silica spheres is retained, despite the removal of lysozyme. Distinct to the post-pyrolysis sample are dark spots (which are probably pores generated by the pyrolysis of the organic constituent of the sample) that cover the silica spheres (see Supporting Information, Figure 1).

The lysozyme/titania nanospheres differed markedly from the lysozyme/silica precipitates, both in their size and the degree of interconnectivity. SEM analysis revealed that the lysozyme/PHF-Ti-derived material was quite polydisperse, with diameters ranging from 100 nm to 1 μm. Individual lysozyme/PHF-Ti spheres were more strongly intercon-

[*] Prof. J. C. Spain
Georgia Institute of Technology
School of Civil and Environmental Engineering
311 Ferst Drive, Atlanta, GA 30332 (USA)
Fax: (+1) 404-894-8266
E-mail: jspace@ce.gatech.edu

Dr. H. R. Luckarift
Air Force Research Laboratory
Airbase Technologies Division, 139 Barnes Drive, Suite #2
Tyndall Air Force Base, FL 32403 (USA)

M. B. Dickerson, Prof. K. H. Sandhage
Georgia Institute of Technology
School of Materials Science and Engineering
771 Ferst Drive, Love Bldg., Atlanta, GA 30332 (USA)

[**] This work was supported by funding from the U.S. Air Force Office of Scientific Research (Walter Kozumbo, Joan Fuller, and Hugh De Long, program managers). H.R.L. was supported by a postdoctoral fellowship from the Oak Ridge Institute for Science and Education (U.S. Department of Energy). The authors acknowledge Rajesh R. Naik and Glenn R. Johnson for helpful discussions and Benjamin Church for help with BET and thermal analyses.



Supporting information for this article is available on the WWW under <http://www.small-journal.com> or from the author.

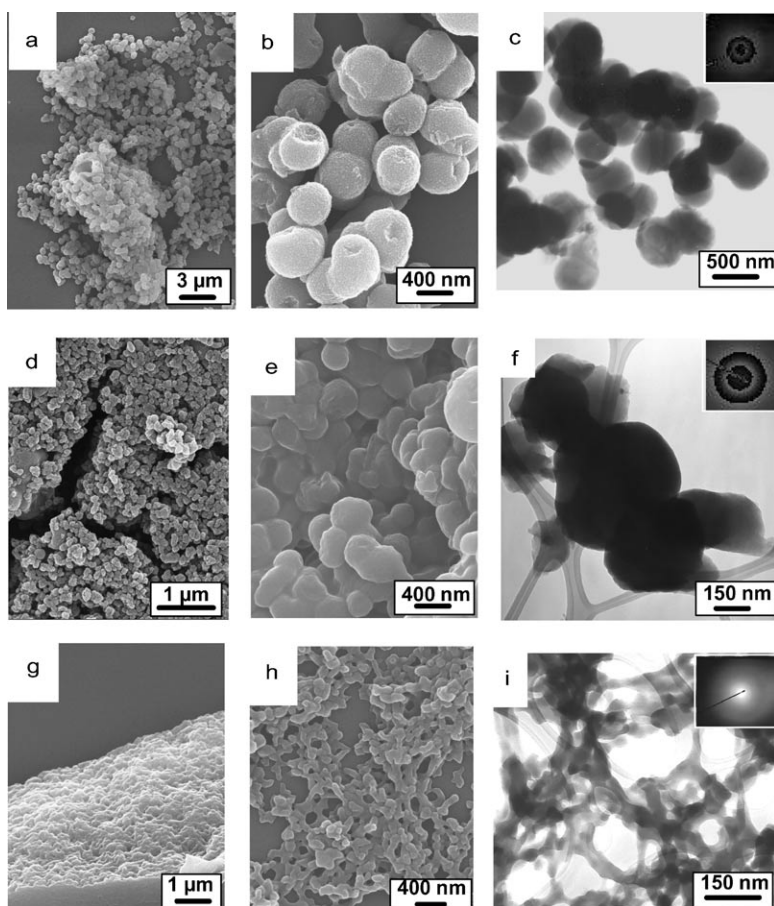


Figure 1. SEM and TEM micrographs of silica and titania nanoparticles formed by precipitation with lysozyme. a, b) SEM and c) TEM micrographs of silica from lysozyme and TMOS; d, e) SEM and f) TEM micrographs of titania from lysozyme and PHF-Ti; g, h) SEM and i) TEM micrographs of titania from lysozyme and Ti-BALDH. Insets: Selected-area electron diffraction (SAED) patterns of precipitates.

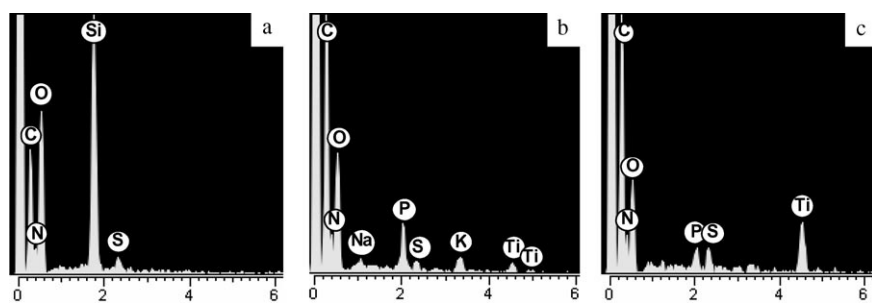


Figure 2. Energy dispersive spectroscopy of lysozyme-mediated silica and titania precipitates. a) Silica precipitated with lysozyme and TMOS; b) titania precipitated with lysozyme and PHF-Ti; c) titania precipitated with lysozyme and Ti-BALDH.

connected than the siliceous material and had a more sintered appearance (Figure 1). EDS analysis indicated that the lysozyme/PHF-Ti material was primarily composed of carbon, oxygen, titanium, potassium, phosphorus, and sulfur (Figure 2). Lysozyme is the probable origin of the carbon and sulfur signal, as noted above, whereas the titanium, oxygen, and potassium peaks are clearly associated with the inorganic precursor. The phosphorous can be traced to the incorporation of phosphate ions from the buffer solution during precipitation. The entrapment of lysozyme within the

titania precipitate was confirmed through analysis with SDS-PAGE of the organic component recovered after dissolution of the titania in sodium hydroxide (as discussed above for the silica-entrapped lysozyme). The substantial organic component of the composite was confirmed by TG analysis, which resulted in a 59.3% loss in dry weight upon heating to 700 °C in air. Additional weight loss, upon heating to 700–900 °C, was attributed to the evaporation of potassium. SAED analysis (inset of Figure 1f) and XRD analysis (not shown) indicated that the precipitated material was amorphous. Subsequent heat treatment of the lysozyme/PHF-Ti composite materials at 600 °C for 4 h resulted in the formation of phase-pure potassium titanyl phosphate (see Supporting Information, Figure 2), a unique nonlinear optical material that has found applications in lasing and low-loss waveguides.^[8]

The morphology of titanium dioxide formed by the interaction of lysozyme and Ti-BALDH differed conspicuously from the precipitates formed from the silicic acid or PHF-Ti precursors. SEM and TEM analyses of the titania precipitate revealed an open, highly interconnected network of very fine particles. The fundamental particles entrapped within the network possess diameters of only 10–50 nm. EDS analyses of the lysozyme/Ti-BALDH product showed an elemental composition similar to lysozyme/PHF-Ti (Figure 2). SDS-PAGE analysis of the organic material recovered after dissolution of the titania in sodium hydroxide again indicated the presence of lysozyme within the composite material. The proportion of combustible components of the material was some-

what higher (76.3%, from TG analysis) than that of either of the previously observed lysozyme/inorganic materials. SAED analysis (inset in Figure 1i) and XRD analysis (not shown) indicated that, unlike previously generated biomimetic titania,^[2] the lysozyme-catalyzed material was amorphous.

The activity of the encapsulated lysozyme was compared with that of the free enzyme to determine the effect of immobilization. The physical entrapment of lysozyme within an inorganic matrix could, in principle, inhibit the ability of lysozyme to attach to a bacterial cell wall and catalyze lysis.

Two assay methods were used to determine the activity of the encapsulated lysozyme. Bacteriolytic activity was investigated with *Micrococcus lysodeikticus* cells and by hydrolysis of a synthetic membrane mimic, the *p*-nitrophenyl β -glycoside of *N*-acetylchitooligosaccharide ((PNP-GlcNAc)₅; PNP = *p*-nitrophenyl, GlcNAc = *N*-acetylglucosamine).^[9] After immobilization of lysozyme in silica, 85(±6.6) % of the free enzyme activity was retained in the silica/lysozyme nanocomposite. A portion of the remaining enzyme activity and protein (approximately 10 %) was detected in the reaction supernatant and subsequent wash fractions. After immobilization of lysozyme in titania, 50(±6.5) % (with PHF-Ti as precursor) and 45(±12.7) % (with Ti-BALDH as a precursor) of the free enzyme activity was retained in the titania/lysozyme nanocomposites. The activity of immobilized lysozyme was comparable irrespective of the assay method used for the investigation (Figure 3a). The thermostability of the free and immobilized lysozyme was investigated to determine whether the inorganic matrices provide an environment that protects the immobilized lysozyme from denaturation. Free lysozyme in solution was denatured by incubation at 75 °C for 1 h (90 % decrease in activity). In comparison, the silica- and titania-encapsulated lysozyme retained 75 % and 20–45 % of the native activity, respectively, when incubated under the same conditions (Figure 3b).

The possibility of immobilizing an additional enzyme (for enhanced functionality) during the lysozyme-mediated precipitation reactions was also investigated. Butyrylcholinesterase was selected as a suitable model enzyme for immobilization due to its versatility in biosensor applications.^[10] Under the precipitation conditions described above, butyrylcholinesterase encapsulated during silica and titania precipitation fully retained the native enzyme activity (Figure 3c). Lysozyme-induced immobilization provided a more economical and efficient encapsulation of butyrylcholinesterase than that we had previously reported with a synthetic silica-forming peptide.^[11]

Lysozyme is a cationic polypeptide with a high isoelectric point ($pI \approx 10.5$) and includes a large percentage of hydroxy- and imidazole-containing amino acid residues, which are characteristic of many biomineralization-mediating biomacromolecules.^[1,12] The ability to immobilize lysozyme has been demonstrated by using a variety of support matrices, all involving attachment or adsorption to a surface.^[13] The limitations associated with surface-bound lysozyme (for example, the loading capacity and poor retention of activity) were overcome here by partially encapsulating the lysozyme within the porous inorganic matrices, thereby retaining the native protein structure and function. The primary physiological role of lysozyme is hydrolysis of the peptidoglycan of bacterial cell walls and resultant cell lysis (that is, a mechanism that involves lysozyme acting in contact with bacterial cell walls). The observation that lysozyme retains its catalytic activity when encapsulated suggests an alternative mechanism for lytic action. The section of protein responsible for the precipitation of silica or titania may be independent from the protein active site. The bactericidal properties of lysozyme are known to be independent of enzymatic activity, as has been confirmed by the retention of bactericidal

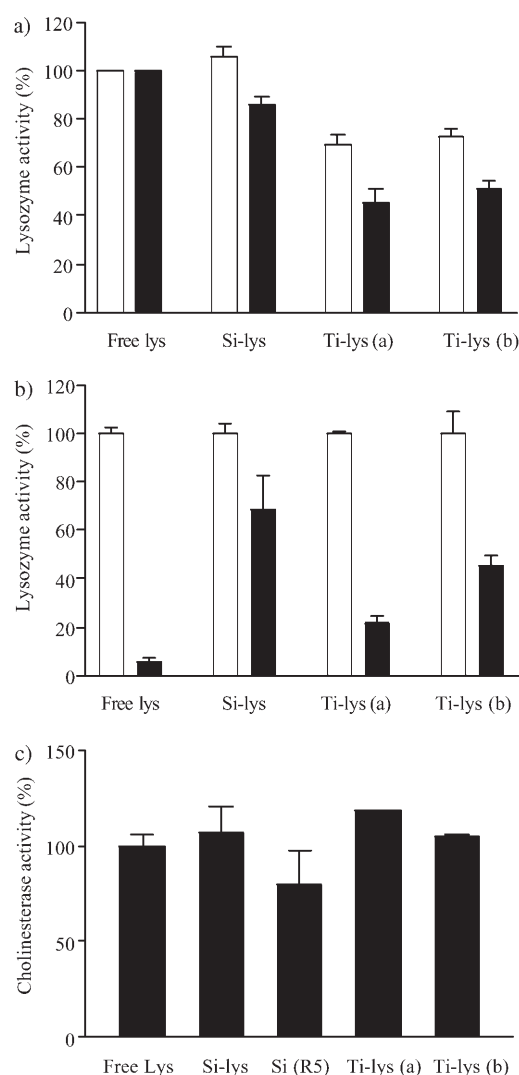


Figure 3. a) Activity of free and immobilized lysozyme in silica or titania nanoparticles. Lysozyme activity determined by lytic assay with *Micrococcus lysodeikticus* cells (□) or with PNP-(GlcNAc)₅ (■). Values quoted in the text are relative to the activity of native lysozyme in solution, taken as 100 %. b) Thermostability of free and immobilized lysozyme in silica or titania nanoparticles: □ = enzyme activity before heat treatment; ■ = enzyme activity after heat treatment for 1 h at 75 °C. c) Activity of butyrylcholinesterase immobilized in lysozyme-catalyzed silica or titania nanoparticles. Free lys = free lysozyme in solution; Si-lys = silica precipitated with lysozyme; Si (R5) = silica precipitated with R5 peptide;^[11] Ti-lys (a) = titania precipitated with lysozyme and Ti-BALDH; Ti-lys (b) = titania precipitated with lysozyme and PHF-Ti.

properties in denatured lysozyme.^[3,14] The mechanism of bactericidal activity in encapsulated lysozyme, however, requires further elucidation.

In summary, lysozyme induces the rapid, room-temperature precipitation of amorphous silica and titania, which, in turn, provide excellent support matrices for additional enzymes added during the reaction. Such lysozyme-mediated precipitation is a one-pot procedure that simultaneously results in lysozyme encapsulation within the silica or titania, with appreciable retention of antimicrobial activity. The inorganic matrices protect the immobilized biomolecules from

physical denaturation that occurs with free enzymes in solution and the lysozyme offers protection from microbial degradation. This attractive biomineralization/bioencapsulation strategy provides an economical and facile route for the synthesis of a wide range of functional bionanocomposites comprising biomacromolecules enclosed within silica or titania nanostructures.

Experimental Section

p-Nitrophenyl-penta-*N*-acetyl- β -chitopentaoside (PNP-(GlcNAc)₅) was from Seikagaku Corp., Tokyo. Lysozyme (EC 3.2.1.17) and butyrylcholinesterase (EC 3.1.1.8) were from Sigma-Aldrich. Butyrylcholinesterase stock solutions were prepared in a cholinesterase-specific buffer (0.1 M NaOH, 0.1 M KH₂PO₄, pH 8). All other chemicals were of analytical grade and were obtained from Sigma-Aldrich. The synthetic peptide, R5, was obtained from New England Peptide, Inc.

For the precipitation of inorganics, a stock solution of lysozyme (100 mg mL⁻¹) was prepared in deionized water and dialyzed prior to use (Slide-A-Lyzer, Pierce Biotechnology). TMOS was hydrolyzed in 1 M hydrochloric acid (1 M final concentration). The precipitation mixture consisted of buffer (800 μ L; 0.1 M NaOH, 0.1 M KH₂PO₄, pH 8), hydrolyzed TMOS (100 μ L; final concentration of 100 mM), and lysozyme (100 μ L; final concentration of 10 mg mL⁻¹). The mixture was agitated for 5 min at room temperature. The resultant particles were removed by centrifugation for 10 s (14 000 *g*) and then washed twice with deionized water. For the formation of titania particles, the precipitation reaction was as described above with either 100 mM PHF-Ti or Ti-BALDH as the inorganic precursor instead of TMOS. Ti-BALDH stock solutions were prepared in water, while PHF-Ti solutions were prepared in water and heated gently (50 °C) to aid solubility.

For encapsulation of butyrylcholinesterase in the precipitates, the precipitation mixture consisted of buffer (800 μ L) containing butyrylcholinesterase (50 units mL⁻¹), precursor (100 μ L; concentrations described above), and lysozyme (100 μ L; 100 mg mL⁻¹). Butyrylcholinesterase enzyme activity was measured spectrophotometrically at 630 nm as described previously.^[11] Entrapped lysozyme was released from silica and titania particles by dissolving the inorganic matrix in 1 M sodium hydroxide for 10 min at 37 °C and the proteins were visualized by denaturing SDS-PAGE. SDS-PAGE (15%) was performed by using a Mini/Protein II apparatus (Amersham Pharmacia) at a constant voltage of 200 V and according to the manufacturer's instructions. Lysozyme activity assays were performed with *Micrococcus lysodeikticus* cells according to the supplier's instructions. The activity of lysozyme was also determined colorimetrically by using the substrate (PNP-(GlcNAc)₅) as reported previously.^[9b]

The morphology of the lysozyme/inorganic composite materials was characterized by scanning (Leo 1530 FEG SEM, Carl Zeiss SMT AG) and transmission (JEOL 100CX II) electron microscopy. Microchemical analyses were conducted by utilizing an Oxford Inca EDS detector attached to the scanning electron microscope, with at least three measurements for each sample. The crystalline phases of the resulting composite materials were evaluated by X-ray diffraction (Philips PW1800, PANalytical) by

utilizing CuK α radiation at a scan rate of 0.6 deg min⁻¹. TG analyses were performed in a Netzsch STA 449 C instrument by heating to 1000 °C at a rate of 10 °C min⁻¹ in a synthetic-air gas stream. Multipoint nitrogen-adsorption BET analysis was conducted in a Quantachrome Autosorb-1c apparatus on samples dried at 120 °C.

Keywords:

biomimetic synthesis • biomineralization • enzyme immobilization • lysozyme • nanomaterials

- [1] a) N. Kroger, R. Deutzmann, M. Sumper, *Science* **1999**, *286*, 1129–1132; b) J. N. Cha, K. Shimizu, Y. Zhou, S. C. Christiansen, B. F. Chmelka, G. D. Stucky, D. E. Morse, *Proc. Natl. Acad. Sci. USA* **1999**, *96*, 361–365.
- [2] J. L. Sumerel, W. Yang, D. Kisailus, J. C. Weaver, J. H. Choi, D. E. Morse, *Chem. Mater.* **2003**, *15*, 4804–4809.
- [3] A. Pellegrini, U. Thomas, R. von Fellenberg, P. Wild, *J. Appl. Bacteriol.* **1992**, *72*, 180–187.
- [4] a) T. Coradin, A. Coupe, J. Livage, *Colloids Surf. B* **2003**, *29*, 189–196; b) C. Jimenez-Lopez, A. Rodriguez-Navarro, J. M. Dominguez-Vera, J. M. Garcia-Ruiz, *Geochim. Cosmochim. Acta* **2003**, *67*, 1667–1676.
- [5] F. Gao, Q. Lu, S. Komarneni, *Chem. Commun.* **2005**, 531–533.
- [6] a) S. K. Deb, *Solid State Commun.* **1972**, *11*, 713–715; b) J. Sun, I. Ichinose, R. Takaki, A. Nakao, T. Kunitake, *Chem. Lett.* **2002**, *7*, 742–743; c) A. C. Rastogi, S. N. Sharma, S. Kohli, in *Microcrystalline and Nanocrystalline Semiconductors-1998* (Eds.: M. J. Sailor, C. C. Tsai, L. T. Canham, K. Tanaka), Materials Research Society, Warrendale, PA, **1999**, pp. 263–268; d) C. Yao, E. B. Slamovich, T. J. Webster, in *Nanoscale Materials Science in Biology and Medicine* (Eds.: C. T. Laurencin, E. A. Botchwey), Materials Research Society, Warrendale, PA, **2005**, pp. 215–220; e) Y. Gao, Y. Masuda, K. Koumoto, *Langmuir* **2004**, *20*, 3188–3194; f) M. Nakamura, T. Aoki, Y. Hatanaka, D. Korzec, J. Engemann, *J. Mater. Res.* **2001**, *16*, 621–626.
- [7] a) A. Kuroda, K. Ogino, *Fragrance J.* **1994**, *22*, 17–21; b) K. Nakano, K. Sakai, O. Yasui, Japanese patent no. 2004307363, **2004**.
- [8] M. N. Satyanarayan, A. N. Deepthy, H. L. Bhat, *Crit. Rev. Solid State Mater. Sci.* **1999**, *24*, 103–189.
- [9] a) D. Shugar, *Biochim. Biophys. Acta* **1952**, *8*, 302–309; b) F. Nanjo, K. Sakai, T. Usui, *J. Biochem.* **1988**, *104*, 255–258.
- [10] a) A. K. Singh, A. W. Flounders, J. V. Volponi, C. S. Ashley, K. Wally, J. S. Schoeniger, *Biosens. Bioelectron.* **1999**, *14*, 703–713; b) Y. A. Cho, H. S. Lee, G. S. Cha, Y. T. Lee, *Biosens. Bioelectron.* **1999**, *14*, 435–438.
- [11] H. R. Luckarift, R. R. Naik, M. O. Stone, J. C. Spain, *Nat. Biotechnol.* **2004**, *22*, 211–213.
- [12] T. Coradin, P. J. Lopez, C. Gautier, J. Livage, *C. R. Palevol.* **2004**, *3*, 443–452.
- [13] a) A. Crapisi, A. Lante, G. Pasini, P. Spettoli, *Process Biochem.* **1993**, *28*, 17–21; b) R. Datta, W. Armiger, D. F. Ollis, *Biotechnol. Bioeng.* **1973**, *15*, 993–1006; c) D. Leckband, R. Langer, *Biotechnol. Bioeng.* **1991**, *37*, 227–237; d) A. A. Vertegel, R. W. Siegel, J. S. Dordick, *Langmuir* **2004**, *20*, 6800–6807.
- [14] a) A. Pellegrini, U. Thomas, N. Bramaz, S. Klauser, P. Hunziker, R. von Fellenberg, *J. Appl. Microbiol.* **1997**, *82*, 372–378; b) H. N. Hunter, W. Jing, D. J. Schibli, T. Trinh, I. Y. Park, S. C. Kim, H. J. Vogel, *Biochim. Biophys. Acta* **2005**, *1668*, 175–189.

Received: October 3, 2005

Published online on March 15, 2006

Silica-immobilized enzyme reactors; application to cholinesterase-inhibition studies

Heather R. Luckarift^{a,*}, Glenn R. Johnson^a, Jim C. Spain^b

^a Air Force Research Laboratory, Airbase Technologies Division, 139 Barnes Drive, Suite #2, Tyndall Air Force Base, FL 32403, USA

^b Georgia Institute of Technology, School of Civil and Environmental Engineering, 311 Ferst Drive, Atlanta, GA 30332, USA

Received 30 March 2006; accepted 19 June 2006

Available online 1 August 2006

Abstract

A rapid and economical method is reported for the preparation of an immobilized enzyme reactor (IMER) using silica-encapsulated equine butyrylcholinesterase (BuChE) as a model system. Peptide-mediated silica formation was used to encapsulate BuChE, directly immobilizing the enzyme within a commercial pre-packed column. The silica/enzyme nanocomposites form and attach simultaneously to the metal affinity column via a histidine-tag on the silica-precipitating peptide. BuChE–IMER columns were integrated to a liquid chromatography system and used as a rapid and reproducible screening method for determining the potency of cholinesterase inhibitors. The IMER preparation method reported herein produces an inert silica-encapsulation matrix with advantages over alternative systems, including ease of preparation, high immobilization efficiency (70–100%) and complete retention of activity during continuous use.

Published by Elsevier B.V.

Keywords: Immobilized enzyme reactor; Butyrylcholinesterase; Silica-encapsulation; Cholinesterase inhibitors

1. Introduction

Immobilization of proteins to solid supports is advantageous for a wide variety of biosensing, bioprocessing and affinity chromatography applications. Immobilized enzyme reactors (IMERs) have found application in catalysis and have also been used with a wide variety of receptor proteins for substrate interaction and inhibition studies [1–7]. The main advantages of immobilized enzyme systems are stability and reusability. In addition, IMERs facilitate continuous on-line analysis, significantly minimizing cost and analysis time. Immobilization of enzymes for IMER applications has been demonstrated using a variety of chemical and physical techniques. Chemical immobilization generally involves enzyme attachment to a matrix via cross-linking or covalent bonding. Physical methods include adsorption of biomolecules to a porous support or ion exchange matrix, or entrapment within an insoluble gel matrix. Several previously reported IMER configurations use silica or monolithic materials as a support matrix for enzyme immobilization

but such systems are often handicapped by poor enzyme loading capacities. Many methods of immobilization and entrapment also cause significant structural deformation of the enzyme, leading to reduction in activity. Significant optimization of the immobilization method is often required and factors such as stability may be sacrificed in favor of increased loading capacity [3–6].

Butyrylcholinesterase (BuChE) and acetylcholinesterase (AChE) are crucial to transmission of nerve impulses in mammals and have received increasing attention due to their potential roles in disorders of the central nervous system, such as Alzheimer's disease and Down's Syndrome [8]. BuChE is of pharmacological and toxicological importance due to its ability to hydrolyze ester-containing drugs and scavenge cholinesterase inhibitors, including organophosphate nerve agents [9]. Inhibition of cholinesterase provides a mechanism for acetylcholine replacement, which has proven to be an effective therapy in treating the cognitive and functional symptoms of Alzheimer's disease [10,11]. IMERs have found increasing application to acetylcholinesterase inhibition studies by employing immobilized acetylcholinesterase or horseradish peroxidase within packed columns [4,12–14]. The previously reported systems however, have specific

* Corresponding author. Tel.: +1 850 283 6034; fax: +1 850 283 6090.
E-mail address: hluckarift@gtcom.net (H.R. Luckarift).

drawbacks such as low loading capacity and long preparation times.

We recently reported a biomimetic silicification reaction that provides a biocompatible and simple method for enzyme immobilization resulting in a stable, heterogeneous catalyst with enhanced mechanical stability and high loading capacity [15,16]. The silicification reaction mixture consists of hydrolyzed tetramethyl orthosilicate (TMOS) and a silica-condensing synthetic peptide (R5). The R5 peptide is the repeat unit of a silaffin protein previously identified from the diatom *Cylindrotheca fusiformis*. In the diatom, silaffins catalyze the precipitation of silica, to form the organism's exoskeleton. The R5 peptide mimics the silica precipitation *in vitro* and forms a network of fused spherical silica nanoparticles (average diameter of 500 nm) [17].

The stability of silica-immobilized enzymes provided an opportunity to explore continuous flow-through reaction systems. Silica-entrapped BuChE was initially investigated in two flow-through systems: (1) a fluidized-bed system and (2) a packed-bed system. The fluidized-bed system proved suitable for continuous operation and retained conversion efficiency for over 1000 column volumes, but the use of the column was limited by the need for upwards flow-through the column, to prevent packing. In the packed-bed system the conversion rate decreased over time; the immobilized enzyme was not inactivated during the continuous flow but rather the overall retention time decreased, due to packing and eventual channeling of the silica particles [15]. The mechanical stability of the silica-immobilized enzyme indicated that it was applicable to flow through applications but the configuration of the apparatus required optimization. In order to avoid these limitations, the aim of the present study was to determine whether IMERs could be prepared using silica-encapsulation *in situ* via his-tag attachment of the silica-immobilized enzyme to metal ion affinity resin. Immobilization of silica to surfaces has recently been reported by attachment of silicatein proteins to a gold surface, using histidine-binding to nickel via a nitrilotriacetic acid chelator [18]. An alternate method involves deposition of silica by electrochemical dip pen nanolithography patterning of histidine-tagged peptides [19]. Simultaneous encapsulation and attachment of an active biomolecule to the surface of a flow-through device however, has not been previously reported. The silica immobilization method reported herein provides a novel method for rapid and highly efficient enzyme encapsulation and is applicable to the preparation of a wide variety of immobilized biomolecules.

2. Experimental

2.1. Materials

Butyrylcholinesterase (E.C.3.1.1.8; from Equine Serum, ~50% protein and activity of 1200 Units/mg protein) was purchased from Sigma–Aldrich (St. Louis, MO). Cholinesterase specific phosphate buffer was used throughout (0.1N NaOH, 0.1 M KH_2PO_4 , pH 8) unless otherwise stated [15]. All other chemicals were of analytical grade and obtained from Sigma–

Aldrich. The synthetic peptides; R5 (SSKKS₆SGSYSGSKGSKRRIL), C-terminus (His)₆-tag R5: (SSKKS₆SGSYSGSKGSKRRILHHHHHHH-COOH), N-terminus (His)₆-tag R5: (H₂NHHHHHHSSKKS₆SGSYSGSKGSKRRIL) were from New England peptides (Gardner, MA).

2.2. Enzyme analysis

The activity of BuChE was determined by the rate of butyrylthiocholine iodide (BuCh-I) hydrolysis in potassium phosphate buffer (25 mM, pH 7.0) containing MgSO_4 (10 mM) and Ellman's reagent (1.26 μM); the reaction produces a yellow anion that can be detected by spectroscopy, where $\epsilon = 13,600 \text{ m}^{-1} \text{ cm}^{-1}$ at 412 nm [12–14,20,21]. A calibration curve of the thiocholine product complex was generated by incubating fixed concentrations of BuCh-I with BuChE until the reaction reached completion (assumed to be 100% conversion). The absorbance was measured at 412 nm and correlated with the product extinction coefficient [20]. Protein concentration was determined by using a bicinchonic acid (BCA) protein assay kit (Pierce Biotechnology, Rockford, IL) with bovine serum albumin as standard.

2.3. His-tag immobilization to agarose beads

A stock solution of the R5 peptide (or (His)₆-R5) (100 mg/ml) was prepared in deionized water. Silicic acid was prepared by hydrolyzing TMOS (final concentration 1 M) in hydrochloric acid (1 mM). Chelating sepharose fast flow metal ion affinity chromatography media was charged with cobalt ions (1 M CoCl_2) according to the manufacturer's instructions (GE Healthcare/Amersham Biosciences, Piscataway, NJ). The silicification mixture consisted of BuChE stock solution (80 μl of 100 U/ml), hydrolyzed TMOS (10 μl) and R5 peptide stock (10 μl of 100 mg/ml). The ratio of (His)₆-R5 peptide and R5 peptide was varied to determine loading capacity but the final peptide concentration of the mixture was maintained at 10 mg/ml throughout. The mixture was left for 30 min to allow the silicification reaction to proceed and then washed with five volumes of buffer.

2.4. IMER preparation

2.4.1. C-His₆-BuChE-IMER and N-His₆-BuChE-IMER

BuChE-IMERs were prepared using HiTrap Chelating HP columns (dimensions: 1.6 cm \times 2.5 cm; 5 ml volume) charged with cobalt ions (1 M CoCl_2) according to the manufacturer's instructions (GE Healthcare/Amersham Biosciences, Piscataway, NJ). The (His)₆-R5 peptide (500 μl of 10 mg/ml) was loaded onto the column and washed according to the manufacturer's instructions. The silicification mixture, consisting of BuChE stock solution (1.6 ml of 100 U/ml), hydrolyzed TMOS (0.2 ml) and R5 peptide stock (0.2 ml) was mixed and added to the column. The column was left for 30 min to allow the silicification reaction to proceed and then washed with five column volumes of buffer.

2.4.2. Si-BuChE-IMER

The Si-BuChE-IMER was prepared as above with the exception of the His₆-R5 peptide.

2.4.3. Soluble-BuChE-IMER

The soluble-BuChE-IMER was prepared by loading soluble enzyme (1.6 ml of BuChE stock solution (100 U/ml)) directly onto the column. The column was left for 30 min before washing with five column volumes of buffer.

After immobilization, the BuChE activity and protein concentration in the eluate and resultant wash fractions were measured to determine the immobilization efficiency. For stability studies, buffer was passed through the columns continuously at a fixed rate (1 ml/min). At regular intervals, the residual enzyme activity on the columns was determined.

The morphology of the silica nanoparticles was characterized by scanning electron microscopy (ICBR Electron Microscopy Core Lab, University of Florida).

2.5. Chromatography conditions

For activity and inhibition studies, the IMERs were attached to an Agilent 1100 series liquid chromatography system. Phosphate buffer (25 mM, pH 7.0) was used as the mobile phase at a flow rate of 1 ml/min, unless otherwise stated, and the eluate was monitored using a diode-array detector (412 nm). BuCh-I was injected onto the IMER columns (concentration range: 10 μ M–250 mM, 20 μ l injections in triplicate) and the peak area of the product was correlated to concentration against a calibration curve. Blank control samples (containing no inhibitor) were injected at regular intervals to monitor the reproducibility and stability of the column. Michaelis–Menten plots were generated of activity (mmoles product/min) at a range of substrate concentrations and specific activity (V_{\max}) values were calculated using GraphPad Prism software (v 3.02). For inhibition experiments a stock solution of inhibitor (100 mM) was prepared in ethanol and diluted into a solution of BuCh-I (200 mM) to give a range of inhibitor concentrations (10 μ M–10 mM). The degree of inhibition was determined according to the formula $I(\%) = (I_i - I_f)/I_i \times 100$, where I_i is the initial steady state absorbance of the substrate, and I_f corresponds to the final activity of the enzyme in the presence of inhibitor. Inhibition curves (percentage activity inhibition versus log [inhibitor]) were plotted and the IC₅₀ values extrapolated using GraphPad Prism software (v 3.02).

3. Results and discussion

3.1. Butyrylcholinesterase immobilization

The effect of additional histidine residues upon the silicification activity was determined using the R5 peptide with six histidine residues (his-tag) attached at either the carboxyl (C)-terminus or amino (N)-terminus. Both (His)₆-tagged peptides catalyzed the precipitation of silica at a rate comparable to the native R5 peptide indicating that the addition of histidines does not affect the precipitation activity of the peptide (data

not shown). The R5 peptide typically produces silica nanoparticles with an average size of \sim 500 nm [15–17]. SEM analysis revealed that the C-(His)₆-R5 peptide catalyzed the formation of silica particles with a size range of approximately 150–700 nm and an average size of \sim 500 nm. The silica particles formed by the N-(His)₆-R5 were slightly larger, with a size range of 700–1200 nm and an average size of \sim 800 nm (data not shown).

The suitability of metal ion affinity chromatography media for enzyme immobilization was determined initially using a slurry of the column packing material in batch experiments in order to optimize the enzyme immobilization conditions. The maximum loading capacity of the silica nanoparticles formed by precipitation with (His)₆-R5 was approximately 20 Units BuChE per milliliter packing media. The enzyme loading could be increased to approximately 30 Units BuChE per milliliter of packing media by using a mixture of one part (His)₆-R5:four parts R5. Encapsulation with (His)₆-R5 alone limits enzyme immobilization to the surface of the agarose beads. The presence of non-tagged peptide, however, increases the formation of an interconnected matrix of silica nanospheres (Fig. 1), therefore greatly increasing the surface area for encapsulation. We previously determined that the silicification reaction yields approximately 1.2 mg of silica from a 100 μ l reaction mixture [15]. The calculated capacity for enzyme loading in the silica nanospheres using the optimized reaction conditions (above) is \sim 22.2 mg enzyme/g silica (2.2%, w/w).

3.2. Butyrylcholinesterase-IMER preparation

The scheme for immobilizing BuChE into a packed column is shown in Fig. 2. A pre-packed metal ion affinity chromatography column charged with cobalt ions selectively retains proteins (or peptides) with histidine or other complex-forming amino acid residues, exposed on the surface of the protein. Therefore a His₆-homologue of the R5 peptide selectively binds to the cobalt ions. When the silicification mixture is applied to the column, silica precipitation occurs and integrates with the peptide already bound to the column, resulting in the concurrent immobilization of the enzyme. Analysis of the packing within the column by SEM confirmed the presence of silica nanospheres attached to the surface of the agarose beads (Fig. 1 c and d).

Four columns were prepared comprising: (1) soluble BuChE (soluble-BuChE-IMER); (2) BuChE immobilized in silica (Si-BuChE-IMER); (3) BuChE immobilized in silica, with N-terminal His₆-peptide (N-His₆-BuChE-IMER); and (4) BuChE immobilized in silica, with C-terminal His₆-peptide (C-His₆-BuChE-IMER). The amount of protein retained during immobilization was determined for each IMER. In the case of the silica-immobilized IMERs, it is difficult to determine what proportion of BuChE was bound to the column because unbound peptide would also be detected in the eluate. The columns that contain the silica however, retained much more total protein (>90%) than the soluble-BuChE-IMER (Table 1). Residual BuChE activity in the eluate and wash fractions was negligible in all cases (less than 1%—data not shown). The enzyme loading for the silica-immobilized columns was approximately 30 Units BuChE per ml packing, in agreement with the maximum immo-

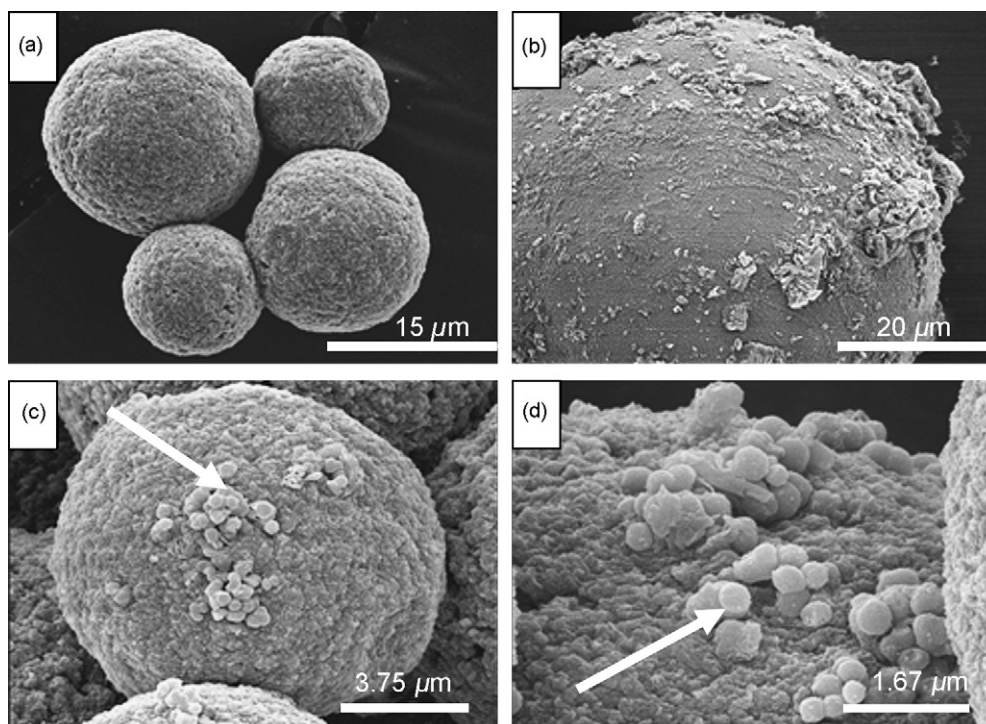


Fig. 1. SEM micrographs of silica nanoparticles attached to agarose beads SEM analysis of agarose beads (a) and immobilized BuChE attached to agarose beads. Using silica nanoparticles formed from N-(His)₆-R5 peptide only (b) or from a mixture of N-(His)₆-R5 peptide and R5 peptide (c and d).

bilization capacity previously obtained during optimization in loose media.

The silica-immobilized IMERs exhibited high substrate conversion efficiency (~60%) irrespective of the presence or absence of the his-tag. Despite the high immobilization efficiency in the absence of a his-tag however, the Si-BuChE-IMER lost activity over time and was attributed to the gradual elution of silica particles from the column during continuous flow. The

physical attachment of the silica particles via the his-tag resulted in stable IMER preparations, which during continuous flow conditions, demonstrated reproducible conversion of BuCh-I for both the C-His₆-BuChE-IMER and N-His₆-BuChE-IMER with no significant loss in enzyme activity or conversion efficiency (Fig. 3). The His₆-BuChE-IMERS were stable over a period of 200 column volumes of continuous flow. The silica immobilization provided greater stability and retention of enzyme activity

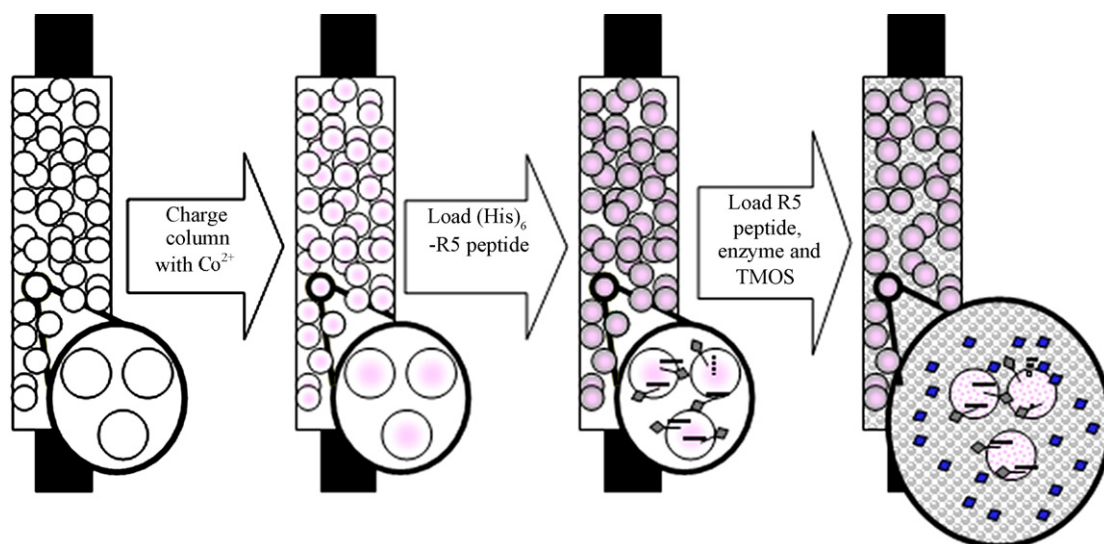


Fig. 2. Scheme for enzyme immobilization in silica nanospheres attached by affinity binding to cobalt-coated resin. Key: agarose beads (○); Co²⁺ coated agarose beads (●); his-tagged peptide (—○); enzyme (■); silica nanospheres (▨).

Table 1
Immobilization efficiency and kinetic parameters of BuChE–IMERs

		Soluble-BuChE–IMER	Si-BuChE–IMER	N-His ₆ -BuChE–IMER	C-His ₆ -BuChE–IMER
Column contents	BuChE	✓	✓	✓	✓
	R5 peptide	×	✓	✓	✓
	His ₆ -R5 peptide	×	×	✓	✓
Protein retained (%) ^a		47.7	92.55	98.69	98.95
Immobilized units (Units) ^b		~93	~158	~160	~131
Immobilization efficiency (%)		58.1	98.7	100	70.6
Enzyme activity (V_{\max}) (μmoles/min)		18.68 ± 0.42	31.58 ± 0.65	32.48 ± 0.92	26.28 ± 1.16

^a ([Protein]_{in} – [Protein]_{out}).

^b ([Units]_{in} – [Units]_{out}).

than the soluble-BuChE–IMER. The initial conversion activity of the soluble-BuChE–IMER was significantly lower (~48%) and it lost activity rapidly.

3.3. Determination of kinetic parameters of BuChE–IMERs

N-His₆-BuChE–IMER and C-His₆-BuChE–IMER columns connected to an LC system exhibited stable performance at a wide range of flow rates from 0.5 to 3 ml/min. Multiple injections of substrate through the columns by means of an auto sampler system provided rapid analysis and demonstrated reproducible conversion efficiency. The percentage conversion of BuCh-I and the product retention time decreased with increasing flow rate as expected due to the reduction in residence time. The column pressure remained stable and below 70 Bar at the range of flow rates tested (data not shown). A flow rate of 1 ml/min was chosen as an optimum balance between high product conversion and low retention time. Under the optimum flow conditions the chromatographic retention time was approximately 5 min and analysis of an injected sample was completed in less than 10 min.

The retention of BuChE activity by each of the IMERs indicated that BuChE was retained on the stationary phase. The relative activity and rate of reaction of BuChE immobilized within the IMERs was determined using Michaelis–Menten plots to determine specific activity (V_{\max}) (Fig. 4). True kinetic parameters cannot be defined using this fixed-bed system, because the initial reaction rates cannot be determined due to the residence

time in the columns which results in complete conversion at low substrate concentrations. The specific activity of the IMERs can, however, be used to compare specific activity between like systems and provides an estimate of immobilization efficiency. For each system, the hydrolysis of BuCh-I followed conventional Michaelis–Menten kinetics and saturating substrate concentration was in excess of 100 mM (Fig. 4).

Because V_{\max} is directly proportional to enzyme concentration, the units of immobilized enzyme can be correlated to V_{\max} as described previously [14] (Table 1). The immobilization efficiency was highest for the IMERs that involved silica-immobilization of the enzyme. However, significant non-specific binding of the free enzyme was observed, which is intriguing considering the low percentage (~1%) of histidine residues in BuChE. Recent reports suggest a non-competitive interaction between BuChE and metal ions such as Ni²⁺ and Co²⁺, which might contribute to the non-specific binding observed in this study [22]. The soluble enzyme, however, was not retained within the soluble-BuChE–IMER during continuous flow operation and some variability in the data obtained from the soluble-BuChE–IMER was recognized and is attributed to the loss in enzyme activity during continuous analysis.

3.4. Inhibition of BuChE–IMERs

The silica-based IMERs showed stable and reproducible conversion of BuCh-I during continuous operation, providing a system that is suitable for a number of applications that would not be feasible with soluble enzyme. The hydrolysis of BuCh-I by cholinesterases is decreased by the presence

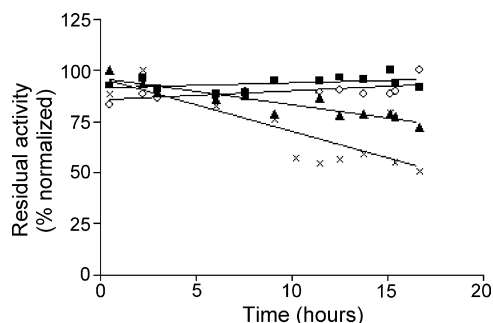


Fig. 3. Stability of BuChE–IMERs during continuous operation. (×) Soluble-BuChE–IMER; (▲) Si-BuChE–IMER; (○) C-His₆-BuChE–IMER; (■) N-His₆-BuChE–IMER. Conversion activity (%) normalized to initial rate. Based on concentration of product (μM) from conversion of 100 μM BuCh-I at a flow rate of 1 ml/min.

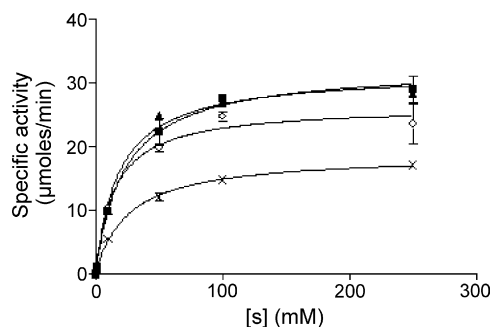


Fig. 4. Michaelis–Menten plots for BuChE–IMERs. (×) Soluble-BuChE–IMER; (▲) Si-BuChE–IMER; (○) C-His₆-BuChE–IMER; (■) N-His₆-BuChE–IMER. Values are mean and SD of triplicate experiments.

Table 2
Effect of cholinesterase inhibitors on BuChE activity in IMERs

Inhibitor	N-His ₆ -BuChE-IMER		C-His ₆ -BuChE-IMER	
	IC ₅₀ (mM)	K _i (mM)	IC ₅₀ (mM)	K _i (mM)
Galantamine	0.65 ± 0.03	0.04	0.49 ± 0.04	0.05
Eserine	0.84 ± 0.03	0.05	0.88 ± 0.03	0.09
Tacrine	5.75 ± 0.15	0.40	4.37 ± 0.62	0.44
Edrophonium chloride	10.02 ± 2.69	0.70	11.69 ± 6.12	1.20

IC₅₀ values represent mean with SD of triplicate experiments.

of inhibitors and can therefore be measured in a continuous flow system for screening cholinesterase inhibitors and ranking of their inhibitory potencies. Four reversible inhibitors of BuChE were investigated; tacrine, eserine (physostigmine), galantamine and edrophonium chloride and were selected on the basis of their potency and mode of inhibition (Table 2). The BuChE-IMERs exhibited a concentration-dependent response to all of the cholinesterase inhibitors. In all cases, increasing inhibitor concentration resulted in concurrent and concentration-dependent reduction of BuCh-I hydrolysis. Galantamine was the most potent of the inhibitors tested. The IC₅₀ values were consistently higher than those determined *in vitro* but demonstrate feasibility of using IMERs to screen the preliminary inhibition characteristics of substrates. The inhibitor potency of eserine was approximately 5 times greater than observed for tacrine, in agreement with previous literature reports [23].

4. Conclusion

The use of silica-encapsulation provides a facile immobilization technique that permits retention of enzyme activity and imparts mechanical properties that facilitate application to flow-through systems, such as IMERs. The IMERs can be used for the screening of specific enzyme inhibitors and the ranking of their inhibitory potencies; an extremely useful parameter in drug discovery. Butyrylthiocholine is not a physiological substrate for human brain butyrylcholinesterase but is used as a synthetic substrate for the enzyme. Therefore, inhibition constants derived using this method can only be representative of relative inhibitor potency. The primary advantage of the IMER system is integration into a liquid chromatography system, which facilitates application to high throughput screening. A wide variety of potential inhibitors can be screened by injecting the test compounds together with substrate and rapidly measuring inhibition kinetics.

A recent report describing immobilization of enzymes onto a microreactor surface using his-tag attachment was limited to commercially available or highly purified enzymes and resulted in very low enzyme loading [24]. The location of the his-tag on the silica-nucleating peptide rather than on the protein eliminates the need for recombinant modification of the protein of interest in order to use this method. The affinity binding of the silica peptide to the column resin provides a system that is durable under continuous use, with retention of activity at flow rates that are directly applicable to on-line chromatography appli-

cations. The IMERs were stable and reusable for analysis of over 250 injections, totaling more than 50 h of continuous use with no significant loss in activity. The automation of IMER analysis by integration into a LC system with an auto-sampler significantly reduces the time and work load required to analyze inhibitor potency, providing reliable and reproducible data within a short time period. The reusability of the IMERs also significantly reduces the amount of enzyme required for analysis.

The IMERs demonstrated in this study are presented as a model system applicable to a range of formats. The loading capacities achieved were sufficient for demonstrating the concept, but analysis of the silica-coated agarose indicated that we have only used a fraction of the surface of the agarose beads and further optimization of the approach will lead to dramatically higher loading capacities. Preliminary investigations indicate that a wide range of enzymes can be readily immobilized using the silica entrapment method [15,16] providing opportunities to create IMER systems of a variety of biomacromolecules with potentially interchangeable components. This bioencapsulation strategy therefore provides an economical and rapid route for synthesizing IMER systems with a number of advantages including; minimal preparation time, high immobilization efficiency and excellent stability. IMERs could be designed to contain an enzyme for biocatalysis or organic synthesis, for rapid screening in medical diagnostics and therapy or for developing IMER columns for affinity chromatography [1,2,25]. In addition, co-immobilization of multienzyme systems is also possible. Such systems can provide continuous cofactor recycling [26], or catalyze multistep processes. The method described is scalable dependent upon the application, for example, in a microfluidic format for biosensors or as large-scale IMERs for biosynthesis.

Acknowledgements

This work was funded by the US Air Force Office of Scientific Research. HRL was supported by a postdoctoral fellowship from the Oak Ridge Institute for Science and Education (US Department of Energy). The authors acknowledge D.M. Eby for useful discussions.

References

- [1] P.L. Urban, D.M. Goodall, N.C. Bruce, *Biotech. Adv.* 24 (2006) 42.
- [2] J. Krenkova, F. Foret, *Electrophoresis* 25 (2004) 3550.
- [3] A.M. Girelli, E.J. Mattei, *J. Chromatogr. B* 819 (2005) 3.
- [4] M. Bartolini, V. Cavrini, V. Andrisano, *J. Chromatogr. A* 1065 (2005) 135.
- [5] N. Markoglou, I.W. Wainer, *J. Chromatogr. A* 948 (2002) 249.
- [6] E. Calleri, C. Temporini, S. Furlanetto, F. Loidice, G. Fracchiolla, G. Mas-solini, *J. Pharma. Biomed. Anal.* 32 (2003) 715.
- [7] V. Sotolongo, D.V. Johnson, D. Wahnnon, I.W. Wainer, *Chirality* 11 (1999) 39.
- [8] E. Giacobini, *Pharmacol. Res.* 50 (2004) 433.
- [9] A. Nese Cokugras, *Turk. J. Biochem.* 28 (2003) 54.
- [10] M. Holden, C. Kelly, *Adv. Psychiatr. Treat.* 8 (2002) 89.
- [11] D.R. Liston, J.A. Nielsen, A. Villalobos, D. Chapin, S.B. Jones, S.T. Hubbard, I.A. Shalaby, A. Ramirez, D. Nason, W. Frost White, *Eur. J. Pharmacol.* 486 (2004) 9.
- [12] M. Bartolini, V. Cavrini, V. Andrisano, *J. Chromatogr. A* 1031 (2004) 27.

- [13] Y. Dong, L. Wang, D. Shangguan, R. Zhao, G. Liu, J. Chromatogr. B 788 (2003) 193.
- [14] V. Andrisano, M. Bartolini, R. Gotti, V. Cavrini, G. Felix, J. Chromatogr. B 753 (2001) 375.
- [15] H.R. Luckarift, J.C. Spain, R.R. Naik, M.O. Stone, Nat. Biotech. 22 (2004) 211.
- [16] R.R. Naik, M.M. Tomczak, H.R. Luckarift, J.C. Spain, M.O. Stone, Chem. Commun. 15 (2004) 1684.
- [17] N. Kroger, R. Duetzmann, M. Sumper, Science 286 (1999) 1129.
- [18] M.N. Tahir, P. Theato, W.E.G. Muller, H.C. Schroder, A. Janshoff, J. Zhang, J. Huth, W. Tremel, Chem. Commun. (2004) 2848.
- [19] G. Agarwal, R.R. Naik, M.O. Stone, J. Am. Chem. Soc. (2003) 7408.
- [20] R.M. Blong, E. Bedows, O. Lockridge, Biochem. J. 327 (1997) 747.
- [21] G.L. Ellman, K.D. Courtney, V. Andres Jr., M. Featherstone, Biochem. Pharmacol. 7 (1961) 88.
- [22] A. Nese Cokugras, D. Cengiz, E.F. Tezcan, J. Protein Chem. 22 (2003) 585.
- [23] K. Hirai, K. Kato, T. Nakayama, H. Hayako, Y. Ishihara, G. Goto, M. Miyamoto, J. Pharmacol. Exp. Ther. 280 (1997) 1261.
- [24] M. Miyazaki, J. Kaneno, S. Yamaori, T. Honda, M. Portia, P. Briones, M. Uehara, K. Arima, K. Kanno, K. Yamashita, Y. Yamaguchi, H. Nakamura, H. Yonezawa, M. Fujii, H. Maeda, Protein Pept. Lett. 12 (2005) 207.
- [25] C. Bertucci, M. Bartolini, R. Gotti, V. Andrisano, J. Chromatogr. B 797 (2003) 111.
- [26] L. Betancor, C. Berne, H. Luckarift, J. Spain. Chem. Commun, in press.

Silica-Immobilized Enzyme Reactors

Heather R. Luckarift

Microbiology and Applied Biochemistry, Air Force Research Laboratory, 139 Barnes

Drive, Suite # 2, Tyndall AFB, FL 32403

Tel: 850-283-6034, Fax: 850-283-6509, Email: hluckarift@gtcom.net

Abstract

Recent studies have demonstrated the applicability and versatility of immobilized enzyme reactors (IMERs) for chemical and biochemical synthesis and analysis. The majority of IMER systems rely on enzymes immobilized to packed matrices within flow-through devices. This review focuses primarily on the use of silica as a support for enzyme immobilization and specific applications of the resulting silica-based IMERs. A number of recently published examples (2000 onwards) are discussed as model systems. The effect of various silica matrices and immobilization techniques upon the enzymatic properties and stability of the biocatalysts is considered. In addition, reports in which the carrier matrix is biologically-derived silica are highlighted as an alternative and versatile technique that provides advantageous recovery, reuse and reproducibility.

Keywords: Immobilized enzymes, Enzyme reactors, IMER, Biocatalysis, Drug discovery, Biosilica.

Introduction and Scope

Enzymes are versatile catalysts that mediate a diversity of metabolic and pharmacological processes. Significant advancements in genetic engineering and protein purification methods have resulted in a wealth of commercially available enzymes which are readily isolated from growing culture. Although the diversity of available enzymes has expanded, issues related to their integration and stability during chemical production and analysis still exist. In their native state, enzymes are soluble in aqueous solutions and as such, are often susceptible to denaturation once separated from their physiological environment. By their nature, enzymes are not consumed during the reactions that they catalyze, but are difficult to reuse and recover as a soluble component from a reaction mixture. This is a primary concern for enzymes which are expensive to prepare and only available in very small amounts. Immobilization of enzymes is therefore often used in an attempt to stabilize and prolong the activity and reusability of the catalyst. Numerous methods for enzyme immobilization have been explored and offer a variety of advantages depending upon the functional and biochemical properties of the enzyme, as well as the final application.^[1-5]

The integration of immobilized enzymes into continuous flow-through systems provides an added advantage to many applications, as the immobilized biocatalyst is stabilized and can be recycled. The resulting immobilized enzyme reactors (IMERs) can also be integrated directly to further analytical methods such as liquid chromatography or mass spectrometry.^[6] In fact, one of the primary applications of many IMER systems is the digestion of proteins for automated sequence analysis by integration with mass spectrometry. The use of IMERs for protein digestion, however, has been reviewed extensively elsewhere and will not be covered herein.^[6-10]

A variety of matrices have been investigated over the years for enzyme immobilization or encapsulation, but for focus, the emphasis within this review is limited to IMERs that utilize

silica as a scaffold. The use of silica-based IMERs has received increasing attention since their appearance in the early 1970's and since then, the use and diversity of applications has grown steadily (Figure 1). The last decade has seen a vast increase in this subject area; presumably due to a parallel development of commercially available chromatographic support matrices that are amenable to IMER development. IMERs now find application in scientific fields as diverse as pharmacology, chemistry, materials science and chemical engineering (Figure 1, inset). With a few exceptions that are included for reference, the work reviewed herein will be restricted to studies reported since the year 2000.

Enzyme immobilization

Enzyme immobilization is generally achieved through covalent binding, ionic or hydrophobic interactions, or physical entrapment. Covalent attachment is one of the most commonly used methods for stabilizing enzyme activity as the enzyme molecule becomes fixed in a manner that limits the conformational changes that can lead to enzyme denaturation.^[11-13] There are intrinsic problems, however, in that covalent attachment can lead to limitations and variations in conformational mobility due to the orientation of the enzyme on the support during immobilization. Immobilization mediated by ionic or hydrophobic interactions, by comparison, is much less rigid but the adsorbed enzyme may leach from its support upon slight changes in the reaction environment (e.g. pH, ionic strength or temperature). Overall, however, immobilization using physical interactions provides an environment that greatly improves the catalytic properties of the biocatalyst, particularly in non-physiological environments.^[14-16] Sol-gel encapsulation has also been widely studied for enzyme immobilization, but the primary drawbacks are poor loading efficiency and enzyme leakage.^[17,18] The limitation has been resolved for some enzymes by

fabrication of support matrices with pore sizes that are specifically tailored to allow substrate flow but prevent enzyme leaching.^[19]

Biosilicification is the formation of nano-patterned siliceous structures in biological systems and is mediated by proteins such as silaffins and silicateins, found in marine diatoms and sponges, respectively.^[20-22] Using biological molecules as scaffold templates, biomimetic silicification reactions have been shown to provide a simple and effective alternative for enzyme encapsulation.^[23,24] The biologically-derived silica particles physically entrap enzymes within silica nanospheres directly as the silica particles form, providing an effective ‘cage’ that limits enzyme denaturation and retains high enzyme activity. The application of biologically-derived silica (biosilica) as a method for enzyme immobilization and preparation of IMERs using this method will be discussed in more detail below.

Immobilized enzyme reactors

The packaging of immobilized enzymes within a flow-through system creates an IMER that can be utilized as a microreactor (for chemical synthesis) or integrated into conventional chromatography systems (for analyte detection).^[25,26] IMERs can be exploited either before (pre-column) or after (post-column) a chromatographic separation or can serve as a chromatographic column in itself. Pre-column conversions would include pre-treatment of analytes such as chiral separation or screening for enzyme inhibition. Location of an IMER before a chromatography column via a switching valve allows the IMER to be separated from denaturing conditions downstream (i.e. organic solvents or pH environments required for subsequent chromatographic separations).^[27,28] Post-column IMERs are primarily designed to enhance detection of a product or analyte.^[29-32] As the diversity of support matrices escalates, the difficulty in defining optimum

characteristics relevant to all applications becomes more difficult. The choice of support is dependent upon the nature and mechanism of the enzyme, the properties of the support and the final application and conditions of use of the resulting IMER. A review of pre and post-column IMER formulations, support matrices and their relative advantages and disadvantages is provided by Girelli *et al.*^[33]

IMERs are useful for the analysis of biological systems only as long as the characteristics of the biomolecule are retained. The ability to study enzyme kinetic characteristics using IMER systems by calculation of Michaelis-Menten Kinetics has been demonstrated to confirm that the immobilized enzyme is not significantly hindered by its orientation and binding.^[8,34]

Lineweaver-Burk plots of reaction rate *vs.* substrate concentration are readily achievable in flow-through IMER systems from which the Michaelis constant (K_m) and the maximum enzyme velocity (V_{max}) can be calculated and mechanisms of inhibition (competitive, noncompetitive etc.) can be determined. Specific enzyme inhibition affinity can also be calculated in IMER systems by measuring the IC_{50} (the inhibitor concentration that results in a 50% reduction in product conversion under saturating substrate conditions) or an inhibition constant (K_i) calculated from the intersect of a Lineweaver-Burk plot.^[35,36]

Silica as an enzyme-immobilization support

Various support matrices have been developed and are now commercially available for enzyme immobilization. Of all available techniques, silica-based derivatized matrices, monolithic chromatography supports and artificial membrane stationary phases are the most commonly used. Using these techniques, the immobilization of enzymes to various stationary phases has now been demonstrated for a wide variety of applications using a range of enzymes, membrane proteins and receptor proteins.^[19,37-41] Silica-based stationary phases of the type used

in liquid chromatography separation columns are commonly used as support matrices for enzyme immobilization to produce IMERs. The primary advantage of the readily available commercial supports is their reproducibility. The silica support, however, must be functionalized to allow for covalent attachment of enzymes. An additional limitation of these columns is that the void volume of packed silica columns may create diffusion and flow limitations. The recent introduction of monolithic polymers as a stationary phase provides an alternative to overcome those limitations.^[10,19,42-45] Monolithic separation media is essentially one single core which does not contain voids between the packing materials. This results in improved mass transfer, as all of the sample and mobile phase must flow through the entire stationary phase. Silica-based monoliths provide an inherent advantage of having equally sized mesoporous structures and large surface areas. The high-throughput of monoliths allow for high flow rates with low back pressures; which enables further coupling to analytical detection systems. Selection of silica monoliths, however, is often a trade off between macroporous structures that permit high flow rates and low back pressures but with significant leaching of protein (due to large pore sizes >50 nm), compared to mesoporous structures with pore diameters more suited to protein retention (3-5 nm) but a concurrent increase in high back pressures even at low flow rates. Besanger *et al.*, for example, reported a mesoporous silica monolith that generates a back pressure of >3500 psi at flow rates of less than 1 $\mu\text{l}/\text{min}$, which excludes further integration with pressure-driven liquid chromatography.^[19] The authors attempted to address the limitation using sol-gel synthesis; using glyceroxysilanes to create mesoporous materials that combines high protein retention of α -glutamyl transpeptidase (loading efficiency >80%) with enhanced flow characteristics. One limitation of this approach was long preparation times of several days, due to multiple aging steps. Variations in fabrication pH and polyethylene glycol concentrations were optimized to minimize shrinkage of the monoliths during preparation and to prevent flow-channeling as a

result of the column pulling away from the capillary surface. Flow rates were low in the final system, with optimal rates less than 1 $\mu\text{l}/\text{min}$. The apparent catalytic activity of the immobilized enzyme, however, was comparable to soluble enzyme for the conversion of L-glutamic acid *p*-nitroanilide to *p*-nitroaniline.^[19] The sol-gel method can be used to produce an aggregate of spherical particles that occurs due to phase separation during sol-gel transition, resulting in a coarse porous matrix with good flow characteristics when packed into a flow-through column. The particles formed using these techniques are of the order of several microns in diameter with interparticle gaps of the same size order that allow the efficient flow of substrate through the column. Sol-gel entrapment of protease, for example, has been demonstrated in an IMER for transesterification reactions.^[42]

An alternative area of IMER development is the use of immobilized artificial membrane (IAM) stationary phases that consist of a monolayer of phospholipid covalently immobilized on an inert silica support, in which enzymes are entrapped in an environment that resembles a biological membrane. IAM stationary phases are particularly useful for studying trans-membrane receptors and drug transport across membranes and for non-covalent immobilization of membrane-associated proteins. A wealth of reports on the use of IAM stationary phases to study drug interactions, particularly across the blood-brain barrier, are documented but not described further herein due to the depth of the subject area.^[46-55]

Biosilica for IMER preparation

Biomimetic silicification reactions provide a rapid and simple alternative method for enzyme immobilization that result in the physical entrapment of enzymes within silica nanospheres as they are formed (Figure 2). The reaction mixture consists of a silica-precipitating

peptide and a silicate precursor (tetramethylorthosilicate) that rapidly (<2 minutes) form silica nanoparticles in aqueous buffered solution. A matrix of spherical silica particles (typically ~500nm in diameter) is formed and provides effective encapsulation of a range of enzymes including esterases, hydrolases, peroxidases and reductases.^[23,35,56-59] The silica particles can be further integrated into flow-through systems by either: i) preparing the silica particles in batch mode and then packing them into a column or by ii) preparing the silica particles within a commercially available pre-packed column, *in situ*, by anchoring them to the column matrix. Both alternatives provide viable methods for fabricating IMERs and examples of each are included within this review. To achieve biosilica formation (and enzyme encapsulation) *in situ*, the silica-precipitating peptide is functionalized with a histidine-rich tail (his-tag), allowing for its retention within a commercial pre-packed column by metal affinity binding between the ‘his-tag’ and a metal coating (cobalt) upon the agarose packing material. The peptide forms silica *in situ* and simultaneously encapsulates enzymes directly at the surface of the agarose and hence within the packed column (Figure 2). To our knowledge, the use of biologically-derived silica matrices (biosilica) as a support matrix for development of IMERs is unique and will be described in more detail throughout this review to highlight the validity of the approach.

IMERs for drug discovery

Many basic biological signaling responses rely upon specific interactions between biomolecules and a respective, and often highly specific, ligand. As such, pharmaceutical research is often directed towards the elucidation of these mechanisms and their regulation or modulation by drug interactions.^[60] Although enzyme activation has a therapeutic role, the mode of action of many commercially available drugs is enzyme inhibition. Pharmacological inhibition of cyclooxygenase, for example, can provide relief from the symptoms of inflammation and pain

and is the mode of action of drugs such as aspirin and ibuprofen.^[61] Serotonin reuptake inhibitors and monoamine oxidase inhibitors can function as antidepressants, due to their ability to prevent the breakdown of neurotransmitters.^[62-64] Screening of therapeutic enzyme inhibitors is often directed towards achieving high specificity and increased potency in order to reduce unspecific interactions (i.e. side effects) and lower toxicity. Examples of IMERs with application to drug discovery and metabolic screening are highlighted in the following sections.

Analysis of cholinesterase inhibition

The pharmacology of cholinesterase enzymes is an area of increasing interest as inhibitors of cholinesterases have therapeutic value for treatment of neurodegenerative diseases such as dementia and Down's syndrome.^[65-67] In addition, cholinesterase inhibitors are the only currently FDA approved treatment for Alzheimer's disease.^[68-70] Cholinesterases such as acetylcholinesterase (AChE) and butyrylcholinesterase (BuChE) catalyze the hydrolysis of acetylcholine; a neurotransmitter in the central nervous system. Cholinesterase inhibitors bind to the enzyme and prevent the enzymatic breakdown of acetylcholine. Acetylcholine accumulates as a result, overwhelming the central nervous system and leading to ataxia (failure of muscle coordination and movements), seizures and ultimately death. In addition, the toxicity of cholinesterase inhibitors, particularly irreversible inhibitors, has led to their use as nerve agents in warfare.^[71,72]

A range of IMER preparation methods have been investigated for immobilization of cholinesterase enzymes in order to screen for enzyme inhibitors (Table 1). A comparison of silica-packed columns and monolithic columns for IMER preparation was recently reported by Bartolini *et al.*^[73] Two modified monoliths (with epoxy or ethylenediamine reactive groups)

were prepared and compared to a silica-packed column for the immobilization of AChE and kinetic characteristics of the columns were determined at a range of flow rates. The monolithic columns demonstrated specific advantages; good stability, enzyme loading is performed *in situ* and conditioning times are short. The loading capacity of the columns were low (~3%), however, compared to silica-packed columns (~29%). The silica-packed column also required a shorter preparation time and at a fraction of the cost. AChE immobilization was also achieved by *in situ* derivatization of epoxide silica that resulted in covalent linkages between the enzyme and the epoxide groups and provided stability to the immobilized enzyme. The loading capacity of the column was high (Table 1) but analysis times were reduced due to a requirement for low flow rates.^[74] By comparison, immobilization of BuChE in biosilica nanoparticles was complete in less than 1 hour with an immobilization efficiency of 100% and a high loading capacity for enzyme (Table 1).^[35] Biosilica-IMERs containing immobilized BuChE were used for screening the drug potency of cholinesterase inhibitors (Figure 3) and were stable for over 2 days of continuous use at flow rates of up to 3 ml/min.^[35]

In an alternative system, AChE was immobilized to silica gel by covalent binding and used to monitor the hydrolysis of acetylcholine and concurrent inhibition by carbamate pesticides (Table 1). The system was reusable, but only a few times and as such was designed as a disposable sensor for pesticides. AChE hydrolyses acetylcholine to release choline and acetic acid. The acid undergoes spontaneous dissociation and releases hydrogen ions which can be detected potentiometrically (change in pH due to increase of hydrogen ions) or conductimetrically (change in conductivity due to increase in ion concentration). Both detection systems in conjunction with the AChE-IMER provided detection limits of less than 1 ppm and within range for detection of carbamates at environmentally relevant levels.^[75]

The interest in cholinesterase enzymes and their reaction metabolites is exemplified by the availability of a commercial polymeric bioreactor available from Bioanalytical Systems Inc. (BASi, West Lafayette, IN) for analysis of acetylcholine and choline. Dong *et al.*, reported a modification to the commercially available product, by the addition of horseradish peroxidase in a post-column IMER that improved sensitivity of detection by 200-fold. Horseradish peroxidase was immobilized to amine-functionalized silica beads and packed into a column and used to monitor the formation of hydrogen peroxide as a measure of acetylcholine concentration in mammalian lysates. The IMER column was stable for up to 8 months with no loss in activity, providing that a biocide was added to prevent the growth of contaminating biofilms.^[76]

Drug metabolism by glucuronidation

Glucuronidation plays a significant role in the pharmacology of many drugs and as such, the determination of non-conjugated and conjugated drug metabolites is a useful tool. The reaction primarily converts toxins and certain drugs to a more water soluble metabolite that can be readily excreted from the body by the kidneys. Uridine diphospho-glucuronosyltransferase (UDPGT), for example, is involved in metabolic detoxification in vertebrates through glucuronidation reactions that facilitate the transport of lipophilic compounds to excretory organs. Non-solubilized UDPGT from rat liver microsomes was covalently immobilized to a functionalized silica support by Schiff base chemistry and a number of reaction variables (i.e. sonication treatments and buffer selection) were investigated during immobilization to determine an optimum configuration.^[77] A high loading capacity for protein (~40 mg protein g⁻¹ silica) was a trade off with a reduction in specific activity that was attributed to destruction of lipids associated with the enzyme during preparation. IMER preparation times of up to 3 days may also contribute to a loss in specific activity. The resulting UDPGT-IMERs, however, was reusable

over a period of 45 days with up to 75% activity retained, depending upon the IMER configuration. The IMER was coupled (pre-column) to a C₁₈ and anion-exchange column in order to separate substrate from product downstream and used for the on-line glucuronidation of 4-methylumbelliferone and acetaminophen.^[77] Immobilization of rat liver microsomes containing UDPGT using silica sol-gel technology to create an IMER for capillary electrochromatography has also been reported and used for the on-line analysis of the metabolism of *p*-nitrophenol and testosterone.^[78] Similarly, β -glucuronidase was immobilized to a monolithic silica based column and used to evaluate the conversion of the cough suppressant dextromethorphan to two metabolites; dextrorphan and 3-hydroxymorphinan. The products are formed by cytochrome P-450 enzymes and undergo glucuronidation reactions *in vivo*. As such, the presence of these metabolites in urine is used to assess the metabolic activity of specific cytochrome P-450 enzymes. The resulting silica-based monolithic IMER of β -glucuronidase provides on-line hydrolysis of the conjugates for rapid analysis of metabolite concentrations in human urine samples.^[79]

Determination of catecholamines

Catecholamines such as norepinephrine, epinephrine and dopamine are an important group of chemical compounds that act as neurotransmitters in the central nervous system (Figure 4).^[80] The work of Markoglou and Wainer has demonstrated the application of IMER systems for the analysis of catecholamines in order to understand the physiological interaction with various adrenergic receptor proteins.^[81-85] Dopamine β -hydroxylase (DBH) and phenylethanolamine N-methyltransferase (PNMT) are essential enzymes involved in the metabolism of catecholamines *in vivo*. These enzymes are essential to nervous signaling and

implicated in neurological disorders such as Schizophrenia and Parkinson's disease.^[86] Drug discovery for targets that can alter the function of these enzymes are therefore a key focus. The immobilization of PNMT and DBH to glutaraldehyde-functionalized silica gel was optimized in batch systems (~ 2.5 mg protein g^{-1} support) and packed into columns.^[81-83] Immobilization of PNMT had some deleterious effects upon enzyme activity but the system was stable at elevated temperatures (up to 60°C) and proved effective at screening the binding characteristics of known inhibitors. An IMER based on immobilized PNMT, for example, was used to demonstrate the *N*-methylation of normetanephrine (Figure 4, $\text{R} = \text{OCH}_3$).^[81] In addition, the PNMT-IMER was coupled with a second DBH-IMER for two-step synthesis of L-epinephrine from dopamine, with product recoveries of $\sim 95\%$ (Figure 4). The technology was extended to incorporate two different forms of DBH (soluble and membrane-bound) by utilizing two differing methods of IMER preparation; an immobilized artificial membrane for the membrane-bound protein and glutaraldehyde-functionalized silica for the soluble protein.^[85]

Screening for prodrug activation

Berne *et al.* describe an IMER containing a bacterial nitrobenzene nitroreductase enzyme that catalyzes the conversion of a nitro group to hydroxylamine resulting in a large electronic change which can be exploited for a variety of biotechnological applications; primarily the activation of prodrugs and proantibiotics for cancer treatments or antibiotic therapy, respectively.^[87] Nitrobenzene nitroreductase was immobilized ($>80\%$ immobilization efficiency) in a silica matrix formed by polyethyleneimine (PEI) that catalyzes the formation of a matrix of interconnected silica particles of ~ 1 μm diameter. PEI has been extensively used for stabilizing enzymes by generating hydrophilic microenvironments that protect the enzyme from

denaturation and the use of PEI as a scaffold for silica formation therefore provides a synergism between the stabilizing effect of PEI and the encapsulation stability of silica nanoparticles. The resulting silica-encapsulated nitroreductase was contained in a stainless steel column to create an IMER for conversion of nitrobenzene, a prodrug (CB1954), and a proantibiotic (nitrofurazone). The IMER showed excellent activity and stability for the screening of prodrugs in non-aqueous solvents such as methanol and acetonitrile. IMER functioning in a non-aqueous system is a primary advantage, due to the relative insolubility of many prodrugs in aqueous solutions. Flow rates within the system were low (1-5 $\mu\text{L}/\text{min}$) but no enzyme leaching or back-pressure problems were reported and stoichiometric conversion of all test substrates was observed, with a concurrent decrease in conversion efficiency with increased flow rates as expected. The system was operated for more than 3 days at room temperature with a flow rate of 5 $\mu\text{L}/\text{min}$ for continuous conversion of nitrobenzene with >90% conversion efficiency (Figure 5).

Screening inhibitors of glyceraldehyde-3-phosphate dehydrogenase

Glyceraldehyde-3-phosphate dehydrogenase (GAPDH) is a target for developing drugs for the treatment of parasitic diseases such as sleeping sickness, due to its role in controlling ATP production in pathogenic parasites.^[88] GAPDH, however, has low stability and loses up to half of its activity within a day. GAPDH isolated from rabbit was covalently immobilized to a wide-pore silica support by glutaraldehyde activation and Schiff-base chemistry.^[89] The loading capacity was 150 μg of enzyme to 100 mg stationary phase with ~95% loading efficiency, but less than 3% of the initial enzyme activity was retained. The low retention of activity was attributed to the instability of the enzyme in aqueous solutions and the significant time delay (6 hours at optimum) for binding to occur. The resulting particles, however, were packed into a

glass column to make a GAPDH-IMER which was stable for 30 days; a significant improvement upon the native enzyme. The IMER was utilized for kinetic measurements of enzyme activities and enzyme inhibition was evaluated with the toxin, agaric acid, to demonstrate that the IMER could be used for screening GAPDH inhibitors.

IMERs for chemical synthesis

Enzymes are useful for synthesis of fine chemicals, production of agrochemicals and pharmaceuticals.^[90-96] In order to employ enzymes in bioprocesses a number of limitations such as enzyme stability, difficulty in separating the product from the catalyst and the inherent difficulty of re-using the catalyst must be overcome. These disadvantages can be alleviated by using IMER systems that provide enzymes immobilized into, or onto, a solid support. The resulting immobilized catalysts are heterogeneous and can be readily separated and recovered; increasing the commercial feasibility of enzyme-based reactions. Separation of products downstream of the process can raise production costs considerably and in this area, the development of continuous flow reaction systems has seen a critical input to improving technology. IMERs have now been developed by a number of groups and demonstrated as a viable alternative to conventional synthesis. The immobilization of subtilisin Carlsberg to fumed silica, for example, was used within a continuous packed-bed reactor for transesterification reactions in hexane.^[97] In the following section, examples of catalysis using IMER systems are chosen to exemplify the application to chemical synthesis.

Preparation of penicillin analogues

Penicillin G acylase (PGA) enzymes catalyze the cleavage of the acyl-chain of penicillins to produce 6-aminopenicillanic acid; providing a commodity product at a scale of 20,000 tons per annum. The enzyme has very broad substrate specificity with utility to the production of semi-synthetic penicillins and β -lactam antibiotics.^[98,99] The enzyme can resolve racemic mixtures of chiral compounds with excellent stereochemistry for a range of substrates. The catalytic versatility of the enzyme has been extended by immobilizing PGA onto chromatography supports and using the enantiomeric selectivity of the enzyme to resolve racemic mixtures.^[100] Immobilization onto supports with various pore sizes and functionalities were recently compared for the development of a PGA-IMER using two preparation methods: i) immobilizing the enzyme and then packing the immobilized catalyst into a column (batch) versus ii) immobilizing the enzyme within a pre-packed column (*in-situ*). Despite the high loading capacity observed with batch preparation (87 mg enzyme g⁻¹ support), a loss of activity was observed upon packing and *in-situ* techniques provided optimal performance in comparison. Immobilization *via* the amino groups of the enzyme showed retention of activity, whereas enzyme activity was abolished when the enzyme was attached via its carboxyl groups.^[101] Microparticulate epoxy-silica supports showed high enzyme loading but the efficiency was greatly superseded by single phase porous silica monoliths where ~250 mg of protein could be loaded to a single column. Using the optimized system, PGA-IMERs were integrated with an liquid chromatography system to determine the PGA-catalyzed hydrolysis of esters. In addition, the resulting column acted as a chiral stationary phase for screening of substrate analogues and non-steroidal anti-inflammatory drugs.^[100] Further downstream chiral separation led to precise determination of enantioselectivity in the synthesis of 2-aryloxyalkanoic acid methyl esters and a variety of substrate analogues.^[102]

Lipase-catalyzed conversions

Lipases are one of the most versatile and hence widely exploited groups of enzymes in biocatalysis.^[103-108] In the previous section we noted that PGA can be utilised to synthesize 2-aryloxyalkanoic acid methyl esters. A similar report utilizes a lipase from *Candida rugosa* for racemic separation of 2-aryloxyalkanoic acids, analogous methyl esters and non-steroidal anti-inflammatory drugs.^[109] Lipase based IMERs were produced by i) physical adsorption of lipase to a silica (RP18) stationary phase and by ii) covalent immobilization of lipase *via* activating agents on aminopropyl-functionalized silica. Immobilization yield by physical adsorption was high but unstable due to weak hydrophobic interactions which allowed the enzyme to leach from the IMER over time; particularly in the presence of solvent. Covalent immobilization eliminated the leaching problems, allowing for chromatographic separation and collection of products for off-line enantioselective analysis.

Lipase from *Candida rugosa* was immobilized to silica gel with relatively low loading capacity (1.9 mg protein g⁻¹ support) but good recovery of activity (~37%) and used as a packed-bed IMER to catalyze the racemic resolution of (S)-ketoprofen from its constituent enantiomers. The optically pure (S)-isomer was obtained with >99% ee at a conversion rate of ~30% and a productivity rate of 1.5 mg g⁻¹ biocatalyst h⁻¹. (S)-ketoprofen is a non-steroidal anti-inflammatory drug used to reduce inflammation and relieve pain; the (R)-isomer has no activity.^[110,111] By comparison, 2-phenoxypropionic acids and their esters are used as herbicides; in this case, the (R)-isomers are biologically active. Lipase from *Candida rugosa* was again immobilized to silica beads and used as a packed-bed reactor for the continuous racemic resolution of 2-(4-chlorophenoxy) propionic acid (46% ee).^[112]

Conversion of nitroarenes

One advantage of immobilizing enzymes is the ability to utilize a biocatalyst in non-physiological environmental conditions. The combination of a metal and a biocatalyst, for example, would ordinarily not be feasible due to the disparate reaction conditions required for optimal activity. An IMER containing biosilica-immobilized hydroxylaminobenzene mutase (HABM) was developed using a simple fluidized-bed design and integrated with a packed-bed reactor containing zinc for conversion of nitrobenzene to *o*-aminophenol with ~90% conversion efficiency during continuous operation over a period of 24 hours. The HABM-IMER system also proved amenable to the formation of a novel homologue of the antibiotic, chloramphenicol (Figure 6).^[56] The system can operate at flow rates of the order of milliliters per minute (for large scale catalysis) but can be reduced in scale to microfluidic formats with flow rates of only microlitres per hour (more suited to screening). A microfluidic HABM-IMER was used in conjunction with an additional microfluidic IMER connected in series that contained biosilica-immobilized soybean peroxidase for the synthesis of 2-aminophenoxazin-3-one; an intermediate in the synthesis of actinomycin antibiotics (Figure 6).^[58]

IMERs as biosensors

The majority of drug interactions rely on reversible inhibitors of enzyme activity. Irreversible enzyme inhibitors, however, can often cause drastic effects upon metabolic functions and are the mechanism of action of many poisons and potent neurotoxins. Ricin, for example, is a potent protein toxin found in castor oil beans. Ricin is an irreversible inhibitor that functions as a glycosidase and inactivates ribosomes so specifically that fewer than ten castor oil beans is sufficient for severe cytotoxicity and potential fatality.^[113,114] As such, ricin and other

neurotoxins also find application as terrorist threat agents. One area of research applicable to IMERs has been the development of biosensor systems to screen irreversible inhibitors despite limitations that are inherent to this type of system; such as enzyme reactivation. Although a close correlation between biosensors and IMERs may seem apparent, according to the strict IUPAC definition of a biosensor, an IMER by itself is not a biosensor. A biosensor is defined as ‘a device that uses specific biochemical reactions mediated by isolated enzymes, immunosystems, tissues, organelles or whole cells to detect chemical compounds, usually by electrical, thermal or optical signals’.^[115] The integration of an IMER with a detection system may therefore lead to the development of a biosensor but IMERs are essentially bioreactors rather than biosensors as the biological component is distinct from the physical transducer.^[114] The distinction, however, is not always evident and examples of biosensors/IMER combinations can be found within the literature. A number of examples of such are included in a review by Fishman et al.^[116] The IMER containing biosilica-immobilized BuChE described earlier for screening the drug potency of cholinesterase inhibitors, for example, was also integrated with an aerosol collection system to develop a biosensor for the detection of organophosphate nerve agents in air.^[59] The system was tested with model organophosphates including paraoxon, demeton-S and malathion. The substrates are all potent inhibitors of BuChE and as such, the BuChE-IMER required reactivation with pyridine-2-aldoxime following every test sample in order to maintain enzymatic activity over repeated use. Despite the inherent limitations, the system proved suitable for detection of organophosphates in air at practical detection limits.^[59]

Conclusions and Future considerations

The application of silica-based IMERs clearly offers practical advantages, providing enzyme reactions that can undergo repeated interrogation or continuous use. The scalability of

the process is an obvious advantage, allowing for large-scale systems applicable to continuous large-scale synthesis, and also to small-scale microfluidic systems that are more suited to preliminary screening. In addition, the IMER process has been shown to be adaptable to a mix and match design in which individual IMER units can be rearranged to change the series of catalytic events, and hence, the product. Coimmobilization of enzymes either in a combined system, or individually as single sequential units will allow for development of complex catalytic sequences. Biologically-derived silica (biosilica) provides a feasible and versatile alternative method for forming a silica matrix that acts as an excellent scaffold for enzyme encapsulation. The biosilica reaction is rapid and simple with high loading capacities and high mechanical stability that has been used in applications such as screening enzyme-drug interactions and for the synthesis of novel chemicals and antibiotic intermediates. The application of IMER technology will doubtless continue, as enzyme immobilization techniques and support matrices continue to be developed.

Acknowledgements

Portions of the research presented herein represent recent research within the Microbiology and Applied Biochemistry program at the Air Force Research Laboratory. This work has been supported by several funding sources including Air Force Office of Scientific Research, Joint Services Technology Office and Air Force Research Laboratory, Material Science Directorate. HRL is an employee of Universal Technology Corporation, 1270 N. Fairfield Road, Dayton, OH.

Table 1. Comparison of IMER preparation methods utilizing cholinesterase enzymes

*The monolith columns included in this table are not silica based but are included for reference and comparison.

†Stability is cited as activity remaining following the time period given

^aPotentiometric detection, ^bConductimetric detection, (-) not applicable or not reported, (ID) internal diameter, acetylcholinesterase (AChE), butyrylcholinesterase (BuChE)

	Monolith disks*		Packed Silica	Biosilica	Epoxide-Silica	Silica-gel
Enzyme	Human AChE	Human AChE	Human AChE	Equine BuChE	Human AChE	Electric-eel AChE
Column matrix	EDA-CIM disk	Epoxy-CIM disk	Silica gel, (40 µm, 300Å)	Biosilica coated agarose beads	Epoxide silica gel (5 µm, 200Å)	Silica gel (40-63 µm, 60Å)
Dimensions	3x12 mm	3x12 mm	3x35 mm	25x20 mm	50x4.6 mm (ID)	3x0.31 cm
Immobilization	<i>In situ</i>	<i>In situ</i>	Batch	<i>In situ</i>	<i>In situ</i>	Batch
Immobilization efficiency	3%	3%	29%	~100%	25%	-
Stability†	<30% (2 mos.)	~80% (2 mos.)	~80% (2 mos.)	100% (15 h)	70% (4 mos.)	Reused 2 – 7 times
Flow Rate (ml/min)	0.2 - 1.4	0.2 - 1.4	0.2 - 1.4	0.5 - 3.0	0.1	0.25 - 1.0
Analysis time (min)	5	5	5	10	20	35–45 ^a 31–37 ^b
Bed volume (mL)	0.34	0.34	0.06	5.0	-	-
Immobilized enzyme (U)	0.18±0.01	0.22±0.01	4.35±0.01	~160	63	150 ^a , 200 ^b
Reference	[73]	[[73]	[73]	[35]	[74]	[75]

Figure 1. Use of silica-immobilized enzyme reactors

Source: Scopus keyword search for *silica immobilized enzyme reactors* in title, abstract and keywords; categorized by year (bar chart) and subject area (inset pie chart).

Figure 2. Preparation of IMERs using biologically-synthesized silica

A mixture of a silica-precipitating peptide and hydrolyzed tetramethylorthosilicate rapidly forms silica in aqueous solution (a), producing a network of silica nanospheres of ~500 nm (b). The particles can be attached to large agarose beads (c) by metal affinity binding; by adding six histidine residues to the peptide (d). *Figure adapted from Journal of Chromatography B, 2006, 843(2), 310-316.*^[35]

Figure 3. Screening of a cholinesterase inhibitor on a BuChE-IMER

Chromatograms showing subsequent injections to a BuChE-IMER of butyrylthiocholine at saturating substrate concentration (a), with 1mM tacrine inhibitor (b) and again with butyrylthiocholine at saturating substrate concentration (c)

Figure 4. Pathway for dopamine metabolism

Dopamine β -hydroxylase (DBH), Phenylethanolamine *N*-methyltransferase (PNMT)

Figure 5. Silica-immobilized nitroreductase IMER

Schematic of the IMER containing silica-encapsulated nitroreductase inside a stainless steel microreactor (specifications shown) and operational stability of the resulting column for the conversion of nitrobenzene (100 μ M) at 5 μ l/min. *Figures reprinted with permission from Biomacromolecules, 2006, 7, 2631-2636.*^[87] Copyright 2006 American Chemical Society.

Figure 6. Enzyme catalyzed conversion of nitroarenes

Hydroxylaminobenzene mutase (HABM), Soybean peroxidase (SBPO)

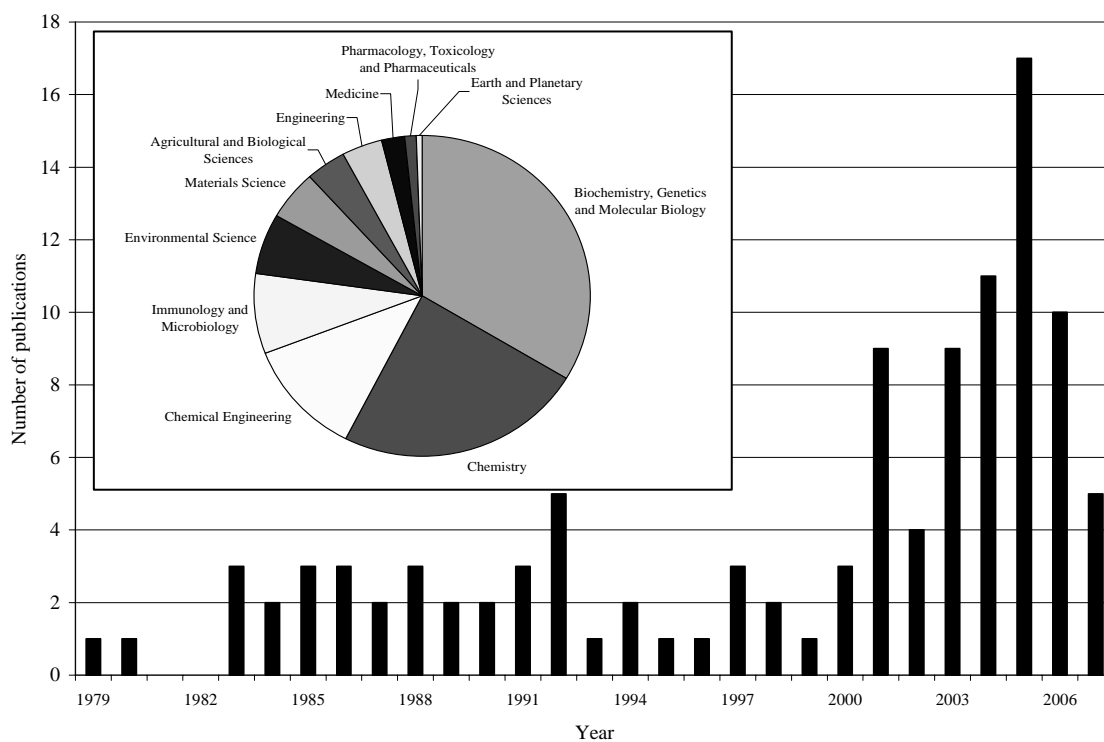
Figure 1.

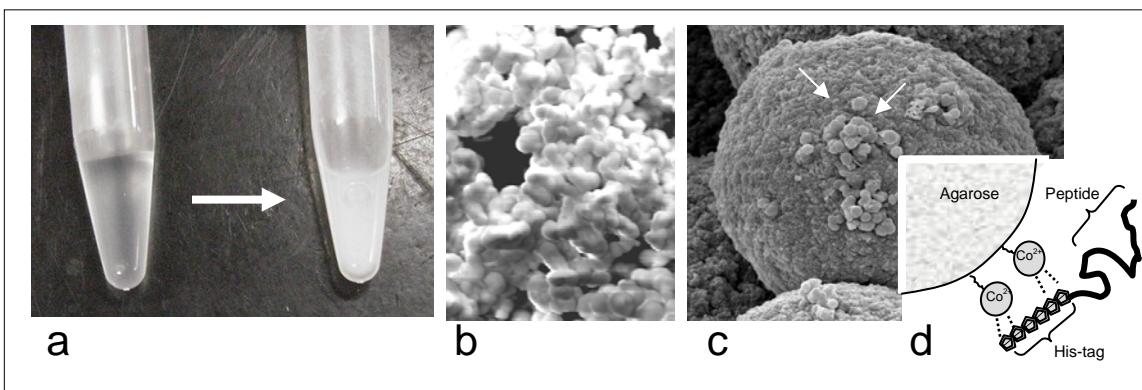
Figure 2.

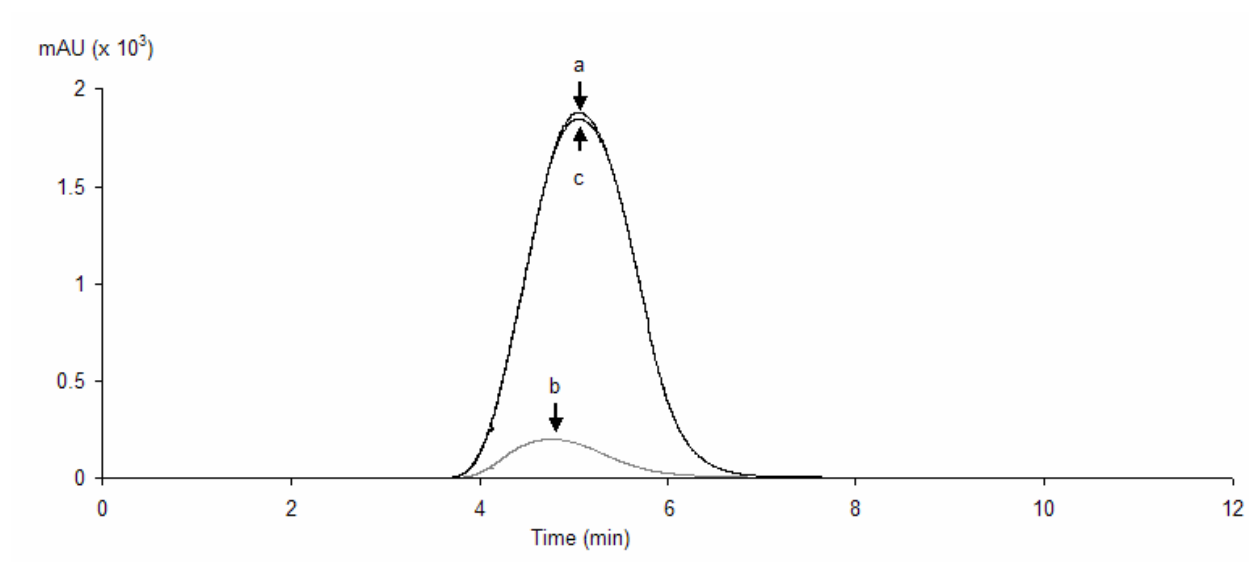
Figure 3.

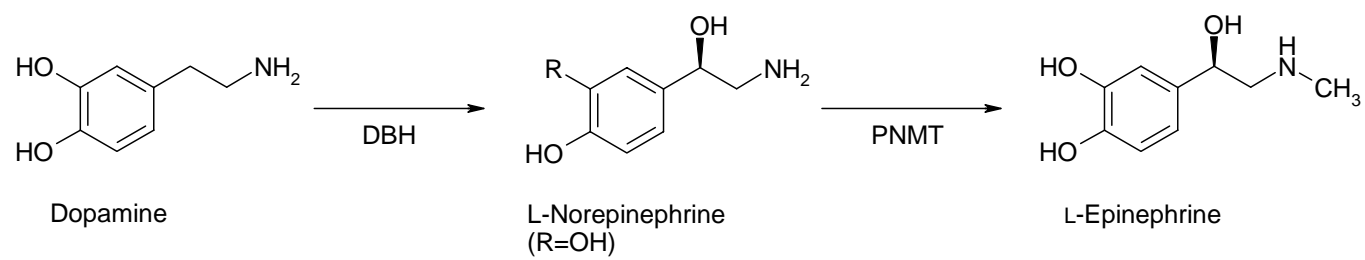
Figure 4.

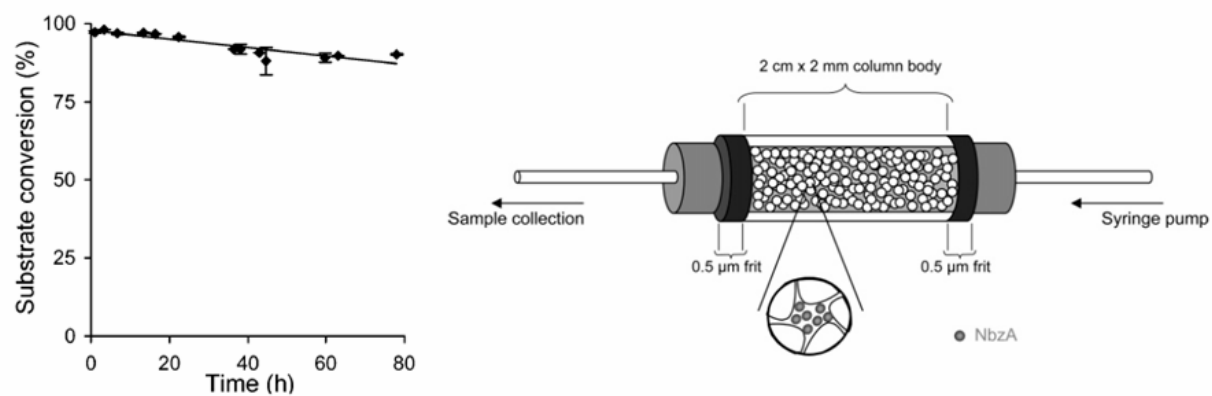
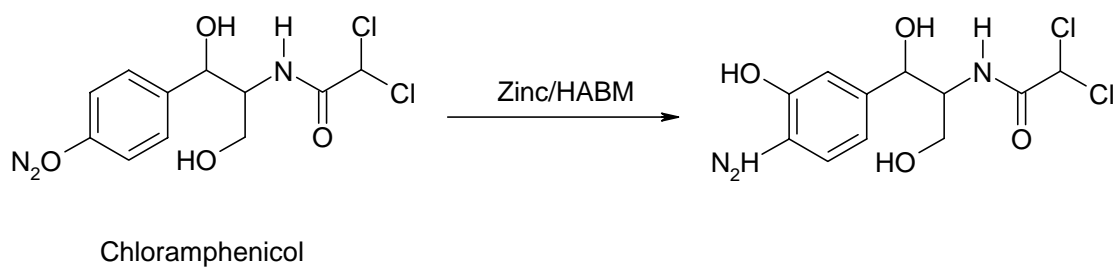
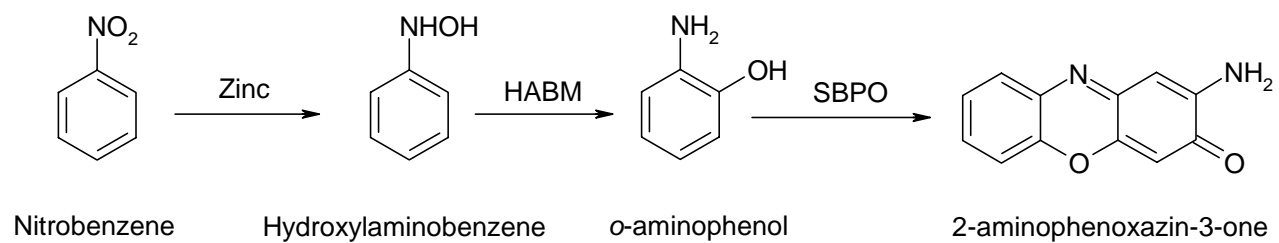
Figure 5.

Figure 6.

References

1. Liang, J. F.; Li, Y. T.; Yang, V. C. Biomedical application of immobilized enzymes. *J. Pharm. Sci.* 2000, 89, 979-990.
2. Cao, L. Immobilised enzymes: science or art? *Curr. Opin. Chem. Biol.* 2005, 9, 217-226.
3. Katchalski-Katzir, E. Immobilized enzymes-learning from past successes and failures. *Trends Biotechnol.* 1993, 11, 471-478.
4. Bornscheuer, U. T. Immobilizing enzymes: how to create more suitable biocatalysts. *Angew. Chem. Int. Ed.* 2003, 42, 3336-3337.
5. Sheldon, R. Enzyme Immobilization: The Quest for Optimum Performance. *Adv. Synth. Catal.* 2007, 349, 1289-1307.
6. Krenkova, J.; Bilkova, Z.; Foret, F. Characterization of a monolithic immobilized trypsin microreactor with on-line coupling to ESI-MS. *J. Sep. Sci.* 2005, 28, 1675-1684.
7. Temporini, C.; Perani, E.; Mancini, F.; Bartolini, M.; Calleri, E.; Lubda, D.; Felix, G.; Andrisano, V.; Massolini, G. Optimization of a trypsin-bioreactor coupled with high-performance liquid chromatography-electrospray ionization tandem mass spectrometry for quality control of biotechnological drugs. *J. Chromatogr. A* 2006, 1120, 121-131.
8. Urban, P. L.; Goodall, D. M.; Bruce, N. C. Enzymatic microreactors in chemical analysis and kinetic studies. *Biotechnol. Adv.* 2006, 24, 42-57.
9. Massolini, G.; Calleri, E. Immobilized trypsin systems coupled on-line to separation methods: recent developments and analytical applications. *J. Sep. Sci.* 2005, 28, 7-21.
10. Kato, M.; Inuzuka, K.; Sakai-Kato, K.; Toyo'oka, T. Monolithic bioreactor immobilizing trypsin for high-throughput analysis. *Anal. Chem.* 2005, 77, 1813-1818.
11. Mateo, C.; Palomo, J. M.; Fernandez-Lorente, G.; Guisan, J. M.; Fernandez-Lafuente, R. Improvement of enzyme activity, stability and selectivity via immobilization techniques. *Enzyme Microbial Technol.* 2007, 40, 1451-1463.
12. Mozahev, V. V.; Melik-Nubarov, N. S.; Sergeeva, M. V.; Sikrnis, V.; Martinek, K. Strategy for stabilizing enzymes. I. Increasing stability of enzymes via their multipoint interaction with a support. *Biocatalysis* 1990, 3, 179-187.
13. Klibanov, A. M. Stabilization of enzymes against thermal inactivation. *Adv. App. Micro.* 1983, 29, 1-28.
14. Palomo, J. M.; Fernandez-Lorente, G.; Mateo, C.; Ortiz, C.; Fernandez-Lafuente, R.; Guisan, J. M. Modulation of the enantioselectivity of lipases via controlled immobilization and medium engineering: hydrolytic resolution of mandelic acid esters. *Enzyme Microbial Technol.* 2002, 31, 775-783.
15. Fernandez-Lafuente, R.; Armisen, P.; Sabuquillo, P.; Fernandez-Lorente, G.; M. Guisan, J. Immobilization of lipases by selective adsorption on hydrophobic supports. *Chem. Phys. Lipids* 1998, 93, 185-197.
16. Petkar, M.; Lali, A.; Caimi, P.; Daminati, M. Immobilization of lipases for non-aqueous synthesis. *J. Mol. Catal. B: Enzymatic* 2006, 39, 83-90.
17. Avnir, D.; Lev, O.; Livage, J. Recent bio-applications of sol-gel materials. *J. Mat. Chem.* 2006, 16, 1013-1030.
18. Gill, I.; Ballesteros, A. Bioencapsulation within synthetic polymers (Part 1): sol-gel encapsulated biologicals. *Trends Biotechnol.* 2000, 18, 282-296.

19. Besanger, T. R.; Hodgson, R. J.; Green, J. R. A.; Brennan, J. D. Immobilized enzyme reactor chromatography: Optimization of protein retention and enzyme activity in monolithic silica stationary phases. *Anal. Chimica Acta* 2006, 564, 106-115.
20. Shimizu, K.; Cha, J.; Stucky, G. D.; Morse, D. E. Silicatein alpha: cathepsin L-like protein in sponge biosilica. *Proc. Nat. Acad. Sci.* 1998, 95, 6234-6238.
21. Cha, J. N.; Shimizu, K.; Zhou, Y.; Christiansen, S. C.; Chmelka, B. F.; Stucky, G. D.; Morse, D. E. Silicatein filaments and subunits from a marine sponge direct the polymerization of silica and silicones in vitro. *Proc. Nat. Acad. Sci.* 1999, 96, 361-365.
22. Kroger, N.; Deutzmann, R.; Sumper, M. Polycationic peptides from diatom biosilica that direct silica nanosphere formation. *Science* 1999, 286, 1129-1132.
23. Luckarift, H. R.; Spain, J. C.; Naik, R. R.; Stone, M. O. Enzyme immobilization in a biomimetic silica support. *Nat. Biotechnol.* 2004, 22, 211-213.
24. Naik, R. R.; Tomczak, M. M.; Luckarift, H. R.; Spain, J. C.; Stone, M. O. Entrapment of enzymes and nanoparticles using biomimetically synthesized silica. *Chem. Commun. (Camb)* 2004, 1684-1685.
25. Burns, K. L.; May, S. W. Separation methods applicable to the evaluation of enzyme-inhibitor and enzyme-substrate interactions. *J. Chromatogr. B. Analyt. Technol. Biomed. Life Sci.* 2003, 797, 175-190.
26. Emneus, J.; Marko-Varga, G. Biospecific detection in liquid chromatography. *J. Chromatogr. A.* 1995, 703, 191-243.
27. Ono, M.; Idei, N.; Nakajima, T.; Itoh, Y.; Kawakami, N.; Shimada, K.; Yamato, S. Simultaneous determination of riboflavin phosphate and other ingredients in a multivitamin pharmaceutical preparation by on-line automated LC coupled with pre-column immobilized enzyme reactor. *J. Pharm. Biomed. Anal.* 2002, 29, 325-334.
28. Yamato, S.; Kawakami, N.; Shimada, K.; Ono, M.; Idei, N.; Itoh, Y. On-line automated high-performance liquid chromatographic determination of total riboflavin phosphates using immobilized acid phosphatase as a pre-column reactor. *J. Chromatogr. A* 2000, 896, 171-181.
29. Wada, M.; Inoue, K.; Thara, A.; Kishikawa, N.; Nakashima, K.; Kuroda, N. Determination of organic peroxides by liquid chromatography with on-line post-column ultraviolet irradiation and peroxyoxalate chemiluminescence detection. *J. Chromatogr. A* 2003, 987, 189-195.
30. Marko-Varga, G.; Dominguez, E.; Hahn-Hagerdal, B.; Gorton, L. Bioselective detection in liquid chromatography by the use of immobilized enzymes. *J. Pharm. Biomed. Anal.* 1990, 8, 817-823.
31. Jansen, H.; Brinkman, U. A.; Frei, R. W. Stereoselective determination of L-amino acids using column liquid chromatography with an enzymatic solid-phase reactor and chemiluminescence detection. *J. Chromatogr.* 1988, 440, 217-223.
32. Werkhoven-Goewie, C. E.; de Ruiter, C.; Brinkman, U. A.; Frei, R. W.; de Jong, G. J.; Little, C. J.; Stahel, O. Automated determination of drugs in blood samples after enzymatic hydrolysis using precolumn switching and post-column reaction detection. *J. Chromatogr.* 1983, 255, 79-90.
33. Girelli, A. M.; Mattei, E. Application of immobilized enzyme reactor in on-line high performance liquid chromatography: a review. *J. Chromatogr. B. Analyt. Technol. Biomed. Life Sci.* 2005, 819, 3-16.

34. Kerby, M. B.; Legge, R. S.; Tripathi, A. Measurements of kinetic parameters in a microfluidic reactor. *Anal. Chem.* 2006, 78, 8273-8280.
35. Luckarift, H. R.; Johnson, G. R.; Spain, J. C. Silica-immobilized enzyme reactors; application to cholinesterase-inhibition studies. *J. Chromatogr. B Analyt. Technol. Biomed. Life Sci.* 2006, 843, 310-316.
36. Andrisano, V.; Bartolini, M.; Gotti, R.; Cavrini, V.; Felix, G. Determination of inhibitors' potency (IC₅₀) by a direct high-performance liquid chromatographic method on an immobilised acetylcholinesterase column. *J. Chromatogr. B. Biomed. Sci. Appl.* 2001, 753, 375-383.
37. Jadaud, P.; Wainer, I. W. The stereochemical resolution of the enantiomers of aspartame on an immobilized alpha-chymotrypsin HPLC chiral stationary phase: the effect of mobile-phase composition and enzyme activity. *Chirality* 1990, 2, 32-37.
38. Gottschalk, I.; Lagerquist, C.; Zuo, S. S.; Lundqvist, A.; Lundahl, P. Immobilized-biomembrane affinity chromatography for binding studies of membrane proteins. *J. Chromatogr. B. Analyt. Technol. Biomed. Life Sci.* 2002, 768, 31-40.
39. Lundqvist, A.; Lundahl, P. Advantages of quantitative affinity chromatography for the analysis of solute interaction with membrane proteins. *J. Biochem. Biophys. Methods* 2001, 49, 507-521.
40. Moaddel, R.; Lu, L.; Baynham, M.; Wainer, I. W. Immobilized receptor- and transporter-based liquid chromatographic phases for on-line pharmacological and biochemical studies: a mini-review. *J. Chromatogr. B Analyt. Technol. Biomed. Life Sci.* 2002, 768, 41-53.
41. Bertucci, C.; Bartolini, M.; Gotti, R.; Andrisano, V. Drug affinity to immobilized target bio-polymers by high-performance liquid chromatography and capillary electrophoresis. *J. Chromatogr. B Analyt. Technol. Biomed. Life Sci.* 2003, 797, 111-129.
42. Kawakami, K.; Sera, Y.; Sakai, S.; Ono, T.; Ijima, H. Development and Characterization of a silica monolith immobilized enzyme micro-bioreactor. *Ind. Eng. Chem. Res.* 2005, 44, 236-240.
43. Josic, D.; Buchacher, A. Application of monoliths as supports for affinity chromatography and fast enzymatic conversion. *J. Biochem. Biophys. Methods* 2001, 49, 153-174.
44. Calleri, E.; Massolini, G.; Lubda, D.; Temporini, C.; Loiodice, F. C.; Caccialanza, G. Evaluation of a monolithic epoxy silica support for penicillin G acylase immobilization. *J. Chromatogr. A* 2004, 1031, 93-100.
45. Ostryanina, N. D.; Vlasov, G. P.; Tennikova, T. B. Multifunctional fractionation of polyclonal antibodies by immunoaffinity high-performance monolithic disk chromatography. *J. Chromatogr. A* 2002, 949, 163-171.
46. Liu, H.; Carter, G. T.; Tischler, M. Immobilized artificial membrane chromatography with mass spectrometric detection: a rapid method for screening drug-membrane interactions. *Rapid Comm. Mass Spec.* 2001, 15, 1533-1538.
47. Krause, E.; Dathe, M.; Wieprecht, T.; Bienert, M. Noncovalent immobilized artificial membrane chromatography, an improved method for describing peptide-lipid bilayer interactions. *J. Chromatogr. A* 1999, 849, 125-133.
48. Luco, J. M.; Salinas, A. P.; Torriero, A. A.; Vazquez, R. N.; Raba, J.; Marchevsky, E. Immobilized artificial membrane chromatography: quantitative structure-retention

- relationships of structurally diverse drugs. *J. Chem. Info. Computer Sci.* 2003, 43, 2129-2136.
49. Masucci, J. A.; Caldwell, G. W.; Foley, J. P. Comparison of the retention behavior of beta-blockers using immobilized artificial membrane chromatography and lysophospholipid micellar electrokinetic chromatography. *J. Chromatogr. A* 1998, 810, 95-103.
 50. Pehourcq, F.; Jarry, C.; Bannwarth, B. Potential of immobilized artificial membrane chromatography for lipophilicity determination of arylpropionic acid non-steroidal anti-inflammatory drugs. *J. Pharm. Biomed. Anal.* 2003, 33, 137-144.
 51. Pidgeon, C.; Stevens, J.; Otto, S.; Jefcoate, C.; Marcus, C. Immobilized artificial membrane chromatography: rapid purification of functional membrane proteins. *Anal. Biochem.* 1991, 194, 163-173.
 52. Pidgeon, C.; Venkataram, U. V. Immobilized artificial membrane chromatography: supports composed of membrane lipids. *Anal. Biochem.* 1989, 176, 36-47.
 53. Stewart, B. H.; Chan, O. H. Use of immobilized artificial membrane chromatography for drug transport applications. *J. Pharm. Sci.* 1998, 87, 1471-1478.
 54. Yang, C. Y.; Cai, S. J.; Liu, H.; Pidgeon, C. Immobilized artificial membranes - screens for drug membrane interactions. *Adv. Drug Delivery Rev.* 1996, 23, 229-256.
 55. Cloix, J. F.; Wainer, I. W. Development of an immobilized brain glutamine synthetase liquid chromatographic stationary phase for on-line biochemical studies. *J. Chromatogr. A* 2001, 913, 133-140.
 56. Luckarift, H. R.; Nadeau, L. J.; Spain, J. C. Continuous synthesis of aminophenols from nitroaromatic compounds by combination of metal and biocatalyst. *Chem. Commun. (Camb)* 2005, 383-384.
 57. Luckarift, H. R.; Balasubramanian, S.; Paliwal, S.; Johnson, G. R.; Simonian, A. L. Enzyme-encapsulated silica monolayers for rapid functionalization of a gold surface. *Coll. Surf. B Biointerfaces* 2007, 58, 28-33.
 58. Luckarift, H.; Ku, B.; Dordick, J.; Spain, J. Silica-Immobilized Enzymes for multi-step synthesis in microfluidic devices. *Biotech. Bioeng.* 2007, 98, 701-705.
 59. Luckarift, H.; Greenwald, R.; Bergin, M.; Spain, J.; Johnson, G. Biosensor system for continuous monitoring of organophosphate aerosols. *Biosens. Bioelectron.* 2007. *In Press*.
 60. Yao, L. X.; Wu, Z. C.; Ji, Z. L.; Chen, Y. Z.; Chen, X. Internet resources related to drug action and human response: a review. *Appl. Bioinformatics* 2006, 5, 131-139.
 61. Dannhardt, G.; Kiefer, W. Cyclooxygenase inhibitors-current status and future prospects. *Eur. J. Med. Chem.* 2001, 36, 109-126.
 62. Asberg, M.; Eriksson, B.; Martensson, B.; Traskman-Bendz, L.; Wagner, A. Therapeutic effects of serotonin uptake inhibitors in depression. *J. Clin. Psychiatry* 1986, 47 Suppl, 23-35.
 63. Lemberger, L.; Fuller, R. W.; Zerbe, R. L. Use of specific serotonin uptake inhibitors as antidepressants. *Clin. Neuropharmacol.* 1985, 8, 299-317.
 64. Youdim, M. B.; Edmondson, D.; Tipton, K. F. The therapeutic potential of monoamine oxidase inhibitors. *Nat. Rev. Neurosci.* 2006, 7, 295-309.
 65. Liston, D. R.; Nielsen, J. A.; Villalobos, A.; Chapin, D.; Jones, S. B.; Hubbard, S. T.; Shalaby, I. A.; Ramirez, A.; Nason, D.; White, W. F. Pharmacology of selective

- acetylcholinesterase inhibitors: implications for use in Alzheimer's disease. *Eur. J. Pharmacol.* 2004, 486, 9-17.
66. Holden, M.; Kelly, C. Use of cholinesterase inhibitors in dementia. *Adv. Psychiatric Treatment* 2002, 8, 89-96.
 67. Darvesh, S.; Walsh, R.; Kumar, R.; Caines, A.; Roberts, S.; Magee, D.; Rockwood, K.; Martin, E. Inhibition of human cholinesterases by drugs used to treat Alzheimer disease. *Alzheimer Dis. Assoc. Disord.* 2003, 17, 117-126.
 68. Giacobini, E. Cholinesterase inhibitors: new roles and therapeutic alternatives. *Pharmacol. Res.* 2004, 50, 433-440.
 69. Birks, J. Cholinesterase inhibitors for Alzheimer's disease. *Cochrane Database Syst Rev* 2006, CD005593.
 70. Hitzeman, N. Cholinesterase inhibitors for Alzheimer's disease. *Am. Fam. Physician* 2006, 74, 747-749.
 71. Bajgar, J. Organophosphates/nerve agent poisoning: mechanism of action, diagnosis, prophylaxis, and treatment. *Adv Clin Chem* 2004, 38, 151-216.
 72. Wiener, S. W.; Hoffman, R. S. Nerve agents: a comprehensive review. *J Intensive Care Med* 2004, 19, 22-37.
 73. Bartolini, M.; Cavrini, V.; Andrisano, V. Choosing the right chromatographic support in making a new acetylcholinesterase-micro-immobilised enzyme reactor for drug discovery. *J. Chromatogr. A* 2005, 1065, 135-144.
 74. Bartolini, M.; Cavrini, V.; Andrisano, V. Monolithic micro-immobilized-enzyme reactor with human recombinant acetylcholinesterase for on-line inhibition studies. *J. Chromatogr. A* 2004, 1031, 27-34.
 75. Suwansa-ard, S.; Kanatharana, P.; Asawatreratanakul, P.; Limsakul, C.; Wongkittisuksa, B.; Thavarungkul, P. Semi disposable reactor biosensors for detecting carbamate pesticides in water. *Biosens. Bioelectron.* 2005, 21, 445-454.
 76. Dong, Y.; Wang, L.; Shangguan, D.; Zhao, R.; Liu, G. Improved method for the routine determination of acetylcholine and choline in brain microdialysate using a horseradish peroxidase column as the immobilized enzyme reactor. *J. Chromatogr. B. Analyt. Technol. Biomed. Life Sci.* 2003, 788, 193-198.
 77. Kim, H. S.; Wainer, I. W. The covalent immobilization of microsomal uridine diphosphoglucuronosyltransferase (UDPGT): initial synthesis and characterization of an UDPGT immobilized enzyme reactor for the on-line study of glucuronidation. *J. Chromatogr. B. Analyt. Technol. Biomed. Life Sci.* 2005, 823, 158-166.
 78. Sakai-Kato, K.; Kato, M.; Toyo'oka, T. On-line drug-metabolism system using microsomes encapsulated in a capillary by the sol-gel method and integrated into capillary electrophoresis. *Anal Biochem* 2002, 308, 278-284.
 79. Calleri, E.; Marrubini, G.; Massolini, G.; Lubda, D.; de Fazio, S. S.; Furlanetto, S.; Wainer, I. W.; Manzo, L.; Caccialanza, G. Development of a chromatographic bioreactor based on immobilized beta-glucuronidase on monolithic support for the determination of dextromethorphan and dextrophan in human urine. *J. Pharm. Biomed. Anal.* 2004, 35, 1179-1189.
 80. Tsunoda, M. Recent advances in methods for the analysis of catecholamines and their metabolites. *Anal. Bioanal. Chem.* 2006, 386, 506-514.

81. Markoglou, N.; Wainer, I. W. Biosynthesis in an on-line immobilized-enzyme reactor containing phenylethanolamine N-methyltransferase in single-enzyme and coupled-enzyme formats. *J. Chromatogr. A* 2002, 948, 249-256.
82. Markoglou, N.; Wainer, I. W. Synthesis and characterization of immobilized dopamine beta-hydroxylase in membrane-bound and solubilized formats. *J. Biochem. Biophys. Methods* 2001, 48, 61-75.
83. Markoglou, N.; Wainer, I. W. Synthesis and characterization of an immobilized phenylethanolamine N-methyltransferase liquid chromatographic stationary phase. *Anal. Biochem.* 2001, 288, 83-88.
84. Markoglou, N.; Hsuesh, R.; Wainer, I. W. Immobilized enzyme reactors based upon the flavoenzymes monoamine oxidase A and B. *J. Chromatogr. B Analyt. Technol. Biomed. Life Sci.* 2004, 804, 295-302.
85. Markoglou, N.; Wainer, I. W. On-line synthesis utilizing immobilized enzyme reactors based upon immobilized dopamine beta-hydroxylase. *J. Chromatogr. B Analyt. Technol. Biomed. Life Sci.* 2002, 766, 145-151.
86. Goto, Y.; Grace, A. A. The Dopamine System and the Pathophysiology of Schizophrenia: A Basic Science Perspective. *Int. Rev. Neurobiol.* 2007, 78C, 41-68.
87. Berne, C.; Betancor, L.; Luckarift, H. R.; Spain, J. C. Application of a microfluidic reactor for screening cancer prodrug activation using silica-immobilized nitrobenzene nitroreductase. *Biomacromol.* 2006, 7, 2631-2636.
88. Oppenheimer, F. R. Topogenesis of glycolytic enzymes in *Trypanosoma brucei*. *Biochem. Soc. Symp.* 1987, 53, 123-129.
89. Bartolini, M.; Andrisano, V.; Wainer, I. W. Development and characterization of an immobilized enzyme reactor based on glyceraldehyde-3-phosphate dehydrogenase for on-line enzymatic studies. *J. Chromatogr. A* 2003, 987, 331-340.
90. Straathof, A. J.; Panke, S.; Schmid, A. The production of fine chemicals by biotransformations. *Curr. Opin. Biotechnol.* 2002, 13, 548-556.
91. Bhat, M. K. Cellulases and related enzymes in biotechnology. *Biotechnol. Adv.* 2000, 18, 355-383.
92. Panke, S.; Held, M.; Wubbolts, M. Trends and innovations in industrial biocatalysis for the production of fine chemicals. *Curr. Opin. Biotechnol.* 2004, 15, 272-279.
93. Michels, P. C.; Khmelnitsky, Y. L.; Dordick, J. S.; Clark, D. S. Combinatorial biocatalysis: a natural approach to drug discovery. *Trends Biotechnol.* 1998, 16, 210-215.
94. Faber, K.; Franssen, M. C. Prospects for the increased application of biocatalysts in organic transformations. *Trends Biotechnol.* 1993, 11, 461-470.
95. Dordick, J. S.; Khmelnitsky, Y. L.; Sergeeva, M. V. The evolution of biotransformation technologies. *Curr. Opin. Microbiol.* 1998, 1, 311-318.
96. Dordick, J. S. Biocatalysis in nonaqueous media. Patents and literature. *Appl. Biochem. Biotech.* 1988, 19, 103-112.
97. Pfomm, P. H.; Rezac, M. E.; Wurges, K.; Czermak, P. fumed silica activated subtilisin carlsberg in hexane in a packed-bed reactor. *AIChE Journal* 2007, 53, 237-242.
98. Kallenberg, A. I.; Van Rantwijk, F.; Sheldon, R. A. Immobilization of Penicillin G acylase: The key to optimum performance. *Adv. Synth. Catal.* 2005, 347, 905-926.
99. Giordano, R. C.; Ribeiro, M. P.; Giordano, R. L. Kinetics of beta-lactam antibiotics synthesis by penicillin G acylase (PGA) from the viewpoint of the industrial enzymatic reactor optimization. *Biotechnol. Adv.* 2006, 24, 27-41.

100. Calleri, E.; Temporini, C.; Massolini, G.; Caccialanza, G. Penicillin G acylase-based stationary phases: analytical applications. *J. Pharm. Biomed. Anal.* 2004, 35, 243-258.
101. Massolini, G.; Calleri, E.; De Lorenzi, E.; Pregnotato, M.; Terreni, M.; Felix, G.; Gandini, C. Immobilized penicillin G acylase as reactor and chiral selector in liquid chromatography. *J. Chromatogr. A* 2001, 921, 147-160.
102. Massolini, G.; Calleri, E.; Lavecchia, A.; Loiodice, F.; Lubda, D.; Temporini, C.; Fracchiolla, G.; Tortorella, P.; Novellino, E.; Caccialanza, G. Enantioselective hydrolysis of some 2-aryloxyalkanoic acid methyl esters and isosteric analogues using a penicillin G acylase-based HPLC monolithic silica column. *Anal. Chem.* 2003, 75, 535-542.
103. Pogori, N.; Xu, Y.; Cheikhousseff, A. Potential aspects of lipases obtained from *Rhizopus fungi*. *Research Journal of Microbiology* 2007, 2, 101-116.
104. Ghanem, A.; Aboul-Enein, H. Y. Application of lipases in kinetic resolution of racemates. *Chirality* 2005, 17, 1-15.
105. Ghanem, A. Trends in lipase-catalyzed asymmetric access to enantiomerically pure/enriched compounds. *Tetrahedron* 2007, 63, 1721-1754.
106. Dominguez de Maria, P.; Sinisterra, J. V.; Tsai, S.-W.; Alcantara, A. R. Carica papaya lipase (CPL): An emerging and versatile biocatalyst. *Biotechnology Advances* 2006, 24, 493-499.
107. Dominguez de Maria, P.; Carboni-Oerlemans, C.; Tuin, B.; Bargeman, G.; Van Der Meer, A.; Van Gemert, R. Biotechnological applications of *Candida antarctica* lipase A: State-of-the-art. *Journal of Molecular Catalysis B: Enzymatic* 2005, 37, 36-46.
108. Villeneuve, P.; Muderhwa, J. M.; Graille, J.; Haas, M. J. Customizing lipases for biocatalysis: A survey of chemical, physical and molecular biological approaches. *Journal of Molecular Catalysis - B Enzymatic* 2000, 9, 113-148.
109. Calleri, E.; Temporini, C.; Furlanetto, S.; Loiodice, F.; Fracchiolla, G.; Massolini, G. Lipases for biocatalysis: development of a chromatographic bioreactor. *J. Pharm. Biomed. Anal.* 2003, 32, 715-724.
110. Mullangi, R.; Yao, M.; Srinivas, N. R. Resolution of enantiomers of ketoprofen by HPLC: a review. *Biomed Chromatogr* 2003, 17, 423-434.
111. Jamali, F.; Brocks, D. R. Clinical pharmacokinetics of ketoprofen and its enantiomers. *Clin Pharmacokinet* 1990, 19, 197-217.
112. Ujang, Z.; Husain, W. H.; Seng, M. C.; Rashid, A. H. A. The kinetic resolution of 2-(4-chlorophenoxy) propionic acid using *Candida rugosa* lipase. *Proc. Biochem.* 2003, 38, 1483-1488.
113. Wedin, G. P.; Neal, J. S.; Everson, G. W.; Krenzelok, E. P. Castor bean poisoning. *Am. J. Emerg. Med.* 1986, 4, 259-261.
114. Challoner, K. R.; McCarron, M. M. Castor bean intoxication. *Ann. Emerg. Med.* 1990, 19, 1177-1183.
115. Biosensor. In *IUPAC Compendium of Chemical Terminology*, 1992, p 148.
116. Fishman, H. A.; Greenwald, D. R.; Zare, R. N. Biosensors in chemical separations. *Annu. Rev. Biophys. Biomol. Struct.* 1998, 27, 165-198.

Biosensor system for continuous monitoring of organophosphate aerosols

Heather R. Luckarift^{a,*}, Roby Greenwald^{b,1},
Mike H. Bergin^b, Jim C. Spain^b, Glenn R. Johnson^a

^a Air Force Research Laboratory, 139 Barnes Drive, Suite #2, Tyndall AFB, FL 32403, USA

^b School of Civil and Environmental Engineering and School of Earth and Atmospheric Sciences,
Georgia Institute of Technology, 311 Ferst Drive, Atlanta, GA, USA

Received 29 January 2007; received in revised form 19 April 2007; accepted 30 April 2007

Available online 6 May 2007

Abstract

An enzyme-based monitoring system provides the basis for continuous sampling of organophosphate contamination in air. The enzymes butyrylcholinesterase (BuChE) and organophosphate hydrolase (OPH) are stabilized by encapsulation in biomimetic silica nanoparticles, entrained within a packed bed column. The resulting immobilized enzyme reactors (IMERs) were integrated with an impinger-based aerosol sampling system for collection of chemical contaminants in air. The sampling system was operated continuously and organophosphate detection was performed in real-time by single wavelength analysis of enzyme hydrolysis products. The resulting sensor system detects organophosphates based on either enzyme inhibition (of BuChE) or substrate hydrolysis (by OPH). The detection limits of the IMERs for specific organophosphates are presented and discussed. The system proved suitable for detection of a range of organophosphates including paraoxon, demeton-S and malathion.
© 2007 Elsevier B.V. All rights reserved.

Keywords: Enzyme immobilization; Butyrylcholinesterase; Organophosphate hydrolase; Biosensor; Impinger; Aerosol sampling

1. Introduction

Organophosphates (OPs) are used throughout the world as pesticides and insecticides. OPs are also toxic to many other organisms, including humans, due to their often irreversible inhibition of essential enzymes of the central nervous system. The potency of OPs has also led to their use as chemical warfare agents (Bajgar, 2004; Wiener and Hoffman, 2004). Currently, the detection of OP exposure is mostly retrospective, because many OPs exist as atmospheric particulate matter not easily detectable by human senses. The threat of terrorist activity is often cited to emphasize the importance of sampling and analysis of airborne contaminants, yet less sinister circumstances can cause public health issues as well. For example, the ventilation of buildings using outdoor air creates a situation whereby building occupants

can be exposed to OPs both by incidental release (e.g. pesticide spraying) as well as a direct targeted attack. Therefore, there is an urgent need for aerosol sampling devices that provide an early warning of OP chemical agent release before the resultant contamination of a building's air supply.

Detection of OPs in air is currently performed by chromatography coupled with mass selective detectors or various types of spectroscopy (Staaf and Ostman, 2005; Bjorklund et al., 2004; Sanchez et al., 2003). Such techniques are time consuming, expensive and often require highly trained personnel, making them impractical for continuous monitoring. The enzymes acetylcholinesterase (AChE), butyrylcholinesterase (BuChE) and organophosphate hydrolase (OPH) have received much attention as alternatives for the detection of OPs and have been demonstrated in a range of amperometric, potentiometric, conductometric and optical formats (Andrescu and Marty, 2006; Walker and Asher, 2005; Mulchandani et al., 2001, 1998; Simonian et al., 2001; Wang et al., 2003; Singh et al., 1999). Detection using BuChE is based upon enzyme inhibition; OPs block the enzyme activity of BuChE leading to a decrease in response proportional to OP concentration. In contrast, detec-

* Corresponding author. Tel.: +1 850 283 6034; fax: +1 850 283 6090.

E-mail address: hluckarift@gtcom.net (H.R. Luckarift).

¹ Present address: Department of Pediatrics, Emory University School of Medicine, 2015 Uppergate Drive, Atlanta, GA, USA.

tion using OPH is based upon hydrolysis of OP substrates. OPH hydrolyzes a range of OPs including pesticides (e.g. parathion and malathion) and chemical warfare agents (e.g. soman, sarin and VX) (Dumas et al., 1989; Di Sioudi et al., 1999; Lai et al., 1995; Rastogi et al., 1997). The products of hydrolysis can be monitored spectrophotometrically or electrochemically. Because OPs are substrates for OPH, catalysis leads to a direct determination of analyte and the signal generated is directly proportional to the concentration of OP.

A primary limitation of many biologically based detection systems is the instability of the biological component. We have recently demonstrated that silicification provides a biocompatible and simple method for enzyme immobilization (Luckarift et al., 2004). Silicification refers to the process that certain organisms use to form hard silica skeletons by deposition of inorganic minerals. The silicification process can be adapted *in vitro* to entrap enzymes of interest within the resulting silica matrix. The silica immobilization method proved suitable for the encapsulation of butyrylcholinesterase (BuChE) with high retention of enzyme activity (>90%). Further modification of the procedure allowed the entrainment of the silica-immobilized enzymes within a fixed bed column; making them amenable to continuous flow systems (Luckarift et al., 2006). In this study, we compare the applicability of silica-immobilized BuChE and OPH for enzyme-based detection of OP contaminated air. The system provides the potential for development of continuous air monitoring devices for detecting OP contamination and integration with an alarm system. A system is envisaged for example whereby an air conditioning supply could be controlled in response to a positive signal.

2. Materials and methods

2.1. Materials

Butyrylcholinesterase (E.C.3.1.1.8; Equine serum, ≈50% protein and activity of 1200 Units/mg protein) was purchased from Sigma–Aldrich and dissolved in cholinesterase specific buffer (Luckarift et al., 2004). The synthetic peptides R5 (SSKKSYSYSGSKGSKRRIL), and the R5-His-tagged variants were purchased from New England peptide (Gardner, MA). Demeton-S was obtained from ChemService (West Chester, PA). All other chemicals were of analytical grade and obtained from Sigma–Aldrich (St. Louis, MO). OPH was kindly provided by Dr. James Wild of Texas A and M University.

2.2. Air sampler design

A schematic diagram of the sampling system is illustrated in Fig. 1. Liquid samples were aerosolized using a Micro-Mist nebulizer manufactured by Hudson RCI. The nebulizers were loaded with 1 ml of solution and operated at an air flow rate of approximately 4 l/min for 4 min. At the end of 4 min, the nebulizer was switched off and the residual volume of sample remaining in the nebulizer was measured to determine the volume of aerosolized sample. Downstream of the nebulizer, aerosolized samples were diluted with approximately 8 l/min of

filtered room air. The combined flow of sample and diluent air was collected in a SKC BioSampler® impinger (SKC, Eighty Four, PA). This device employs three glass jets to impact a gas or aerosol sample into a liquid reservoir. The airflow through the impinger jets was maintained at sonic speed by providing a stable flow rate of 12 l/min. At this gas flow rate, the impinger has been documented by its manufacturer to have an aerosol collection efficiency of 80% for 0.3 μm particles to ~100% for particles greater than 1.0 μm.

Here, the liquid reservoir in the impinger was composed of phosphate buffer (25 mM, pH 7.0, 10 mM MgSO₄, 126 μM 5,5'-dithiobis (2-nitro-benzoic acid) [Ellman's reagent]) and was continuously circulated at a flow rate of ~20 ml/min using a piston pump (Fluid Metering Inc. Model QV). After the aerosolized sample was entrained into the circulating liquid stream, the mobile phase passed through a passive debubbling device to remove air bubbles. The bubble-laden flow was diverted to waste while the bubble-free flow was directed through the IMER columns and into a single wavelength absorbance detector. The flow rate was maintained at 2 ml/min by a second piston pump positioned between the debubbler and the IMER columns so that the sample was under positive pressure as it was pushed through the column and negative pressure as it was pulled through the detector. Downstream of the detector, the sample was diverted to waste.

The relationship between the concentration of a compound in the air and that in the impinger liquid can be expressed as $C_A = C_l(Q_l/Q_A)$. Where C_A is the atmospheric concentration of the organophosphate of interest, C_l is the concentration in the impinger liquid, Q_l is the liquid flow rate through the impinger and Q_A is the air flow rate within the impinger. Hence for a measured liquid concentration the atmospheric concentration can be determined.

2.3. IMER preparation and chromatography conditions

Immobilized enzyme reactor columns (IMERs) were prepared as described previously (Luckarift et al., 2006), with either BuChE (0.6 mg) or OPH (0.66 mg). In preliminary experiments, IMERs were connected to an Agilent 1100 series liquid chromatography system and liquid samples (20 μl) were injected directly via an auto injection system. For aerosol sampling, the IMER columns were integrated with a BioSampler® Impinger and attached to a Hewlett Packard 1050 series single wavelength detector (Fig. 1). Phosphate buffer (25 mM, pH 7.0, 10 mM MgSO₄, 126 μM 5,5'-dithiobis (2-nitro-benzoic acid) [Ellman's reagent]) was used as the mobile phase throughout unless otherwise stated.

2.3.1. OPH-IMERs

OPH-catalyzed hydrolysis of OPs was monitored continuously at 412 nm for malathion and demeton-S and 400 nm for paraoxon. Ellman's reagent within the mobile phase reacts with free thiols generated by hydrolysis of malathion or demeton-S to produce a detectable chromophore at 412 nm. Detection of paraoxon was by direct determination of the hydrolysis product, *p*-nitrophenol (PNP) at 400 nm. Signal intensity for all substrates

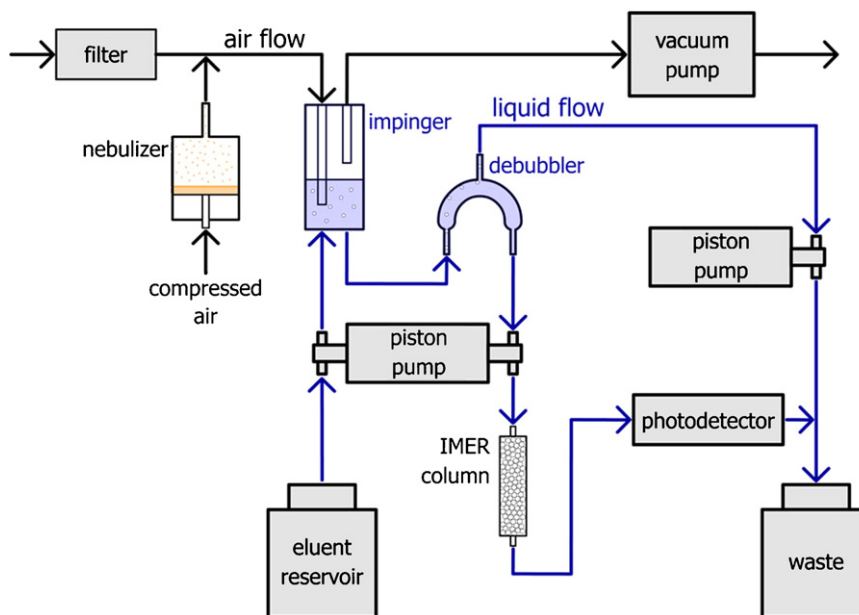


Fig. 1. Schematic for the laboratory characterization of an organophosphate measurement system.

was recorded as the product peak area. Goodness of fit (r^2) for linear regression lines was determined using GraphPad Prism software (v3.02).

2.3.2. BuChE-IMERs

Butyrylthiocholine iodide (BuCh-I) (20 μ M in phosphate buffer) was pumped continuously through the column and product was monitored continuously at 412 nm. The degree of inhibition was determined by calculating the change in peak height compared to initial steady state absorbance for a range of OP concentrations (0.1–5 mM).

2.3.3. BuChE reactivation

After incubation with OP, BuChE-IMERs were reactivated by flowing four column volumes (20 ml) of pyridine-2-aldoxime (PAM) (5 mM) through the column at 4 ml/min, followed by four column volumes of buffer (containing 126 μ M Ellman's reagent and 20 μ M BuCh-I) at 4 ml/min. Long-term reactivation studies were performed on an Agilent 1100 series liquid chromatography system with buffer as one mobile phase and the PAM reactivator (5 mM) as a second mobile phase.

3. Results and discussion

3.1. Enzyme based IMER biosensors

Immobilized enzyme reactor (IMER) biosensors were constructed with either OPH or BuChE as the immobilized enzyme component as described previously for BuChE (Luckarift et al., 2006). Briefly, IMERs are prepared using silica-encapsulation *in situ* via histidine-tag attachment of the silica/enzyme nanocomposites to a packed column by metal affinity binding. Effective loading and retention of the enzyme activity was achieved. The protein concentration of the eluate indicated greater than

90% loading efficiency; in agreement with previous studies for BuChE (Luckarift et al., 2006). The IMER columns gave stable and reproducible conversion of substrate over a 24 h period. In addition, the IMER columns could be stored at 4 °C and reused over a period of 5 days with no loss in activity (data not shown).

3.2. Detection of OPs by OPH-catalyzed hydrolysis in liquid

Detection using the biosensor containing OPH is based on the hydrolysis of OP substrates and the concentration of product formed. Three OP pesticides were selected as representative substrates; paraoxon is representative of OPs with phosphotriester bonds (P–O bond), demeton-S and malathion are representative of phosphonothioate pesticides (P–S bond). Initially the IMERs containing silica-immobilized OPH were tested by direct injection of paraoxon in the liquid phase. OPH catalyzed the hydrolysis of paraoxon to yield p-nitrophenol (PNP) and pro-

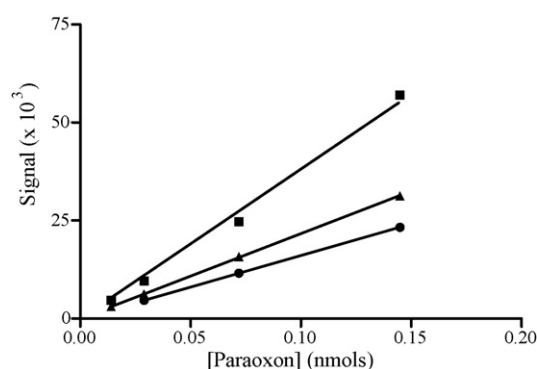


Fig. 2. OPH catalyzed hydrolysis of paraoxon as a function of flow rate. Paraoxon was injected to an OPH column ($n=1$) and signal intensity (peak area at 400 nm) of the hydrolysis product was measured at a range of flow rates: (■) 1 ml/min; (▲) 1.5 ml/min; (●) 2 ml/min.

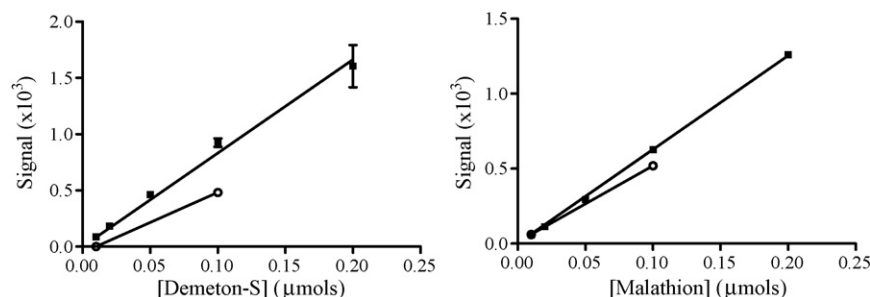


Fig. 3. Detection of demeton-S and malathion by OPH-catalyzed hydrolysis. Substrates (demeton-S and malathion) were injected into OPH columns and signal intensities of hydrolysis products were measured compared to an (enzyme-free) control column. Ellman's reagent was present in the mobile phase (126 μM). OPH-IMER column (■), Enzyme-free control column (○). Data points are mean \pm S.E. ($n = 3$).

duced a concentration-dependent response to paraoxon at a range of flow rates (Fig. 2). A more rapid signal response was observed by increasing the liquid flow rate through the impinger, but there was a concurrent decrease in signal intensity and hence the sensitivity of the system resulting from the reduced residence time. Detection of paraoxon in the absence of the OPH-IMER was minimal (less than 10% relative signal intensity).

Detection of hydrolysis products by spectrophotometric analysis is limited to substrates that produce a strong chromophore. Inclusion of Ellman's reagent within the reaction, however, enhances the detection of free thiol groups generated by the hydrolysis of P–S bonds (as in demeton-S and malathion) (Lai et al., 1995; Rastogi et al., 1997). Detection of demeton-S produced a linear response in the range 0.01–0.2 μmol ($r^2 = 0.9816$) and the signal intensity was significantly enhanced compared to that in an enzyme-free column (Fig. 3). Malathion was also detectable following OPH catalysis and produced a linear response in the same substrate concentration range (0.01–0.2 μmol ; $r^2 = 0.9998$), but the signal was not significantly different from an enzyme-free control at low concentrations (Fig. 3).

3.3. Aerosol sampling system configuration and characterization

The applicability of the IMERs connected to an aerosol sampling system was investigated. Initially, a control column containing no enzyme was connected to the system shown in the schematic (Fig. 1) to determine the efficiency and reproducibility of aerosol collection. The impinger device entrains contaminant particles into a fixed volume of buffer. The liquid flow rate into the impinger was controlled at a rate that could be adjusted to vary the collection efficiency and dilution factor. Aerosol samples collected within the impinger were pumped through the IMER columns and into a single-wavelength detector. PNP was selected as a model compound for calibration because it contains a strong chromophore that can be detected at 400 nm. The response for PNP was linear in the range 0.1–5 μmol ($r^2 = 0.994$). The response time was approximately 6 min and was a function of the combined residence time of the impinger, debubbler and IMER column. System parameters such as the impinger liquid flow rate can be modified to change the response time of the instrument.

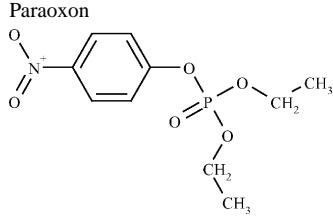
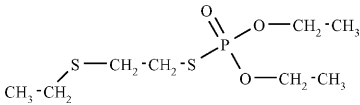
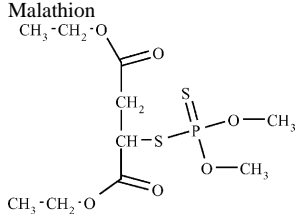
3.4. Detection of OPs in air by OPH-catalyzed hydrolysis

The OPH-IMER was connected to the impinger aerosol sampling system to determine the efficiency and reproducibility of the system during continuous operation. Paraoxon was aerosolized via an atomizer at a range of concentrations and the corresponding signal demonstrated first order reaction kinetics in the range 0–2.5 ppm ($r^2 = 0.994$). The signal intensity for detection of PNP as a product of OPH hydrolysis was in agreement with the signal observed for PNP provided directly to the system, confirming complete hydrolysis of paraoxon at the concentrations tested (Fig. 4a). The lower detection limit for paraoxon was equivalent to an ambient concentration of $\sim 0.52 \mu\text{mol}/\text{m}^3_{\text{AIR}}$ (using the equation described previously). Malathion and demeton-S produced lower responses than paraoxon (Table 1A). The lower detection limits for both demeton-S and malathion was an ambient concentration of $\sim 21 \mu\text{mol}/\text{m}^3_{\text{AIR}}$. The sensor responses of various OP substrates varied considerably due to variations in the substrate specificity of OPH as noted previously (Di Sioudi et al., 1999; Dumas et al., 1989) and the chromogenic intensity of hydrolysis products when complexed with Ellman's reagent. The K_m value for OPH catalyzed hydrolysis of demeton-S, for example, is approximately 10-fold higher than for paraoxon (Lai et al., 1995).

3.5. Detection of OPs by BuChE inhibition in air

The activity of BuChE can be determined by monitoring the hydrolysis of butyrylthiocholine iodide (BuCh-I) and measuring the concurrent formation of product upon reaction with Ellman's reagent to produce a detectable yellow anion (Luckarift et al., 2006 and references therein). OPs inhibit the hydrolysis of BuCh-I producing a decrease in signal intensity that is directly proportional to inhibitor concentration. Buffer was pumped continuously through the impinger at a fixed flow rate (20 ml/min) to give a constant substrate concentration of BuCh-I (20 μM), which yielded steady state continuous hydrolysis of BuCh-I to thiocholine. Paraoxon, demeton-S and malathion were investigated as representative cholinesterase inhibitors. All substrates were delivered to the aerosol sampling system via an atomizer and the inhibition of the steady state signal was measured. The inhibition of BuChE by paraoxon produced a second order kinetic response within the range 5–50 ppb

Table 1
Signal intensity for a range of OPs in the aerosol sampling system

	<div> <div>Paraoxon</div>  </div>		<div> <div>Demeton-S</div>  </div>		<div> <div>Malathion</div>  </div>	
	513 ppb	2.6 ppm	513 ppb	2.6 ppm	513 ppb	2.6 ppm
(A) OPH-IMER column						
Signal	2329 ± 346	12254 ± 402	40.5 ± 23	187.2 ± 44	30.1 ± 1.8	ND
Intensity ^a	100%	100%	1.7%	1.5%	1.3%	–
	Paraoxon		Demeton-S		Malathion	
	26 ppb	52 ppb	52 ppb	260 ppb	52 ppb	260 ppb
(B) BuChE-IMER column						
Signal	15.45 ± 2.475	51.55 ± 5.445	1.1†	2.7 ± 0.44	1.9†	ND
Intensity ^a	100%	100%	2.1%	–	3.7%	–

All values are mean ± S.E. ($n = 3$). Where noted (†), values are ($n = 1$). ND: not determined.

^a Signal intensity relative to Paraoxon.

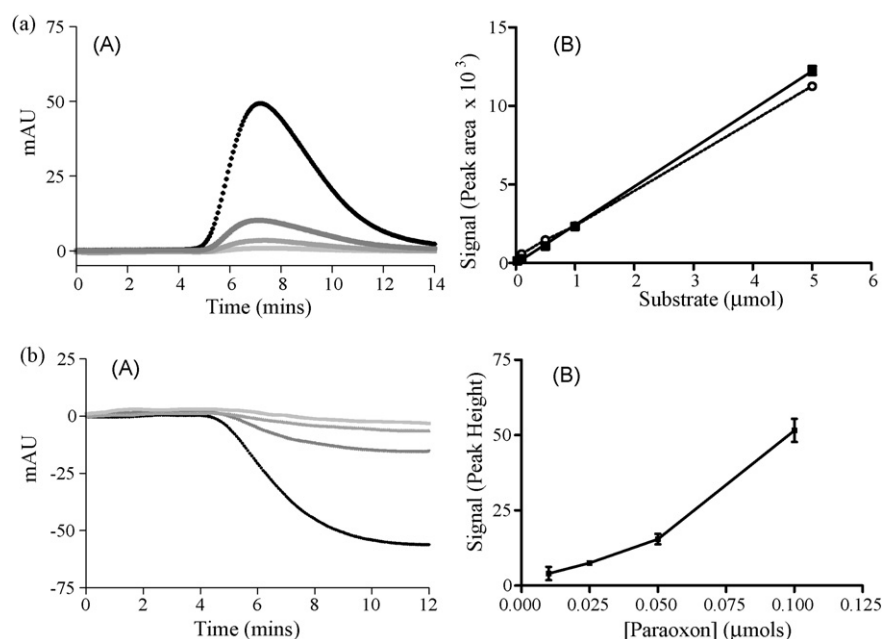


Fig. 4. (a) Detection of paraoxon by hydrolysis using the aerosol sampling system. (A) OPH-catalyzed hydrolysis of paraoxon as a function of paraoxon concentration. (B) Linear correlation of substrate concentration to signal (peak area); *p*-nitrophenol (PNP) was detected directly through a blank column (○) or as a product of paraoxon hydrolysis by OPH-IMER (■). Data points are mean \pm S.E. ($n=3$). (b) Detection of paraoxon by inhibition using the aerosol sampling system. (A) BuChE inhibition by paraoxon as a function of paraoxon concentration. (B) Correlation of substrate concentration to signal (decrease in peak height). Data points are mean \pm S.E. ($n=3$).

(Fig. 4b). The signal response was reproducible with standard deviations of $<10\%$ and was reproducible among three independent OPH-IMERs (data not shown). Inhibition of BuChE by paraoxon was linear at low concentrations but became saturated and lost linearity at concentrations above 25 ppb paraoxon. The lower detection limit for paraoxon based upon inhibition was approximately 5 ppb, equivalent to an ambient concentration of $\sim 0.21 \mu\text{mol}/\text{m}^3_{\text{AIR}}$. The sensitivity of the BuChE-IMER was in the order paraoxon $>$ malathion $>$ demeton-S (Table 1B). The sensitivity for the BuChE-IMER is in agreement with known inhibition of acetylcholinesterase enzymes by OPs (Simonian et al., 2001).

3.6. Biosensor reactivation and stability

BuChE becomes inactivated when exposed to OPs (Gulla et al., 2002; Mulchandani et al., 2001). In order to evaluate the performance utility of the BuChE-IMER it was necessary to reactivate the column and determine the recovered activity. Following inhibition of the BuChE-IMER, the column was treated with pyridine-2-aldoxime (PAM); a reactivator of OP-inhibited cholinesterase enzymes (Kovarík et al., 2004; Gulla et al., 2002). BuChE was irreversibly inhibited to some extent by paraoxon and demeton-S and there was a continuous decrease in enzymatic activity during repeated use of the IMER columns for inhibition experiments, even with use of the reactivator (Fig. 5). Loss of activity, however, was only detected when a saturating substrate concentration was used for activity measurements. At lower substrate concentrations, enzyme activity ($>70\%$) was retained providing reproducible and stable activity measurements for the entirety of the experiment (Fig. 5).

Despite the need to reactivate the BuChE biosensor, both OPH and BuChE biosensors were reusable over a number of samples with no loss in activity in agreement with the stability of the IMER columns demonstrated in previous studies (Luckarift et al., 2006). Detection of malathion and demeton-S resulted in low signals and caused persistent inhibition of the BuChE-IMER (data not shown). As a result, estimation of the detection level of these simulants by inhibition was limited to a small number of assays.

An important characteristic of both the OPH and BuChE biosensors was the stability and reproducibility of the signal response over successive samples (Supplemental Fig. 1). The

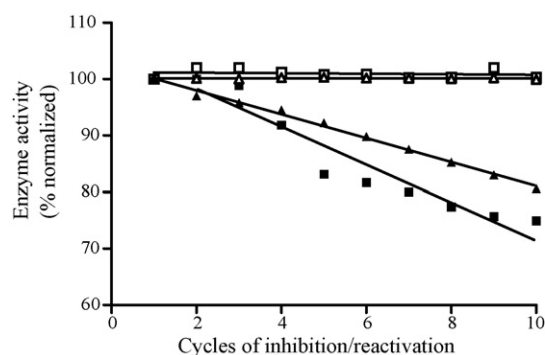


Fig. 5. Reactivation of BuChE following inhibition by demeton-S and paraoxon. Paraoxon and demeton-S were injected to BuChE columns ($20 \mu\text{l}$ of 5 mM). Following reactivation with pyridine-2-aldoxime (four column volumes of 5 mM at 4 ml/min), BuChE-I was supplied at high/saturated ($20 \mu\text{l}$ of 20 mM) and low ($2 \mu\text{l}$ of 20 mM) substrate concentrations to measure retention of enzyme activity. Paraoxon: [high BuChE-I] (▲), [low BuChE-I] (△); Demeton-S: [high BuChE-I] (■), [low BuChE-I] (□). Data points are mean ($n=2$).

stability of the signal also indicates no significant carryover of sample between subsequent analyses, which has been observed as a problem of inhibition-based biosensors.

4. Conclusion

The integration of IMER columns with an aerosol sampling system proved suitable for the detection of OPs and provided reliable and reproducible data for OPs including paraoxon, demeton-S and malathion. In the case of the OPH-IMERs, a difference between sensor responses with various OP substrates is due to variations in the substrate specificity of OPH (Di Sioudi et al., 1999; Dumas et al., 1989). The sensitivity of the systems for demeton-S and malathion differed by an order of magnitude relative to detection of paraoxon for both OPH and BuChE detection systems. Increased sensitivity and a correspondingly lower detection limit for the OPH-IMER can potentially be attained by utilizing variants of OPH with altered substrate preferences. For example, OPH has low catalytic activity towards demeton-S. Genetically modified OPH, however, shows increased catalytic activity towards P–S bonds which could be utilized to enhance the biosensor response (Simonian et al., 2004).

For a continuous air-sampling detector it is not necessary to immediately identify the agent, but simply to provide an early warning. The single wavelength absorbance detector used in this study limits the detection range of specific organophosphates. The addition of a high-pressure liquid chromatography column and spectral analysis in-line with the current detection system would allow the discrimination and quantification of specific OPs detected by the system. Such integration would provide a detection response that could be followed by a more detailed examination of the nature of the contaminant. The system could, therefore, warn against any compound that can act as a cholinergic neurotoxin, irrespective of its origin. This system is adaptable, for example, to monitoring pesticide concentrations in public water supplies or integration with the HVAC intake to a building.

The sensitivity and detection limits demonstrate the potential of the system as a proof of concept, but further optimization of the system will be required to enhance applicability. The system has inherent limitations, for example the OPH-IMER does not require a continuous supply of enzyme substrate, but the BuChE-IMER does. The detection of OPs by the aerosol sampling system is however, simple, rapid and directly applicable to kinetic response measurements. With additional optimization, the biosensor system described may find application for real-time detection of chemical agents under environmental conditions.

Acknowledgements

This work was supported by funding from the U.S. Air Force Office of Scientific Research. HRL was supported by Oak Ridge Institute for Science and Education (U.S. Department of Energy). The authors acknowledge Joseph D. Wander for useful discussions.

Appendix A. Supplementary data

Supplementary data associated with this article can be found, in the online version, at doi:10.1016/j.bios.2007.04.023.

References

- Andreescu, S., Marty, J.-L., 2006. *Biomol. Eng.* 23, 1–15.
- Bajgar, J., 2004. *Adv. Clin. Chem.* 38, 151–216.
- Bjorklund, J., Isetun, S., Nilsson, U., 2004. *Rapid Commun. Mass Spectrom.* 18 (24), 3079–3083.
- Di Sioudi, B.D., Miller, C.E., Lai, K., Grimsley, J.K., Wild, J.R., 1999. *Chem. Biol. Interact.* 119–120, 211–223.
- Dumas, D.P., Caldwell, S.R., Wild, J.R., Raushel, F.M., 1989. *J. Biol. Chem.* 264 (33), 19659–19665.
- Gulla, K.C., Gouda, M.D., Thakur, M.S., Karanth, 2002. *Biochim. Biophys. Acta* 1597, 133–139.
- Kovarik, Z., Radi, Z., Berman, H.A., Simeon-Rudolf, V., Reiner, E., Taylor, P., 2004. *Biochemistry* 43, 3222–3229.
- Lai, K., Stolowich, N.J., Wild, J.R., 1995. *Arch. Biochem. Biophys.* 318 (1), 59–64.
- Luckarift, H.R., Spain, J.C., Naik, R.R., Stone, M.O., 2004. *Nat. Biotech.* 22, 211–213.
- Luckarift, H.R., Johnson, G.R., Spain, J.C., 2006. *J. Chromatogr. B* 843, 310–316.
- Mulchandani, A., Chen, W., Mulchandani, P., Wang, J., Rogers, K.R., 2001. *Biosens. Bioelectron.* 16, 225–230.
- Mulchandani, A., Mulchandani, P., Kaneva, I., Chen, W., 1998. *Anal. Chem.* 70, 4140–4145.
- Rastogi, V.K., DeFrank, J.J., Cheng, T.-C., Wild, J.R., 1997. *Biochem. Biophys. Res. Commun.* 241, 294–296.
- Sanchez, C., Ericsson, M., Carlsson, H., Colmsjo, A., 2003. *J. Chromatogr. A* 993 (1–2), 103–110.
- Simonian, A.L., Efremenko, E.N., Wild, J.R., 2001. *Anal. Chim. Acta* 444, 179–186.
- Simonian, A.L., Flounders, A.W., Wild, J.R., 2004. *Electroanalysis* 16 (22), 1896–1906.
- Singh, A.K., Flounders, A.W., Volponi, J.V., Ashley, C.S., Wally, K., Schoeniger, J.S., 1999. *Biosens. Bioelectron.* 14, 703–713.
- Staaf, T., Ostman, C., 2005. *J. Environ. Monit.* 7 (4), 344–348.
- Walker, J.P., Asher, S.A., 2005. *Anal. Chem.* 77, 1596–1600.
- Wang, J., Krause, R., Block, K., Musameh, M., Mulchandani, A., Schoning, M.J., 2003. *Biosens. Bioelectron.* 18, 255–260.
- Wiener, S.W., Hoffman, R.S., 2004. *J. Intensive Care Med.* 19, 22–37.

Enzyme-encapsulated silica monolayers for rapid functionalization of a gold surface

Heather R. Luckarift^a, Shankar Balasubramanian^b, Sheetal Paliwal^b,
Glenn R. Johnson^a, Aleksandr L. Simonian^{b,*}

^a Air Force Research Laboratory, 139 Barnes Drive, Suite # 2, Tyndall AFB, FL 32403, United States

^b Materials Research and Education Center, Samuel Ginn College of Engineering, Auburn University, 275 Wilmore, Auburn, AL 36849, United States

Available online 22 August 2006

Abstract

We report a simple and rapid method for the deposition of amorphous silica onto a gold surface. The method is based on the ability of lysozyme to mediate the formation of silica nanoparticles. A monolayer of lysozyme is deposited via non-specific binding to gold. The lysozyme then mediates the self-assembled formation of a silica monolayer. The silica formation described herein occurs on a surface plasmon resonance (SPR) gold surface and is characterized by SPR spectroscopy. The silica layer significantly increases the surface area compared to the gold substrate and is directly compatible with a detection system. The maximum surface concentration of lysozyme was found to be a monolayer of 2.6 ng/mm² which allowed the deposition of a silica layer of a further 2 ng/mm². For additional surface functionalization, the silica was also demonstrated to be a suitable matrix for immobilization of biomolecules. The encapsulation of organophosphate hydrolase (OPH) was demonstrated as a model system. The silica forms at ambient conditions in a reaction that allows the encapsulation of enzymes directly during silica formation. OPH was successfully encapsulated within the silica particles and a detection limit for the substrate, paraoxon, using the surface-encapsulated enzyme was found to be 20 μM.

© 2006 Elsevier B.V. All rights reserved.

Keywords: Surface plasmon resonance; Silica; Organophosphate hydrolase; Enzyme immobilization; Paraoxon

1. Introduction

Immobilization of enzymes on solid substrates, such as silicon [1,2], polymers [3] and glass [4] is of great interest for a variety of applications including biocatalysis, biosensors and formation of protein arrays for biological screening. Often, the platform is merely an inactive support for the biomolecule. Recent interest however, has advanced to attaching biomolecules directly to a transducer surface to allow *in situ* and real-time detection of enzymatic activity [5,6].

Surface plasmon resonance (SPR) is a versatile analytical method for real-time monitoring of interactions at a solid/liquid transducer surface. SPR uses the principle of total internal reflectance occurring at the interface between materials with differing refractive indices. An evanescent wave penetrates the interface (modified with a thin layer of gold) and couples with

surface plasmons (oscillating free electrons). The interaction causes a change in reflectivity and a concurrent change in resonance angle, which correlates to the refractive index (RI) of the adjacent medium. The RI is therefore directly related to changes in surface concentration of interacting ligands. The change in RI is continuously monitored to produce a sensorgram of refractive index unit (RIU) as a function of time [7–9]. SPR has proven to be particularly useful for the analysis of biological systems and can be used for example, to determine kinetic parameters and reaction characteristics [9,10]. SPR has been recently used to study enzymatic reactions on various surfaces and microarrays. Kim et al. [11] for example, performed enzymatic reactions on surface bound substrates and measured adsorbed enzyme concentrations and substrate cleavage rates by the use of combined SPR and surface-plasmon enhanced fluorescence techniques. SPR has also been demonstrated as a method for determining the kinetics of surface enzyme reactions based on Langmuir adsorption and Michaelis–Menten kinetics [12,13]. SPR is adaptable to a wide range of biomolecular reactions as labelling of ligands or receptor molecules is not required. The use of SPR for biological

* Corresponding author. Tel.: +1 334 844 4485; fax: +1 334 844 3400.
E-mail address: simonan@eng.auburn.edu (A.L. Simonian).

systems however, generally requires the development of specific methods to attach biomolecules on the sensor surface and orient the molecules for optimal biological activity. Maintaining an interaction between biomolecules and the SPR waveguide surface generally requires covalent modification, which can change biological function and lower the catalytic activity as the orientation of the enzyme active site is hindered by attachment [14].

Recent studies have shown that silica formation can be catalyzed by simple peptides or proteins, such as lysozyme, in a silicification reaction analogous to the formation of silica in biological systems [15–18]. The lysozyme-precipitated silica nanoparticles proved suitable for immobilization of other enzymes. The silicification reaction yields a network of fused silica nanospheres, providing a high surface area for encapsulation and permitting high enzyme loading capacities [19]. We now report herein, a versatile method for immobilization of biomolecules directly onto a SPR transducer surface by encapsulating biomolecules within a lysozyme-mediated self-assembled layer of silica particles. The immobilization of lysozyme is based on non-specific physical adsorption of the protein to the gold SPR surface through a combination of electrostatic and surface interactions [20]. Non-specific binding will therefore result in the formation of a film of lysozyme upon the gold surface, which is then available to participate in the silicification reaction and direct the assembly of a layer of silica at the surface. Physical adsorption generally causes little conformational change of the enzyme and no reagents or pretreatment and activation of the surface is required. A disadvantage is enzyme leaching during continuous use, as the binding is primarily due to weak hydrogen bonding and Van der Waals forces [21]. Previous literature reports however, indicate that lysozyme retains its tertiary structure when adsorbed to a hydrophilic interface, no significant denaturation occurs, and in addition, the binding is irreversible [22].

The fabrication of SPR chips, consisting of gold films coated with thin silicon dioxide layers has been recently reported [23]. The method however, involves vapor-deposited silica layers that showed a lack of stability in aqueous buffer solutions and is unsuitable for enzyme immobilization. A sol–gel technique has been successfully applied to generate stable gold/silica interfaces, which allowed further functionalization but preparation required multi-step attachment using biotin and streptavidin binding chemistries [24]. The lysozyme-mediated silica formation described herein provides a method for coating a gold surface with a thin layer of silica particles, greatly increasing the surface area of the transducer. In addition, the silica provides a matrix for the encapsulation of additional biomolecules, significantly enhancing the functionality of the resulting silica layers by directing the attachment of immobilized biomolecules directly at the gold surface.

2. Experimental

2.1. Enzymes and reagents

Potassium phosphate buffer (0.1N NaOH, 0.1 M KH_2PO_4 , pH 8) was used throughout unless otherwise stated. Paraoxon was obtained from ChemService, West Chester, PA. All other

reagents and chemicals were of analytical grade and obtained from Sigma–Aldrich (St. Louis, MO). Silicic acid was prepared as described previously [19]. Organophosphorus hydrolase (OPH) was generously provided by James Wild and his research group (Texas A&M University). The enzyme purification method has been described previously [25].

2.2. Formation of silica nanoparticles on the gold surface

The formation of silica particles was characterized by SPR using SPREETATM sensors (Texas Instruments) with two analysis channels. A gold surfaced SPR sensor module, and its supporting hardware and software (SPREETA, Texas Instruments) were coupled to a continuous-flow cell to allow contact with reaction solutions. Experimental setup and cleaning steps were performed as previously described [26]. The sensor was docked with the fluidics block and reference measurements were obtained with air and water as baseline measurements. An *in situ* washing step (0.12N NaOH, 1% Triton-X) was performed to ensure that the surface remained hydrophilic. A further baseline with phosphate buffer was taken as a reference measurement. Initially, lysozyme (1 mg/ml) was non-specifically adsorbed to the gold surface and any excess was removed by washing with phosphate buffer. Silicification was carried out *in situ* by introducing TMOS (100 mM tetramethyl orthosilicate in 1 mM HCl) to the lysozyme-modified surface. This process was repeated with different lysozyme concentrations (5, 25 and 50 mg/ml) to determine the optimum enzyme concentration. All immobilization procedures were performed at room temperature ($\sim 22^\circ\text{C}$). Immobilization steps were monitored by measuring the change in refractive index (RI) as a function of time followed by integration using SPREETA software. Net responses were calculated by comparison of ‘working’ and ‘control’ channels. Calculations and statistical analysis were performed with OriginPro 7.5 software (OriginLab Corporation, Massachusetts, USA).

2.3. Calculation of adlayer thickness and surface coverage

The adlayer thickness and surface coverage of each monolayer was calculated using the formula described by Jung et al [27,28]; $d_a = (l_d/2) \times [(n_{\text{eff}} - n_b)/(n_a - n_b)]$, where d_a is the thickness of the adlayer, l_d the characteristic decay length of an evanescent wave at 307 nm, n_{eff} the effective RI of the adlayer (from the SPR signal), n_b the RI of the buffer (from reference reading), and n_a is the RI of the adlayer material assuming an RI of 1.57 for protein and an RI of 1.43 for biosilica [29].

2.4. Enzyme assay for immobilized organophosphate hydrolase activity

OPH was encapsulated within the silica matrix by adapting the method described above. The initial protein monolayer was established using a solution of 25 mg/ml lysozyme to coat the SPR surface. A solution of 100 mM TMOS containing OPH was then passed over the surface for approximately 45 min to yield the silica layer and co-encapsulate OPH during the silicification reaction. The SPR surface was rinsed thoroughly

with buffer to remove any loosely associated enzyme and silica prior to further analysis. Enzyme activity was determined by measuring the hydrolysis of paraoxon as described previously [30]. Paraoxon (1–500 μ M) was circulated across the surface at a flow rate of 100 μ l/min for 2 min. Enzyme activity was determined by collecting 200 μ l of the paraoxon hydrolysis product (*p*-nitrophenol). The absorbance of the hydrolysis product was measured at 405 nm using a UV–vis fiber optic spectrophotometer (Ocean Optics Inc., Dunedin, FL).

2.5. Scanning electron microscopy

For scanning electron microscopy imaging, glass slides coated with a chromium adhesion layer (~ 2 nm) followed by ~ 50 nm gold film were used. The gold slides were cleaned with freshly prepared piranha solution (3:1, H_2SO_4 and H_2O_2 . *Cauti-*on: Piranha solution is dangerous and should be handled with care) followed by thorough rinsing with DI water. The slides were then sonicated in acetone (5 min), rinsed with DI water, and sonicated in ethanol (5 min) before plasma cleaning in air (5 min). The slides were prepared as described above with a range of lysozyme concentrations, followed by silica formation in the presence of 100 mM TMOS. The samples were then coated with a thin layer of gold (~ 10 nm) and imaged using a JEOL JSM 7000F field emission scanning electron microscope (JEOL USA, Inc., Peabody, MA).

3. Results and discussion

3.1. SPR analysis of lysozyme and silica nanocomposite films

SPR spectroscopy revealed rapid adsorption of lysozyme to the gold waveguide surface (Fig. 1a). The change in surface density results in small changes in RI at the interface and a corresponding shift in the resonance angle. Upon introduction of lysozyme, an initial rapid signal increase was observed and was attributed to the change in the bulk refractive index of the circulating solution. The change in RI then increased gradually, corresponding to the adsorption of lysozyme to the gold surface. Surface saturation was indicated by a plateau in the RI signal. The decrease in the RI during the wash step was due to removal of unbound lysozyme. The RI signal change increased linearly with higher protein concentrations (Fig. 1b). The lysozyme adlayer also thickened with increasing lysozyme concentration but showed a plateau at 25 and 50 mg/ml (Table 1),

Table 1
Effect of lysozyme concentration on thickness of lysozyme and silica adlayers

[Lysozyme] (mg/ml)	Thickness of protein adlayer, <i>d</i> (nm)	Surface coverage (molecules/mm ²)	Thickness of silica adlayer, <i>d</i> (nm)
1	0.934	5.23E+10	3.74
5	0.978	5.47E+10	3.75
25	1.963	1.10E+11	6.56
50	2.029	1.14E+11	6.60

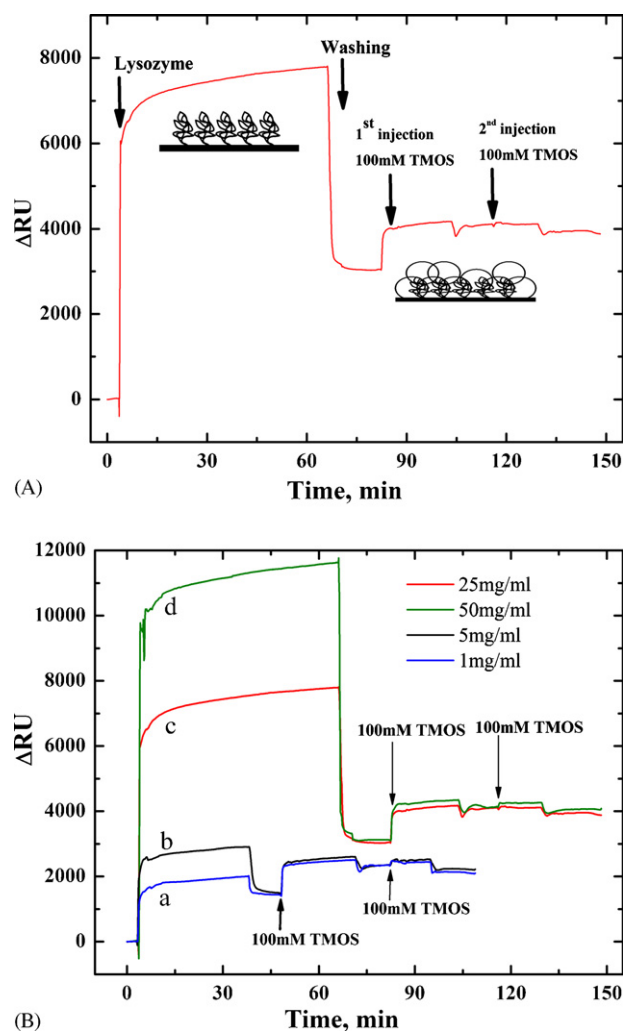


Fig. 1. (A) SPR spectroscopy response showing the binding of lysozyme and formation of silica at the SPR surface. Sensorgram shows addition of 25 mg/ml lysozyme, followed by washing. 100 mM TMOS was added as a precursor for silica formation. (B) Formation of lysozyme-mediated silica coating on gold. SPR response of lysozyme deposited to the gold surface at a range of concentrations: 1 mg/ml (curve a), 5 mg/ml (curve b), 25 mg/ml (curve c) and 50 mg/ml (curve d). Addition of TMOS (100 mM) is indicated by an arrow.

indicating that the gold surface was saturated at high protein concentrations. The surface coverage of lysozyme was calculated and revealed a maximum surface concentration of ~ 2.6 ng/mm² ($\sim 1.10 \times 10^{11}$ molecules/mm²) and a maximum film thickness of ~ 2 nm (± 0.047) (Table 1). The measured maximum coverage of lysozyme at saturation is in agreement with the theoretical surface density for a monolayer of lysozyme (1.8–2.7 ng/mm²), based on a protein with a molecular mass of 14 kDa and dimensions of 4.5 nm \times 3.0 nm \times 3.0 nm [20,21]. SEM images of the monolayer showed a glass-like film of lysozyme across the surface of the waveguide (Fig. 2a).

The bound lysozyme molecules mediated the formation of a silica adlayer *in situ*. Introduction of a solution of TMOS caused a rapid increase in RI, indicating changes in surface refraction consistent with the formation of a second distinct adlayer of silica (Fig. 1B). The reaction was rapid and approximately 90% of silica formation occurred within the first minutes of contact.

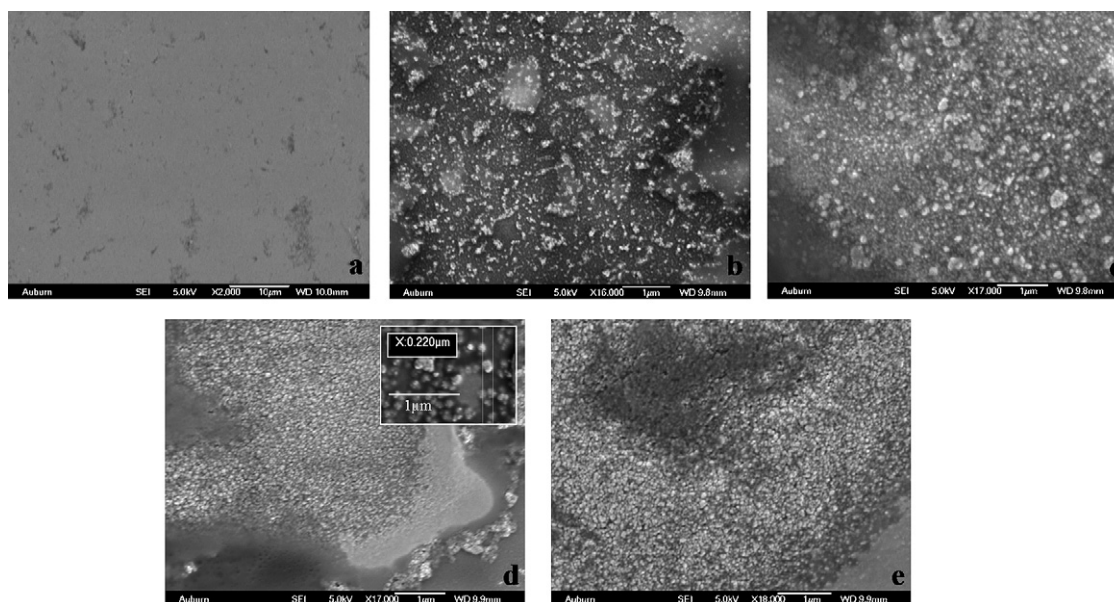


Fig. 2. SEM images of silica-encapsulated OPH at the SPR surface. Gold surface modified with (a) lysozyme (25 mg/ml); (b) lysozyme (1 mg/ml) with 100 mM TMOS; (c) lysozyme (5 mg/ml) with 100 mM TMOS; (d) lysozyme (25 mg/ml) with 100 mM TMOS; (e) lysozyme (25 mg/ml) with 100 mM TMOS and OPH (0.1 mg/ml).

Washing the silica layer with buffer did not decrease the signal significantly, indicating that the silica was firmly attached to the surface. The change in the RI was used to calculate the deposition characteristics of the silica particles. The maximum thickness of the layer was calculated to be ~ 6.6 nm (Table 1). The thickness of the silica layer did not increase following a second injection of TMOS suggesting that the surface was saturated with silica and conditions were not substrate limited. SEM analysis confirmed the formation of an interconnected, dense coating of silica nanospheres formed upon the gold surface. At low concentrations of lysozyme, a scattered deposition of silica was observed with silica particles having an average size ~ 10 nm (Fig. 2). When lysozyme was present in excess, however, dense coatings of interconnected aggregates of much larger silica particles (~ 230 nm) formed in addition to the initial monolayer of silica nanospheres (Fig. 2c and d). In aqueous static suspensions, lysozyme forms silica spheres of approximately 570 nm diameter [15]. The reduction in size of the silica particles observed here is attributed the formation of the silica particles under continuous flow conditions. Silica spheres are the lowest free energy structure formed in a static environment, but application of a dynamic flow will affect the formation and aggregation of silica.

Even though the SEM shows the size of the nanoparticle as 230 nm the thickness measured by SPR for the silica layer is significantly less (~ 7 nm). The results are consistent with the immediate formation of a thin film of silica directly at the surface which provides a template for subsequent formation of larger silica particles, as observed for many silicification reactions [31]. The surface plasmon resonance phenomenon occurs at the metal–liquid interface and is highly sensitive to specific interactions at the interface which may be on the order of only a few nanometers. Although a generated evanescent wave can travel up to ~ 300 nm in the z direction [27], the medium beyond the interface will affect the observed RI. The inability to see the

depth of the whole silica structure using SPR in the present work is in agreement with previous literature reports where silica layers of greater than 44 nm did not show significant SPR response [23].

The lysozyme is presumably attached at the surface in an orientation which does not diminish its ability to mediate silica formation. Variations in TMOS concentration may theoretically affect the thickness of the silica layer. Preliminary control experiments in static suspensions however, revealed that silica formation does not occur if the TMOS concentration is below 25 mM (data not shown), accordingly, silica adlayer formation was not investigated at lower precursor concentrations. In control experiments, no formation of silica particles was observed in the absence of lysozyme. Bovine serum albumin (BSA) adsorbed to the gold surface but did not precipitate silica in the presence of TMOS, confirming that lysozyme is integral to the silica formation at the surface (data not shown).

3.2. Encapsulation of organophosphate hydrolase

The further biofunctionalization of the silica particles at the surface was investigated using organophosphate hydrolase (OPH) as a model system. The gold surface was saturated with lysozyme as defined above and used to mediate the formation of silica particles containing various concentrations of OPH. The silica particles formed on the gold surface as described above and examination using SEM clearly showed that the surface was coated with a film of evenly distributed spheres (Fig. 2e). The addition of OPH to the hydrolyzed TMOS solution did not result in any significant changes in the morphology of the silica surface (Fig. 2d and e). OPH encapsulated within the silica coating maintains activity, confirmed by the hydrolysis of paraoxon and the activity of OPH correlates with protein concentrations used in the encapsulation step (Fig. 3a). The kinetic parameters of the

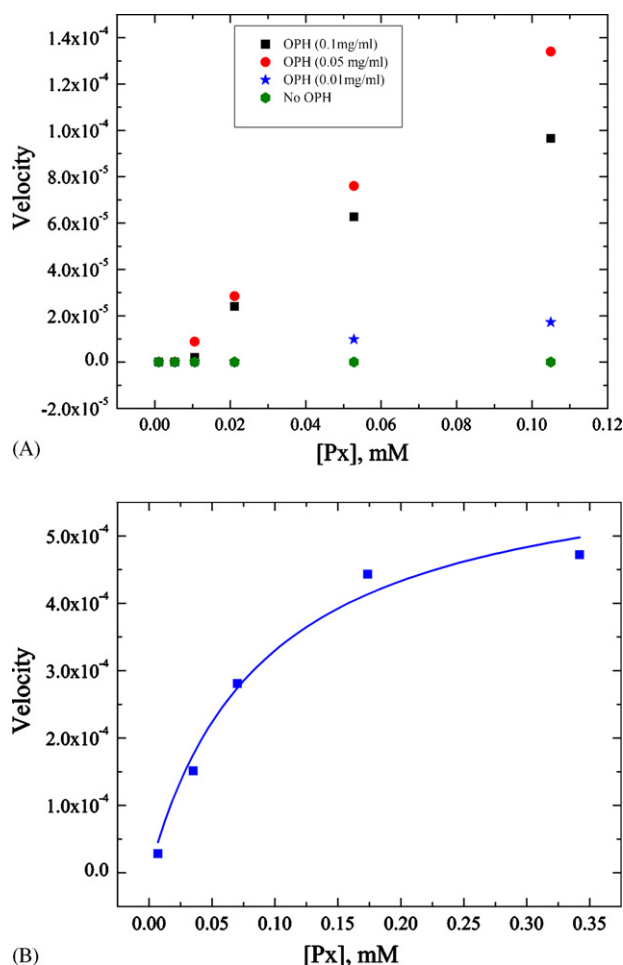


Fig. 3. Paraoxon hydrolysis by silica-encapsulated organophosphate hydrolase immobilized to the SPR surface. (A) Hydrolase activity in relation to OPH concentrations present during silicification step at a range of substrate concentrations. (B) Michaelis–Menten plot of immobilized OPH (0.5 mg/ml during silicification) to reveal maximal velocity of reaction.

encapsulated enzyme were determined by contacting the encapsulated enzyme at the surface with paraoxon at a range of concentrations. At low concentrations of paraoxon (20–100 μ M), the silica-encapsulated OPH shows a linear response (Fig. 3a) but enzyme activity becomes saturated at paraoxon concentrations above 300 μ M (Fig. 3b). A reproducible detection limit of 20 μ M paraoxon was achieved with OPH concentrations greater than 0.05 mg/ml. A decrease in the concentration of encapsulated OPH resulted in a proportional reduction in detection sensitivity. The kinetic parameters of the encapsulated OPH ($K_m = 0.09(\pm 0.022)$) were determined (Fig. 3b) and are in good agreement with the kinetics of OPH in solution [32] indicating that immobilization of OPH in silica does not significantly hinder the mass transport of substrate.

4. Conclusion

The formation of silica using lysozyme precipitation provides a simple and rapid method for the deposition of silica films directly to a gold surface. The silica layer proved sufficiently stable under continuous flow conditions to allow measurement

of enzyme kinetic parameters. The silica deposition and surface immobilization of OPH demonstrated in this study provides a model system with potential application to a range of formats. The surface encapsulated OPH could be reused continually for over 2 days, but lost activity gradually over the time period, concurrent with a loss of silica film thickness (data not shown). The immobilization efficiency and stability achieved were sufficient for demonstrating the concept, but further analysis of the silica coating is required to optimize the approach. The formation of a silica layer on the gold surface significantly increases the surface area at the transducer interface and potentially enhances the sensitivity of SPR spectroscopy applications [33]. The silica layer also proved suitable for encapsulation of OPH and the immobilized enzyme retained activity over a period of several hours, providing accurate and reproducible measurements of immobilized enzyme kinetics. The immobilization technique described provides a versatile method for enzyme encapsulation that selectively immobilizes proteins directly on a transducer surface with no requirement for surface modification before immobilization. OPH is not directly tethered to the SPR surface, which may limit any restriction in the orientation of the active site, as often observed when enzymes are covalently attached to a surface.

The approach may lead to development of a versatile method for the immobilization of enzymes on an SPR transducer surface that might be applied to biosensors or protein microarrays [34–36]. In addition, the methodology developed for OPH immobilization on the gold surface may be applied to other electrochemical detection platforms.

Acknowledgements

This work was supported by the Auburn University Detection and Food Safety Center and NSF Grant (CTS-0330189). H.R.L. was supported by a postdoctoral fellowship managed by the Oak Ridge Institute for Science and Education (U.S. Department of Energy) and funding from the Air Force Office of Scientific Research (Walt Kozumbo, Program Manager). This work could not be accomplished without OPH, generously provided from Dr. J. Wild's Laboratory at TAMU.

References

- [1] T. Laurell, J. Drott, L. Rosengren, *Biosens. Bioelectron.* 10 (1995) 289–299.
- [2] A. Subramanian, S.J. Kennel, P.I. Oden, K.B. Jacobson, J. Woodward, M.J. Doktycz, *Enzyme Microb. Technol.* 24 (1999) 26–34.
- [3] A. Vilkanauskaitė, T. Erichsen, L. Marcinkevičienė, V. Laurinavicius, W. Schuhmann, *Biosens. Bioelectron.* 17 (2002) 1025–1031.
- [4] R.H. Taylor, S.M. Fournier, B.L. Simons, H. Kaplan, M.A. Hefford, *J. Biotechnol.* 118 (2005) 265–269.
- [5] A.W. Flounders, A.K. Singh, J.V. Volponi, S.C. Carichner, K. Wally, A.S. Simonian, J.R. Wild, J.S. Schoeniger, *Biosens. Bioelectron.* 14 (1999) 715–722.
- [6] S.E. Letant, B.R. Hart, S.R. Kane, M.Z. Hadi, S.J. Shields, J.G. Reynolds, *Adv. Mater.* 16 (2004) 689–693.
- [7] R.J. Green, R.A. Frazier, K.M. Shakesheff, M.C. Davies, C.J. Roberts, S.J.B. Tendler, *Biomaterials* 21 (2000) 1823–1835.
- [8] J. Homola, S.S. Yee, G. Gauglitz, *Sens. Actuators B: Chem.* 54 (1999) 3–15.
- [9] D.G. Myszkowski, *FASEB J.* 14 (2000) A1511–A1511.

- [10] Y.R. Kim, H.J. Paik, C.K. Ober, G.W. Coates, S.S. Mark, T.E. Ryan, C.A. Batt, *Macromol. Biosci.* 6 (2006) 145–152.
- [11] J.H. Kim, S. Roy, J.T. Kellis, A.J. Poulouse, A.P. Gast, C.R. Robertson, *Langmuir* 18 (2002) 6312–6318.
- [12] H.J. Lee, A.W. Wark, R.M. Corn, *Langmuir* 22 (2006) 5241–5250.
- [13] H.J. Lee, A.W. Wark, T.T. Goodrich, S.P. Fang, R.M. Corn, *Langmuir* 21 (2005) 4050–4057.
- [14] C.D. Hodneland, Y.S. Lee, D.H. Min, M. Mrksich, *Proc. Natl. Acad. Sci. U.S.A.* 99 (2002) 5048–5052.
- [15] H.R. Luckarift, M.B. Dickerson, K.H. Sandhage, J.C. Spain, *Small* 2 (2006) 640–643.
- [16] J.N. Cha, K. Shimizu, Y. Zhou, S.C. Christiansen, B.F. Chmelka, G.D. Stucky, D.E. Morse, *Proc. Natl. Acad. Sci. U.S.A.* 96 (1999) 361–365.
- [17] T. Coradin, P.J. Lopez, G. Gautier, J. Livage, *Comptes Rendus Palevol.* 3 (2004) 443–452.
- [18] N. Kroger, R. Deutzmann, M. Sumper, *Science* 286 (1999) 1129–1132.
- [19] H.R. Luckarift, J.C. Spain, R.R. Naik, M.O. Stone, *Nat. Biotechnol.* 22 (2004) 211–213.
- [20] J.M. Kleijn, D. Barten, M.A.C. Stuart, *Langmuir* 20 (2004) 9703–9713.
- [21] C.A. Haynes, W. Norde, *Colloids Surf. B* 2 (1994) 517–566.
- [22] T.J. Su, J.R. Lu, R.K. Thomas, Z.F. Cui, J. Penfold, *Langmuir* 14 (1998) 438–445.
- [23] S. Szunerits, R. Boukherroub, *Electrochem. Commun.* 8 (2006) 439–444.
- [24] D.K. Kambhampati, T.A.M. Jakob, J.W. Robertson, M. Cai, J.E. Pemberton, W. Knoll, *Langmuir* 17 (2001) 1169–1175.
- [25] J.K. Grimsley, J.M. Scholtz, C.N. Pace, J.R. Wild, *Biochemistry* 36 (1997) 14366–14374.
- [26] S. Balasubramanian, I.B. Sorokulova, V.J. Vodyanoy, A.L. Simonian, *Biosens. Bioelectron.* 22 (2007) 948–955.
- [27] L.S. Jung, C.T. Campbell, T.M. Chinowsky, M.N. Mar, S.S. Yee, *Langmuir* 14 (1998) 5636–5648.
- [28] A.N. Naimushin, S.D. Soelberg, D.K. Nguyen, L. Dunlap, D. Bartholomew, J. Elkind, J. Melendez, C.E. Furlong, *Biosens. Bioelectron.* 17 (2002) 573–584.
- [29] J. Aizenberg, V.C. Sundar, A.D. Yablon, J.C. Weaver, G. Chen, *PNAS* 101 (2004) 3358–3363.
- [30] B.D. Di Sioudi, C.E. Miller, K. Lai, J.K. Grimsley, J.R. Wild, *Chem. Biol. Interact.* 119/120 (1999) 211–223.
- [31] E.G. Vrieling, S. Hazelaar, W.W.C. Gieskes, Q. Sun, T.P.M. Beelen, R.A.V. Santen, *Silicon biomineralization: towards mimicking biogenic silica formation in diatoms*, in: W.E.G. Muller (Ed.), *Progress in Molecular and Subcellular Biology*, Springer-Verlag, Berlin, 2003.
- [32] A.L. Simonian, A.W. Flounders, J.R. Wild, *Electroanalysis* 16 (2004) 1896–1906.
- [33] S. Oh, J. Moon, T. Kang, S. Hong, J. Yi, *Sens. Actuators B* 114 (2006) 1096–1099.
- [34] T.J. Lin, K.T. Huang, C.Y. Liu, *Biosens. Bioelectron.* 22 (2006) 513–518.
- [35] H. Huang, Y. Chen, *Biosens. Bioelectron.* 22 (2006) 644–648.
- [36] M.G. Kim, Y.B. Shin, J.M. Jung, H.S. Ro, B.H. Chung, *J. Immunol. Meth.* 297 (2005) 125–132.

Three-Dimensional Immobilization of β -Galactosidase on a Silicon Surface

Lorena Betancor,^{1,2} Heather R. Luckarift,¹ Jae H. Seo,³ Oliver Brand,³ Jim C. Spain²

¹Air Force Research Laboratory, Tyndall AFB, Florida 32403

²School of Civil and Environmental Engineering, Georgia Institute of Technology, 311 Ferst Drive, Atlanta, Georgia 30332; telephone: 404-894-0628; fax: 404-894-0628; e-mail: jspain@ce.gatech.edu

³School of Electrical and Computer Engineering, Georgia Institute of Technology, Atlanta, Georgia 30332

Received 13 March 2007; revision received 12 June 2007; accepted 25 June 2007

Published online 11 July 2007 in Wiley InterScience (www.interscience.wiley.com). DOI 10.1002/bit.21570

ABSTRACT: Many alternative strategies to immobilize and stabilize enzymes have been investigated in recent years for applications in biosensors. The entrapment of enzymes within silica-based nanospheres formed through silicification reactions provides high loading capacities for enzyme immobilization, resulting in high volumetric activity and enhanced mechanical stability. Here we report a strategy for chemically associating silica nanospheres containing entrapped enzyme to a silicon support. β -galactosidase from *E. coli* was used as a model enzyme due to its versatility as a biosensor for lactose. The immobilization strategy resulted in a three-dimensional network of silica attached directly at the silicon surface, providing a significant increase in surface area and a corresponding 3.5-fold increase in enzyme loading compared to enzyme attached directly at the surface. The maximum activity recovered for a silicon square sample of 0.5×0.5 cm was 0.045 IU using the direct attachment of the enzyme through glutaraldehyde and 0.16 IU when using silica nanospheres. The immobilized β -galactosidase prepared by silica deposition was stable and retained more than 80% of its initial activity after 10 days at 24°C. The ability to generate three-dimensional structures with enhanced loading capacity for biosensing molecules offers the potential to substantially amplify biosensor sensitivity.

Biotechnol. Bioeng. 2008;99: 261–267.

© 2007 Wiley Periodicals, Inc.

KEYWORDS: enzyme immobilization; silica; β -galactosidase; three-dimensional immobilization; silicon; biosensors

Introduction

Enzymes are commonly used in biosensors because of their high specificity. Biosensor applications require a highly

active immobilized enzyme system that allows the maintenance of an efficient connection between the sensing molecule and the transduction component of the biosensor. Because of their moderate stability, many alternative strategies to immobilize and stabilize enzymes have been explored to improve the feasibility and applicability of a wide range of biosensor applications. Such strategies include covalent immobilization, physical adsorption, cross-linking, encapsulation, or entrapment (Boyukbayram et al., 2006; Létant et al., 2004; Malhotra et al., 2005; Rauf et al., 2006; Subramanian et al., 1999).

Clearly, enzyme loading will be increased in a relatively thick densely packed layer as opposed to a thin adsorbed or covalently attached monolayer. Diffusion and mass transfer limitations, however, can limit the sensor signal to only a proportion of the enzyme that is active at (or near to) the sensing element (Williams and Blanch, 1994). The search for a strategy that allows an increase of the surface area with the concomitant increase in sensitivity of the biosensor, without compromising the activity of the sensing molecule is therefore an important advancement in biosensor design (Charles et al., 2004; Laurell et al., 1995; Luckarift et al., 2007; Vepari and Kaplan, 2006).

The sol-gel encapsulation of enzymes has recently undergone important developments motivated by its wide applications in biosensors (Avnir et al., 2006; Pierre, 2004). Nevertheless, one of the primary drawbacks of the sol-gel technique is enzyme leakage (Blandino et al., 2000). The problem has in some instances been addressed by designing protocols for the preparation of matrices with a pore size adequate to allow the flow of substrates and products but small enough to prevent the elution of the entrapped

Lorena Betancor's present address is Department of Biochemistry, University of Cambridge, 80 Tennis Court Road, Old Addenbrookes Site, Cambridge CB2 1GA, UK. Correspondence to: J.C. Spain

Contract grant sponsor: Air Force Office of Scientific Research

biocomponent (Blandino et al., 2001; Lu et al., 2006). Enzyme leakage can also be limited by pre-immobilization of enzyme on a solid support before encapsulation in sol-gel (Betancor et al., 2005).

The entrapment of enzymes through biomimetic silicification reactions provides an efficient method for the preparation of robust immobilized derivatives of a variety of enzymes (Berne et al., 2006; Luckarift et al., 2006b, 2004). Among the advantages of the immobilization technique are an absence of enzyme leaching and good mechanical properties; both key criteria for biosensor purposes. The study of silicification reactions has recently provided chemical mechanisms for biological silica formation (Belton et al., 2005; Kroger et al., 2001; Sumper and Kröger, 2004). Amino groups have proven to be crucial in the reactions, leading us to explore the possibility of directly involving amino groups from a functionalized surface in the precipitation of silica as a simple method to covalently associate silica-immobilized enzymes directly and simultaneously to a planar surface.

The use of glutaraldehyde chemistry as a simple and efficient method for enzyme immobilization is well established (Betancor et al., 2006; Honda et al., 2005; Yucel et al., 2007). Glutaraldehyde and APTS are common coupling agents used in binding proteins to silicon surfaces (Longo et al., 2006; Williams and Blanch, 1994). APTS is used to functionalize the surface, forming amino groups which are further activated with glutaraldehyde to form a layer of aldehyde groups which react with the amino groups of protein.

Here, we have compared the immobilization of a β -galactosidase on a silicon surface by (i) direct attachment to the surface via glutaraldehyde and (ii) an indirect attachment by chemical association of β -galactosidase entrapped within silica particles.

β -galactosidase from *E. coli*, a tetramer of 465 kDa (Jacobson et al., 1994), was used as a model enzyme because it has been well characterized, is readily quantified, and has been incorporated in several types of biosensors for the detection and quantification of lactose (Goktug et al., 2005; Sharma et al., 2004; Tkac et al., 2000; Watanabe et al., 1991).

Materials and Methods

Chemicals

β -galactosidase from *E. coli* (Grade VIII), monoclonal anti- β -galactosidase antibody produced in mouse (G6282), (3-aminopropyl)triethoxysilane (APTS) and glutaraldehyde (Grade II, 25%) were obtained from Sigma-Aldrich (St. Louis, MO). Secondary Antibody; FITC (Fluorescein Conjugate), Polyclonal Goat Anti-Mouse IgG was purchased from Southern Biotech (Birmingham, AL). The synthetic peptide R5 (SSKKSYSYSGSKGSK RRIL) was obtained from New England Peptides (Gardner, MA).

Potassium phosphate buffer (25 mM, pH 7.0) was used throughout unless otherwise indicated. All other reagents were of analytical grade.

The experiments in this work were performed at least in triplicate and the results are presented as its mean value and corresponding confidence limits.

Functionalization of the Silicon Samples

Single-crystalline lightly doped silicon wafers (0.5×0.5 cm squares) were cleaned in 10% nitric acid at 80°C for 20 min followed by thorough rinsing with distilled water. The cleaned silicon wafers were activated as described previously (Williams and Blanch, 1994). All solutions were applied by placing 20 μL onto the sample surface. Amino-activated silicon samples were prepared by incubating with 10% APTS (v/v) in distilled water for 4 h at 80°C before rinsing thoroughly with distilled water. For glutaraldehyde-activated silicon samples (Glu-Si), the surface was subsequently incubated with 15% (v/v) glutaraldehyde in potassium phosphate buffer 25 mM, pH 7 at 25°C for a minimum of 8 h. Excess glutaraldehyde was removed by thoroughly rinsing with distilled water.

Enzyme Activity Assays

β -galactosidase activity was determined spectrophotometrically by increase in absorbance at 405 nm caused by the hydrolysis of *o*-nitrophenyl- β -D-galactopyranoside (oNPG). The reaction mixture contained 20 mM oNPG and 1 mM MgCl_2 in potassium phosphate buffer. To determine the activity bound to the surface, the samples were incubated in the reaction mixture with gentle agitation. Periodically, samples of the reaction mixture were withdrawn for determination of A_{405} . One enzyme unit (IU) was defined as the amount of enzyme that catalyzes the formation of 1 μmol of product per minute under the specified conditions.

Enzyme Immobilization

Immobilization of the Soluble β -Galactosidase

Immobilization of the soluble enzyme on the silicon surface was carried out by either (1) immersion or (2) evaporation. For immobilization by immersion; activated samples were incubated with 0.08 IU/mL (in 250 μL) at 25°C . Periodically, samples of the supernatant were withdrawn and analyzed for enzyme activity. After 2 h of incubation, the silicon samples were thoroughly rinsed and stored in buffer at 4°C .

For immobilization by evaporation; immobilization was performed by applying the enzyme solution (10 μL volume containing 2 IU/mL) directly on the activated surface at 25°C for 15 min until completely dry. The samples were then rinsed thoroughly and stored in buffer at 4°C .

Silica Entrapment of β -Galactosidase

Silica-entrapment was performed as described previously (Luckarift et al., 2004). Enzyme solutions (0.5 mL) containing 0.02 IU/mL in potassium phosphate buffer (25 mM, pH 8.0) were mixed with 0.125 mL of R5 peptide (100 mg/mL) and 0.125 mL of hydrolyzed tetramethyl orthosilicate (TMOS) solution. The TMOS was hydrolyzed by dilution in hydrochloric acid (1 mM) to a final concentration of 1 M. The particles were agitated for 2 min at 22°C, collected by centrifugation for 10 s (14,000g) and then washed twice in phosphate buffer before use.

Immobilization of the Silica Entrapped Enzyme on the Activated Samples (NH_2 -Si-Enz)

To attach the silica particles to the amino-activated surface, the silica-entrapment was performed directly on the activated surface. Enzyme solutions (10 μL) containing 2 IU/mL in potassium phosphate buffer (25 mM, pH 8.0) were mixed on the sample surface with 2.5 μL of R5 (100 mg/mL) and 2.5 μL of hydrolyzed TMOS solution. After the silica precipitation the samples were washed four times by incubation in buffer with gentle agitation.

Loading Capacity Experiments

The loading capacities of Glu-Si with soluble enzyme and the amino-activated samples with the silica-entrapped enzyme were determined by immobilizing increasing concentrations (2–20 UI/mL) of β -galactosidase, as described above.

Detection of Immobilized β -Galactosidase on Glu-Si

Each silicon sample was incubated with 2 mL of a 1/2,000 dilution of monoclonal anti- β -galactosidase antibody in phosphate buffered saline (PBS) for the detection of native or denatured enzyme molecules. The incubation was carried out for 3 h at 25°C. Samples were then washed thoroughly with PBS and further incubated with a 1/2,000 dilution of secondary antibody (fluorescein conjugated) for 3 h at 25°C. Samples were washed thoroughly with PBS and kept in the same buffer at 4°C for further analysis.

Fluorescence at the surface was imaged on a Zeiss Axiovert 200 microscope equipped with a Zeiss filter set #9 (EX: BP 450-490, FT 510, EM: LP 515). Images were recorded using a Zeiss AxioCam MRc digital camera.

Results and Discussion

Immobilization of Soluble β -Galactosidase to Silicon Samples

A silicon wafer surface was functionalized with APTS and glutaraldehyde to form a layer of aldehyde groups

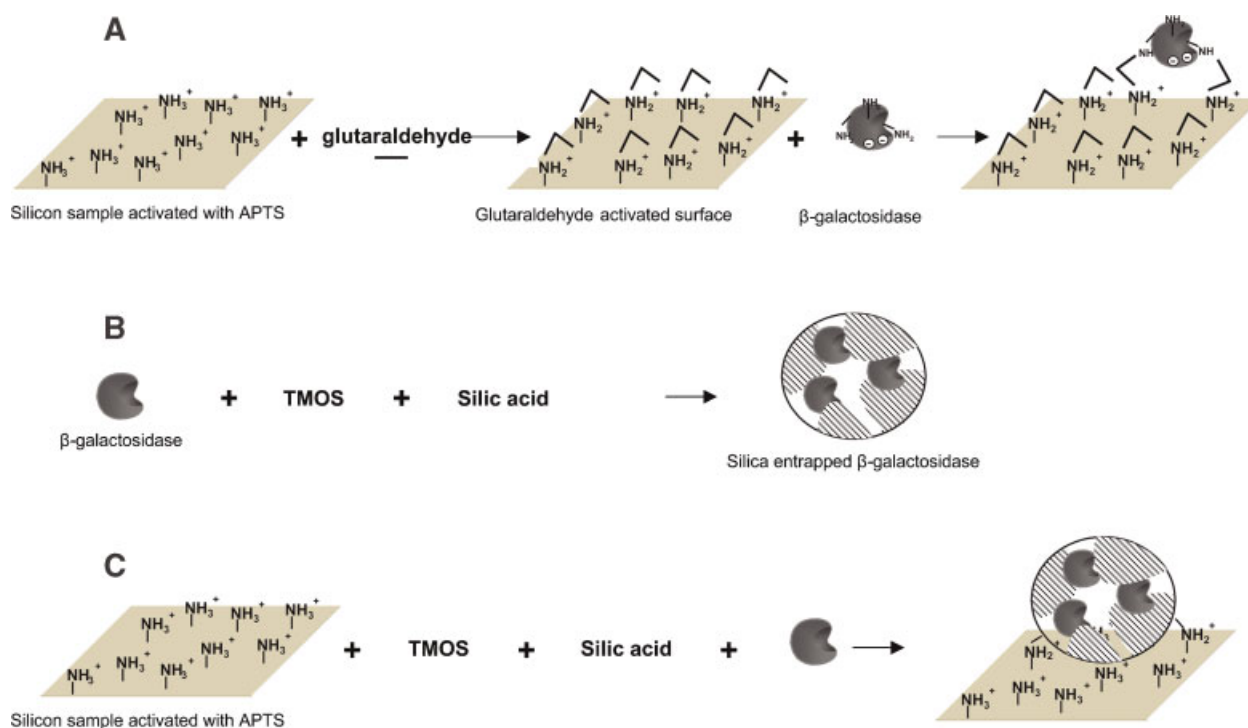
which react with the amino groups of β -galactosidase (Scheme 1A). The Glu-Si were submerged in enzyme solution and immobilization was followed by measuring activity of the remaining free enzyme in the supernatant (Fig. 1). Almost 89% (± 4.5) of the initial enzyme activity was immobilized within 2 h. As an alternate strategy, immobilization of the same amount of enzyme could be achieved by using evaporation to drive immobilization. The evaporation method significantly reduced the incubation time required for complete immobilization to 15 min and yielded substantially higher immobilization efficiencies consistent with previously reported values for the immobilization of β -galactosidase from *E. coli* (Pessela et al., 2007; Fig. 2). Non-specific adsorption of enzyme using either method was 18.5% (± 0.5). Enzyme attached by non-specific binding, however, was readily removed by washing.

The immobilization of β -galactosidase through glutaraldehyde chemistry was confirmed by fluorescence microscopy using antigen-antibody interactions (Fig. 3). Fluorescence microscopy showed an evenly distributed fluorescence signal in the functionalized samples and no signal for a negative control containing a non-functionalized silicon wafer incubated with β -galactosidase (Fig. 3).

Immobilization efficiencies of approximately 60% ($56.35\% \pm 6.16$) were obtained for enzyme loadings lower than 0.06 IU (Fig. 4). When the initial β -galactosidase activity was increased further, a percentage of the activity remained in the supernatant due to saturation of the surface, which decreased the immobilization yield. A maximum loading capacity of the activated silicon samples of 0.045 IU, however, was obtained at high enzyme concentrations despite the lower overall immobilization yield (Fig. 4).

Immobilization of Silica-Encapsulated β -Galactosidase to Silicon Samples

In order to further enhance the stability and loading capacity of the silicon samples we next investigated the formation of three-dimensional silica-immobilized enzymes directly at the surface (Scheme 1C). Because amino groups are critical for biological silica formation, we explored the integration of amino groups from a functionalized surface with the precipitation of silica particles, in order to covalently associate silica-immobilized enzymes directly and simultaneously to a planar surface. Silicon samples were functionalized with amino groups by activation with APTS and used to prepare surface-immobilized β -galactosidase. The biomimetic procedure for silica-entrapment of enzymes (Luckarift et al., 2004) was performed directly on the surface of the functionalized samples. Silica precipitation occurred rapidly for enzyme concentrations of 0.1–2 IU. No activity was found in the wash fractions following immobilization. The strategy led to immobilization of 3.5 times more enzyme activity than in the Glu-Si, where enzyme attachment was most likely limited to a surface-associated monolayer (Fig. 5).



Scheme 1. Immobilization strategies used in this work. **A:** Immobilization of soluble β -galactosidase to Glu-Si. **B:** Entrapment of β -galactosidase in silica particles. **C:** Immobilization of silica-encapsulated β -galactosidase to silicon samples. [Color figure can be seen in the online version of this article, available at www.interscience.wiley.com.]

The amount of immobilized enzyme bound to the silicon surface increased linearly with increasing concentration of enzyme in the reaction solution. The immobilization yield of the resulting samples, however, remained constant at 9.7% (± 1.0) irrespective of the starting concentration. This effect was not observed with the β -galactosidase directly bound to

the surface through glutaraldehyde (Fig. 5) which reached a plateau concentration as the surface became saturated. In comparison, entrapment of enzyme (Scheme 1B; even at higher enzyme concentrations) resulted in an immobilization yield of 45.3% (± 0.2) when the silica particles were freely suspended in buffer. The low activity on the silicon surface is therefore attributed to mass transfer problems associated with diffusion of substrate and product into the silica particles and access to the enzyme's active site. Mass transfer limitations are presumed to arise from the packing of the silica particles upon the surface rather than the entrapment of the enzyme within the silica particle. This limitation has been previously reported in the design of three-dimensional structures for biosensors (Charles et al., 2004).

The sensitivity of a putative biosensor would increase with an increased amount of active enzyme associated with it. Therefore, despite having a low immobilization yield, with 3.5 times more activity the 3D method clearly overcomes the saturation limitation of direct attachment onto the surface.

Silicon samples that had been washed but not activated with APTS did not retain any enzyme activity after the silica deposition step indicating that the APTS functionalization was essential to associate the silica particles to the surface. SEM micrographs of the silica-immobilized enzyme attached to the silicon samples revealed an uneven coverage by a three-dimensional network of silica particles (Fig. 6).

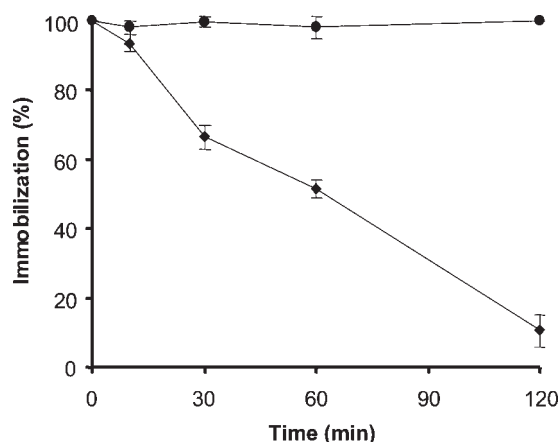


Figure 1. Time course of β -galactosidase immobilization onto Glu-Si. Enzyme activity in supernatant (◆) from enzyme incubated by immersion with silicon wafer; control (●) from enzyme activity in buffer. Immobilization (%) = activity in the supernatant/initial activity $\times 100$.

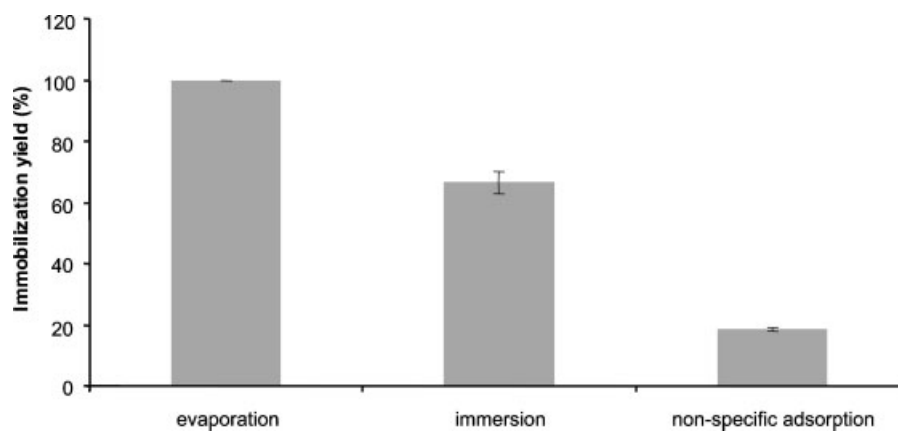


Figure 2. Immobilization yield obtained by various immobilization methods. Immobilization yield (%) = activity bound to the sample/initial activity \times 100.

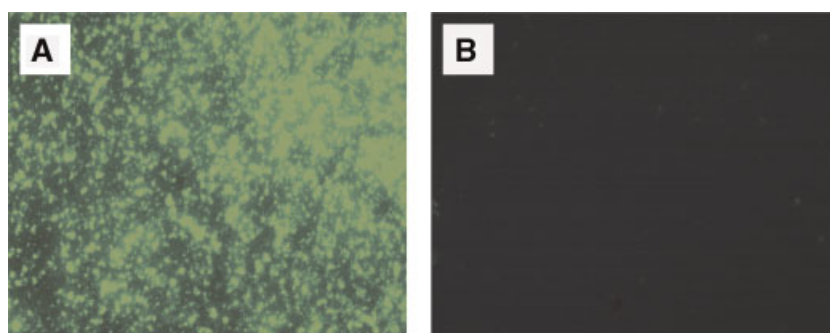


Figure 3. Detection of immobilized β -galactosidase by fluorescence microscopy. Immobilized samples were treated sequentially with a monoclonal antibody and a secondary FITC-conjugated antibody. **A:** β -galactosidase immobilized to a functionalized silicon sample. **B:** control (non-functionalized sample incubated with β -galactosidase). [Color figure can be seen in the online version of this article, available at www.interscience.wiley.com.]

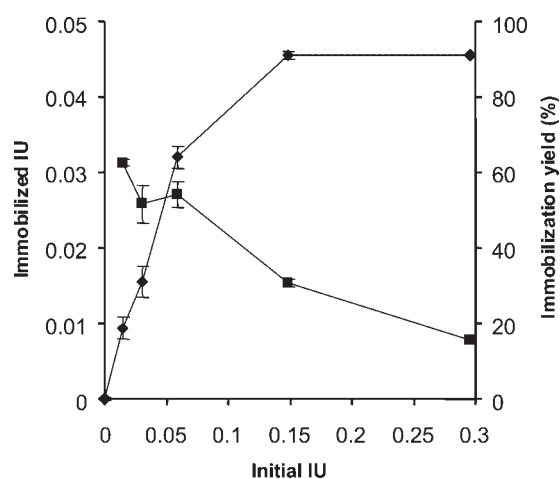


Figure 4. Loading capacity of the Glu-Si. β -galactosidase was applied to a Glu-Si at a range of concentrations. Immobilization yield (%) (■); immobilized IU (◆). Immobilization yield (%) = activity bound to the sample/initial activity \times 100.

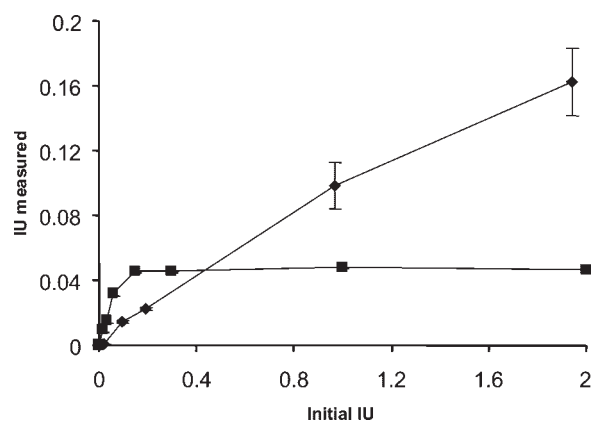


Figure 5. Loading capacity of functionalized silicon samples upon silica-enzyme entrapment. Immobilization of β -galactosidase on Glu-Si (■); immobilization of $\text{NH}_2\text{-Si-Enz}$ (◆).

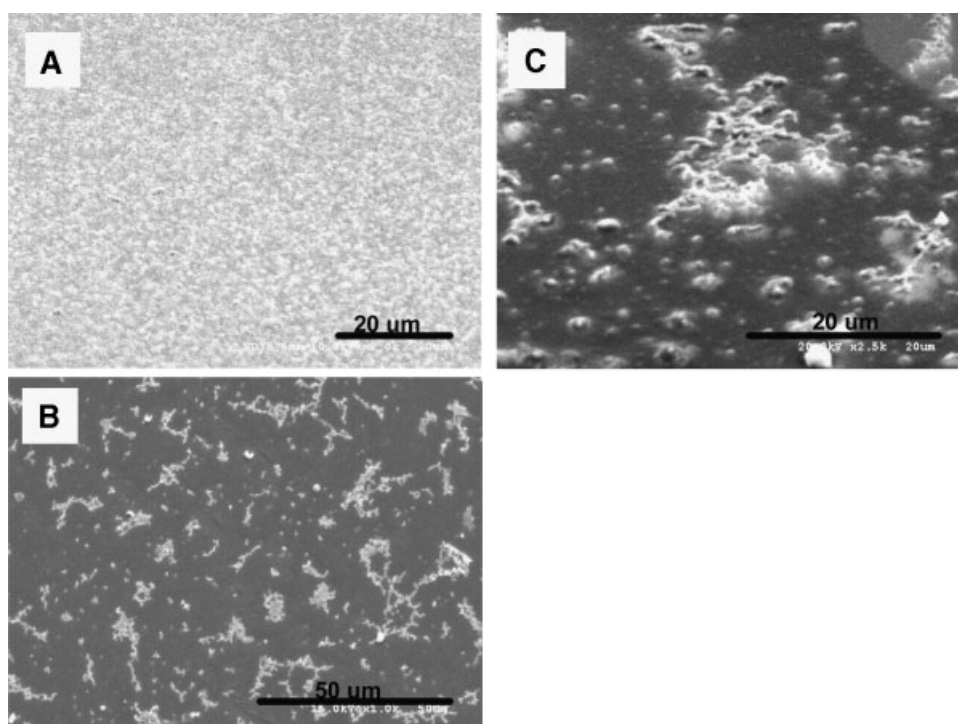


Figure 6. SEM micrographs of $\text{NH}_2\text{-Si-Enz}$. **A–C** show different areas of the immobilized samples. Samples were sputter coated with gold before analysis.

Enzyme stability issues are always of high significance in the production of a stable and reproducible biosensor. Furthermore, the practical application of otherwise interesting putative sensing enzymes is often hindered by their poor stability (Kim et al., 2006). The immobilization of enzymes on unusual surfaces and especially by covalent attachment is sometimes detrimental to the stability of

the enzyme (Brena et al., 2003). The immobilized samples prepared herein by silica deposition retained more than 80% of their initial activity after 10 days at 24°C and their stability proved slightly better than the enzyme directly bound to the surface by glutaraldehyde (Fig. 7). Moreover, the activity of the samples remained unchanged when stored at 4°C for more than 4 weeks (data not shown).

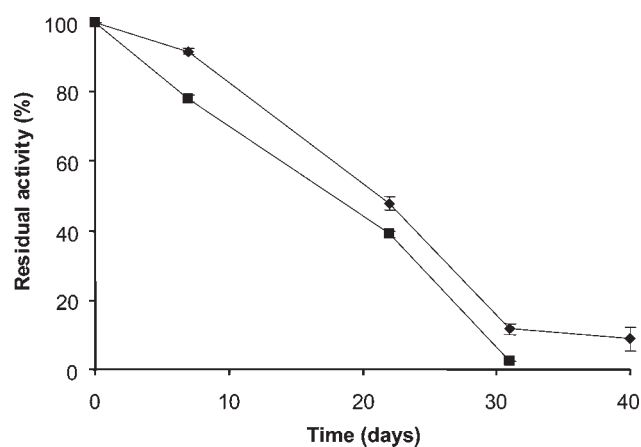


Figure 7. Storage stability of different immobilized samples. ■: β -galactosidase immobilized on Glu-Si. ♦: $\text{NH}_2\text{-Si-Enz}$. The stability experiment was carried out at 25°C and pH 7.

Conclusions

In this work, we have demonstrated a method for three-dimensional enzyme immobilization by involvement of amino groups of a functionalized silicon surface with the biomimetic reactions used to deposit silica. Unlike other attempts to attach silica particles to silicon substrates, where extremely high temperatures were used (900°C ; Zou and Yang, 2006), the system described works under conditions suited to the physiological requirements of biomolecules. In addition, immobilization, attachment and hence stabilization of the enzyme occur simultaneously providing a simple and rapid method for preparation.

The use of silica particles to build a three-dimensional structure not only provides an increased capacity for the immobilization of β -galactosidase but also an improved stability of the sensor molecule. The loading capacities obtained demonstrate the applicability of the concept for biosensors where high loadings of stable sensing molecules are needed. Analysis of the silica-coatings, however,

indicates a non-uniform deposition of silica on the surface. A similar observation was also made for the lysozyme-mediated precipitation of silica at a gold surface (Luckarift et al., 2006b) and for covalent immobilization strategies in general (Subramanian et al., 1999). The preliminary technique described here with further optimization could, however, provide significant enhancement to increase the sensitivity of biosensors or as a strategy for three-dimensional sensors (Charles et al., 2004; Rubina et al., 2004).

This work was supported by funding from the Air Force Office of Scientific Research. L.B and H.R.L were supported by postdoctoral fellowships from the Oak Ridge Institute for Science and Education (US Department of Energy). The authors thank Prof. Nils Kroger and Dr. Nicole Poulsen for help with the fluorescence microscopy.

References

- Avnir D, Coradin T, Lev O, Livage J. 2006. Recent bio-applications of sol-gel materials. *J Mater Chem* 16(11):1013–1030.
- Belton DJ, Patwardhan SV, Perry C. 2005. Spermine, spermidine and their analogues generate tailored silicas. *J Mater Chem* 15(3):4629–4638.
- Berne C, Betancor L, Luckarift HR, Spain JC. 2006. Application of a microfluidic reactor for screening cancer prodrug activation using silica-immobilized nitrobenzene nitroreductase. *Biomacromolecules* 7(9):2631–2636.
- Betancor L, Lopez-Gallego F, Hidalgo A, Alonso-Morales N, Mateo C, Dellamora-Ortiz G, Fernandez-Lafuente R, Guisan JM. 2006. Different mechanisms of protein immobilization on glutaraldehyde activated supports: Effect of support activation and immobilization conditions. *Enzyme Microb Technol* 39(4):877–882.
- Betancor L, Lopez-Gallego F, Hidalgo A, Fuentes M, Podrasky O, Kuncova G, Guisan JM, Fernandez-Lafuente R. 2005. Advantages of the pre-immobilization of enzymes on porous supports for their entrapment in sol-gels. *Biomacromolecules* 6(2):1027–1030.
- Blandino A, Macias M, Cantero D. 2000. Glucose oxidase release from calcium alginate gel capsules. *Enzyme Microb Technol* 27(3–5):319.
- Blandino A, Macias M, Cantero D. 2001. Immobilization of glucose oxidase within calcium alginate gel capsules. *Process Biochem* 36(7):601.
- Boyukbayram AE, Kiralp S, Toppare L, Yagci Y. 2006. Preparation of biosensors by immobilization of polyphenol oxidase in conducting copolymers and their use in determination of phenolic compounds in red wine. *Bioelectrochemistry* 69(2):164–171.
- Brena BM, Irazoqui G, Giacomini C, Batista-Viera F. 2003. Effect of increasing co-solvent concentration on the stability of soluble and immobilized β -galactosidase. *J Mol Catal B Enzym* 21(1/2):25–29.
- Charles PT, Goldman ER, Rangasamy JG, Schauer CL, Chen M-S, Taitt CR. 2004. Fabrication and characterization of 3D hydrogel microarrays to measure antigenicity and antibody functionality for biosensor applications. *Biosens Bioelectron* 20(4):753–764.
- Goktug T, Sezginurk MK, Dinckaya E. 2005. Glucose oxidase- β -galactosidase hybrid biosensor based on glassy carbon electrode modified with mercury for lactose determination. *Analytica Chimica Acta* 551(1/2): 51–56.
- Honda T, Miyazaki M, Nakamura H, Maeda H. 2005. Immobilization of enzymes on a microchannel surface through cross-linking polymerization. *Chem Commun* 40:5062–5064.
- Jacobson RH, Zhang XJ, DuBose RF, Matthews BW. 1994. Three-dimensional structure of β -galactosidase from *E. coli*. *Nature* 369(6483):761–766.
- Kim J, Grate JW, Wang P. 2006. Nanostructures for enzyme stabilization. *Chem Eng Sci* 61(3):1017–1026.
- Kroger N, Deutzmann R, Sumper M. 2001. Silica-precipitating peptides from diatoms. The chemical structure of silaffin-1a from *cylindrotheca fusiformis*. *J Biol Chem* 276(28):26066–26070.
- Laurell T, Drott J, Rosengren L. 1995. Silicon wafer integrated enzyme reactors. *Biosens Bioelectron* 10(3/4):289–299.
- Létant SE, Hart BR, Kane SR, Hadi MZ, Shields SJ, Reynolds JG. 2004. Enzyme immobilization on porous silicon surfaces. *Adv Mater* 16(8): 689–693.
- Longo L, Vasapollo G, Guascito M, Malitesta C. 2006. New insights from X-ray photoelectron spectroscopy into the chemistry of covalent enzyme immobilization, with glutamate dehydrogenase (GDH) on silicon dioxide as an example. *Anal Bioanal Chem* 385(1):146–152.
- Lu Y, Jiang Z-Y, Xu S-W, Wu H. 2006. Efficient conversion of CO₂ to formic acid by formate dehydrogenase immobilized in a novel alginate-silica hybrid gel. *Catalysis Today* 115(1–4):263–268.
- Luckarift HR, Balasubramanian S, Paliwal S, Johnson GR, Simonian AL. 2007. Enzyme-encapsulated silica monolayers for rapid functionalization of a gold surface. *Colloids Surf B Biointerfaces* 58(1):28–33.
- Luckarift HR, Dickerson MB, Sandhage KH, Spain JC. 2006b. Rapid, room-temperature synthesis of antibacterial bionanocomposites of lysozyme with amorphous silica or titania. *Small* 2(5):640–643.
- Luckarift HR, Spain JC, Naik RR, Stone MO. 2004. Enzyme immobilization in a biomimetic silica support. *Nat Biotech* 22(2):211.
- Malhotra BD, Singhal R, Chaubey A, Sharma SK, Kumar A. 2005. Recent trends in biosensors. *Curr Appl Phys* 5(2):92.
- Pessela BCC, Dellamora-Ortiz G, Betancor L, Fuentes M, Guisan JM, Fernandez-Lafuente R. 2007. Modulation of the catalytic properties of multimeric β -galactosidase from *E. coli* by using different immobilization protocols. *Enzyme Microb Technol* 40(2):310–315.
- Pierre AC. 2004. The sol-gel encapsulation of enzymes. *Biocatalysis Bio-transformation* 22(3):145–170.
- Rauf S, Ihsan A, Akhtar K, Ghauri MA, Rahman M, Anwar MA, Khalid AM. 2006. Glucose oxidase immobilization on a novel cellulose acetate-polymethylmethacrylate membrane. *J Biotechnol* 121(3):351–360.
- Rubina AY, Pan'kov SV, Dementieva EI, Pen'kov DN, Butygin AV, Vasiliskov VA, Chudinov AV, Mikheikin AL, Mikhailovich VM, Mirzabekov AD. 2004. Hydrogel drop microchips with immobilized DNA: Properties and methods for large-scale production. *Anal Biochem* 325(1):92–106.
- Sharma SK, Singhal R, Malhotra BD, Sehgal N, Kumar A. 2004. Lactose biosensor based on Langmuir-Blodgett films of poly(3-hexyl thiophene). *Biosens Bioelectron* 20(3):651–657.
- Subramanian A, Kennel SJ, Oden PI, Jacobson KB, Woodward J, Doktycz MJ. 1999. Comparison of techniques for enzyme immobilization on silicon supports. *Enzyme Microb Technol* 24(1–2):26–34.
- Sumper M, Kröger N. 2004. Silica formation in diatoms: The function of long-chain polyamines and silaffins. *J Mater Chem* 14(14):2059–2065.
- Tkac J, Sturdik E, Gemeiner P. 2000. Novel glucose non-interference biosensor for lactose detection based on galactose oxidase-peroxidase with and without co-immobilised β -galactosidase. *Analyst* 125(7): 1285–1289.
- Vepari CP, Kaplan DL. 2006. Covalently immobilized enzyme gradients within three-dimensional porous scaffolds. *Biotechnol Bioeng* 93(6): 1130–1137.
- Watanabe E, Takagi M, Takei S, Hoshi M, Shu-gui C. 1991. Development of biosensors for the simultaneous determination of sucrose and glucose, lactose and glucose, and starch and glucose. *Biotechnol Bioeng* 38(1): 99–103.
- Williams RA, Blanch HW. 1994. Covalent immobilization of protein monolayers for biosensor applications. *Biosens Bioelectron* 9(2):159.
- Yucel D, Ozer N, Hasirci V. 2007. Construction of a choline biosensor through enzyme immobilization on a poly(2-hydroxyethyl methacrylate)-grafted Teflon film. *J Appl Polym Sci* 104(5):3469–3477.
- Zou M, Yang D. 2006. Nanoindentation of silica nanoparticles attached to a silicon substrate. *Tribology Lett* 22(2):189–196.

Application of a Microfluidic Reactor for Screening Cancer Prodrug Activation Using Silica-Immobilized Nitrobenzene Nitroreductase

Cécile Berne,^{†,‡,§} Lorena Betancor,^{†,‡,§} Heather R. Luckarift,[†] and Jim C. Spain^{*,‡}

Air Force Research Laboratory, 139 Barnes Drive, Building 1117, Suite #2, Tyndall AFB, Florida 32403, and School of Civil and Environmental Engineering, Georgia Institute of Technology, 311 Ferst Drive, Atlanta, Georgia 30332

Received February 22, 2006; Revised Manuscript Received June 6, 2006

The nitroreductase-catalyzed conversion of a strong electron-withdrawing nitro group to the corresponding electron-donating hydroxylamine is useful in a variety of biotechnological applications. Activation of prodrugs for cancer treatments or antibiotic therapy are the most common applications. Here, we show that a bacterial nitrobenzene nitroreductase (NbzA) from *Pseudomonas pseudoalcaligenes* JS45 activates the dinitrobenzamide cancer prodrug CB1954 and the proantibiotic nitrofurazone. NbzA was purified by affinity chromatography and screened for substrate specificity with respect to prodrug activation. To facilitate screening of alternate potential prodrugs, polyethyleneimine-mediated silica formation was used to immobilize NbzA with high immobilization yields and high loading capacities. Greater than 80% of the NbzA was immobilized, and enzyme activity was significantly more stable than NbzA in solution. The resulting silica-encapsulated NbzA was packed into a microfluidic microreactor that proved suitable for continuous operation using nitrobenzene, CB1954, and the proantibiotic nitrofurazone. The flow-through system provides a rapid and reproducible screening method for determining the NbzA-catalyzed activation of prodrugs and proantibiotics.

Introduction

Nitroreductases have received increasing attention due to their ability to activate prodrugs for in vitro drug therapy. Reduction of a strong electron-withdrawing nitro group to the corresponding electron-donating hydroxylamine results in a very large electronic change, providing an effective enzyme-mediated electronic “trigger”.¹ Nitroreductase enzymes, therefore, find significant biotechnological application in the generation of strong cytotoxins by directed enzyme-prodrug therapy (DEPT).¹ A wide range of compounds based on dinitrobenzamide motifs have been synthesized and examined as prodrug candidates. The monofunctional prodrug 5-aziriny-2,4-dinitrobenzamide (CB1954), for example, can be activated to form a cytotoxic DNA cross-linking hydroxylamine derivative by bacterial nitroreductases.^{2–4} DEPT using *Escherichia coli* nitroreductase and CB1954 has been demonstrated to be an effective means to kill cancerous cells^{1,5,6} and is in phase 1 clinical trials.⁴ For successful application to DEPT therapy, nitroreductases should have high substrate affinity, specificity, and turnover so that sufficient cytotoxin can be generated to kill the tumorous cells. The nitroreductase (NTR) purified from *E. coli* is the most effective and hence extensively studied enzyme for DEPT to date. However, only a very small fraction of the available metabolic diversity of nitroreductases has been explored to date, because screening methods are inefficient. It could be important to screen a wide range of bacterial nitroreductases with the potential ability to be more efficient prodrug activators.

Nitroreductases are also known to activate nitrofurantoin antibiotics that are used to treat burns, skin grafts, and genitourinary infections.^{7,8} The activation of the antibiotics leads to a hydroxylamine intermediate that reacts with DNA and causes its fragmentation.⁸ Reduction of nitrofurantoin antibiotics is critical for their activation, and bacteria with mutations in nitroreductase genes develop nitrofurantoin resistance.^{7,9}

Enzyme immobilization provides a versatile physicochemical tool that allows the reuse or continuous use of enzymes, facilitates substrate and product recovery, prevents product contamination, and in certain instances, improves the properties of the biocatalyst.^{10,11} Immobilized enzymes have a significant impact in microfluidic applications,¹² for analytical devices used in peptide mapping¹³ and for biocatalytic applications.¹⁴ The entrapment of enzymes on silica-based particles formed through biomimetic silicification reactions has recently been reported as a very efficient method for enzyme immobilization resulting in high thermostability, volumetric activity, and mechanical stability.^{15,16} Silica formation in biogenic systems is mediated by cationic proteins and peptides,¹⁷ but a range of simple polyamine molecules¹⁸ can mediate an analogous reaction¹⁵ that combines the advantages of silica encapsulation with a significant reduction in cost. Polyethyleneimine (PEI), for example, precipitates silica in the presence of silicic acid.¹⁹ This water-soluble cationic polymer has been extensively used for stabilizing enzymes by generating hydrophilic microenvironments that protect the enzyme from denaturation.^{20,21} However, to our knowledge, there are no reports of silica encapsulation of enzymes using PEI as a mediator.

The nitrobenzene nitroreductase (NbzA) from *Pseudomonas pseudoalcaligenes* JS45 (AC A4468) is able to reduce nitrobenzene to hydroxylaminobenzene.²² Characterization of NbzA revealed inducible control of NbzA expression by nitrobenzene

* To whom correspondence should be addressed. Phone: (404) 894 0628. Fax: (404) 894 8266.

[†] Air Force Research Laboratory.

[‡] Georgia Institute of Technology.

[§] Both authors contributed equally to this work.

and high affinity for this substrate (low K_m), indicating that nitrobenzene is the physiological substrate for NbzA.²² NbzA also plays a role during the degradation of 2,4,6-trinitrotoluene by *P. pseudoalcaligenes* JS45, where it catalyzes the reduction of the explosive compound to 2,4-dihydroxylamino-6-nitrotoluene.²³

Despite the potential pharmacological role of nitroreductases, there are few literature reports demonstrating the immobilization of such enzymes. The majority of the work focuses on biosensing applications.^{24,25} The immobilization of a nitroreductase by entrapment in silica particles mediated by PEI is reported herein. The immobilized enzyme preparation was highly stable in a microreactor used as a continuous-flow system to assess nitroreductase activity with nitrobenzene, CB1954, and nitrofurazone.

Experimental Section

Materials. All chemicals were of analytical or HPLC grade and purchased from Sigma-Aldrich (St. Louis, MO). Potassium phosphate buffer (25 mM, pH 7.0) was used throughout unless otherwise indicated.

Expression and Purification of the Nitrobenzene Nitroreductase (NbzA) from *Pseudomonas pseudoalcaligenes* JS45. PCR was used to amplify the *nbzA* gene²⁶ (682 bp, without the start codon) from *P. pseudoalcaligenes* JS45 genome (G. Zylstra, unpublished data). The primers used were: (forward) 5'-CCC ATG GGG CAT CAT CAC CAT CAC CAT CCG ACC AGC CCG TTC ATT G-3' and (reverse) 5'-AAG CTT GGC CTA TAC GGA ATT ACC TGG-3', including the *Nco*I and *Hind*III restriction sites, respectively (bold), and a sequence encoding for six histidine residues (italic). The amplified fragment was cloned into pCR-TOPO vector (TOPO-TA cloning kit, Invitrogen, Carlsbad, CA). After a double digestion by *Nco*I and *Hind*III followed by extraction from an agarose gel, the fragment containing *nbzA* was cloned into the commercial expression vector pBAD-HisA (Invitrogen, Carlsbad, CA), digested with the same enzymes, and designated plasmid pCBJS08. The *Nco*I digestion of pBAD-A released 33 kb from the (His)₆ tag, the Xpress epitope, and the enterokinase cleavage site of the vector. The smaller (His)₆ tag included on the 5' primer was used for the purification. The plasmid pCBJS08 was transformed into *E. coli* Top10 (F⁻ *mcrA* Δ (*mrr-hsdRMS-mcrBC*) ϕ 80*lacZ* Δ M15 Δ *lacX74* *recA1* *araD139* Δ (*ara-leu*)7697 *galU* *galK* *rpsL* (Str^R) *endA1* *nupG*, Invitrogen, Carlsbad, CA), to give the strain *E. coli* Top10 pBAD-*nbzA*.

An overnight culture from a single colony (1/100, v/v) of *E. coli* Top10 pBAD-*nbzA* was inoculated into Luria broth containing ampicillin (100 microgram/mL). Cultures were grown at 37 °C to an optical density of 0.6–0.8 at 600 nm. L-Arabinose (0.002%) was added, and the cells were incubated at 22 °C for an additional 16 h to induce the expression of the recombinant nitrobenzene nitroreductase.

Cells were harvested via centrifugation (7 000g) for 10 min at 4 °C, washed twice, and suspended in saline potassium phosphate buffer (50 mM, pH 7.0, 500 mM NaCl). The cells were lysed by 3 passes through a French pressure cell (16 000 psi). Cell debris and unbroken cells were removed by centrifugation (10 000g for 20 min at 4 °C). The supernatant containing heterologous NbzA was loaded on a Co²⁺-NTA affinity column (HiTrap Chelating HP, GE Healthcare, Piscataway, NJ) and equilibrated with saline potassium phosphate buffer. After washing with the same buffer, proteins were eluted with a gradient of 500 mM imidazole in saline potassium phosphate buffer. The (His)₆-tagged NbzA was eluted with 100 mM imidazole. Fractions with NbzA activity were dialyzed overnight against potassium phosphate buffer at 4 °C, using a Slide-A-Lyzer 10 000 MWCO (Pierce Biotechnology, Rockford, IL).

NbzA Activity. Reductase activity was determined spectrophotometrically (Cary 50 spectrophotometer, Varian Sunnydale, CA) by monitoring the decrease in absorbance at 340 nm due to the oxidation of NADPH. The reaction mixture contained 100 μ M nitrobenzene and

250 μ M NADPH in potassium phosphate buffer.²² Assays were performed at 25 °C and continuously mixed with a magnetic stirrer. For the determination of kinetic parameters with nitrobenzene, nitrofurazone, and CB1954, the NbzA activity measurements were performed as described above by varying the substrate concentration in the reaction mixture. One enzyme unit (IU) was defined as the amount of enzyme that catalyzes the oxidation of 1 μ mol of NADPH per minute under the specified conditions.

NbzA Immobilization. NbzA immobilization was carried out as previously described by Luckarift et al.¹⁵ Samples (0.5 mL) of enzyme solutions (protein concentration from 0.025 to 2.0 mg/mL) in potassium phosphate buffer (25 mM, pH 8.0) were mixed with 0.125 or 1.25 mL of 10% polyethyleneimine (PEI) (pH 8.0) (final PEI concentrations 1% and 10%, respectively) and 0.125 or 0.375 mL of a hydrolyzed tetramethyl orthosilicate (TMOS) solution (final TMOS concentrations 1% and 3%, respectively). The TMOS was hydrolyzed by dilution in hydrochloric acid (1 mM) to a final concentration of 1 M. The mixture was agitated for 2 min at 22 °C, and the particles were collected by centrifugation for 10 s (14 000g) and washed twice in phosphate buffer before use in subsequent experiments. Immobilization yield was defined as the percentage of the initial activity that was immobilized considering the activity remaining in the supernatant. Expressed activity was defined as the ratio of the measured activity of the immobilized enzyme to the difference between the initial activity and the activity in the supernatant.

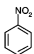
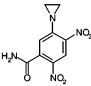
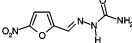
The morphology of the resulting silica particles was characterized by scanning electron microscopy (SEM) (School of Electrical and Computer Engineering, Georgia Institute of Technology, Atlanta, GA).

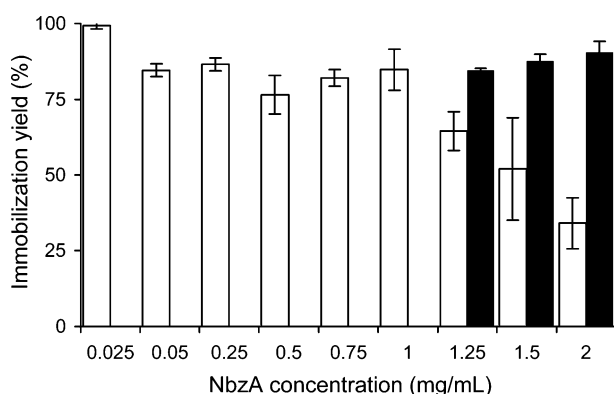
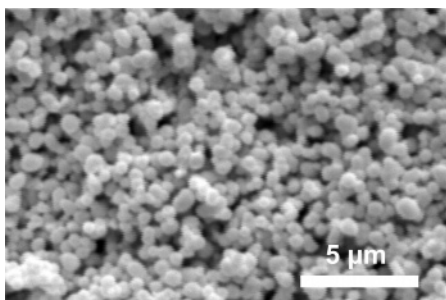
Stability Experiments. Free enzyme solutions and immobilized enzyme suspensions containing 0.05 IU/mL were incubated in phosphate buffer at 40 °C for thermostability experiments or in the presence of acetonitrile (15%) or methanol (50%) for solvent stability experiments. Samples were withdrawn periodically, and enzyme activity was determined as described above.

Microcolumn Experiments. A stainless steel Microbore column (2 cm \times 2 mm, Upchurch Scientific, Oak Harbor, WA) with 0.5 μ m frits was filled with a total of 6 IU of silica-encapsulated NbzA (PEI 1%). Packing was performed by sequentially filling the column with samples of a suspension of the silica-encapsulated NbzA pumped through the column using phosphate buffer (5 μ L/min). The microcolumn was washed with 5 column volumes of phosphate buffer prior to use. All flow-through experiments were carried out at room temperature (22 °C) using a syringe pump (PHD 2000 infusion, Harvard Apparatus, Natick, MA). To determine the substrate conversion, phosphate buffer containing 100 μ M substrate solution (nitrobenzene, CB1954, or nitrofurazone) and 250 μ M NADPH was pumped at flow rates ranging from 1 to 5 μ L/min. After changes in flow rates, samples were collected and analyzed after 5 column volumes had been pumped through the microreactor. The stability of the microreactor was assayed with a continuous flow of phosphate buffer containing 100 μ M nitrobenzene and 250 μ M NADPH at a flow rate of 5 μ L/min. Periodically, samples of the eluate were collected and analyzed by HPLC to determine the degree of nitrobenzene conversion. Due to the spontaneous degradation of NADPH and in order to maintain saturating conditions for the enzyme, the nitrobenzene solution was made fresh every 8 h during continuous use.

Analytical Methods. Conversions were monitored by HPLC using a Spherisorb C8 column (5U, 250 mm, Alltech, Deerfield, IL) with a mobile phase of acetonitrile and water (containing 0.05% and 0.1% trifluoroacetic acid, respectively). The concentration of acetonitrile was increased from 20% to 60% over 13 min, with a flow rate of 1.5 mL/min. Compounds were monitored by UV detection at a single wavelength of 254 nm. Protein concentration was determined by using a BCA (bicinchoninic acid) protein assay reagent kit (Pierce Biotechnology, Rockford, IL) with bovine serum albumin as a standard.

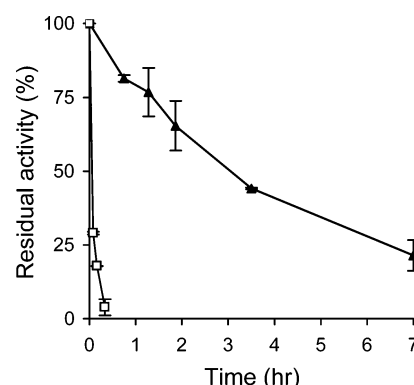
Table 1: K_m Values (μM) of Different Bacterial Nitroreductases

	Soluble NTR	Soluble NTR	Soluble YwrO	Soluble NbzA	PEI silicaencapsulated NbzA (Apparent K_m)
	<i>Escherichia coli</i> ^{1,2,45}	<i>Enterobacter</i> ²⁷	<i>Bacillus amyloliquefaciens</i> ³	<i>P. pseudoalcaligenes</i> JS45	
Nitrobenzene					
	NT ¹	NT	NT	2.3 (\pm 0.35)	2.0 (\pm 0.23)
CB 1954					
	862	NT	618	11.7 (\pm 1)	33.7 (\pm 4.5)
Nitrofurazone					
	64	714	NT	1763 (\pm 572)	5123 (\pm 687)

¹ NT; not tested.**Figure 1.** Effect of immobilization efficiency with increasing NbzA concentration. NbzA was immobilized using PEI 1% and TMOS 1% (white bars) or PEI 1% and TMOS 3% (black bars).**Figure 2.** SEM micrograph of the PEI-mediated silica microparticles containing silica-encapsulated NbzA. Samples were sputtered with gold before analysis.

Results and Discussion

NbzA Expression and Purification. The nitrobenzene nitroreductase (NbzA) from *P. pseudoalcaligenes* JS45 was purified from *E. coli* Top10 with a yield of approximately 1 mg purified (His)₆-tagged protein per liter of culture. Initial attempts to heterologously express the protein using the 3 kDa purification tag from pBAD-HisA (containing the entire (His)₆ tag, Xpress epitope, and enterokinase cleavage site of the vector) led to expression of an inactive protein, presumably due to the additional sequence regions of the vector (data not shown). To

**Figure 3.** Thermal stability of soluble and PEI silica-encapsulated NbzA. Open squares, soluble NbzA; solid triangles, PEI silica-encapsulated NbzA. The PEI silica immobilized and soluble NbzA preparations contained 0.05 IU/mL and were incubated at 40 °C in potassium phosphate buffer. PEI silica-encapsulated NbzA was prepared with 1% PEI.

clone an active protein, a shorter (His)₆ tag was inserted into the 5' PCR primer, and the purification tag was removed from the pBAD-HisA by *Nco*I enzymatic digestion.

The molecular weight of the soluble (His)₆ tag heterologous NbzA was 33 kDa, which is consistent with the size of the protein purified from *P. pseudoalcaligenes* JS45.²² The K_m for nitrobenzene of the (His)₆ tag NbzA purified from *E. coli* in this study was 2.3 (\pm 0.4) μM , consistent with NbzA purified from whole cells of *P. pseudoalcaligenes* (5 μM)²² (Table 1), indicating that heterologous expression and addition of histidines at the N terminus did not substantially modify the protein activity toward nitrobenzene.

NbzA Immobilization. PEI is an inexpensive polyaminated polymer that has been shown to direct the formation of structured silicas in which the morphology can be manipulated by variations in the reaction conditions.¹⁹ We investigated the immobilization of NbzA by entrapment in a silica matrix deposited from a silicic acid solution using PEI as mediator. The immobilization was stable and highly efficient for enzyme concentrations ranging from 0.03 to 1 mg/mL with immobilization yields higher than 80% (Figure 1). The remaining enzyme activity (less than 20%) was detected in the supernatant and in

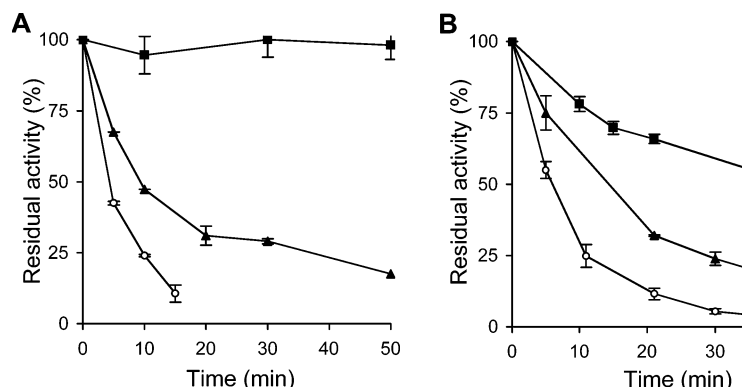


Figure 4. (A) Stability of soluble and PEI silica-encapsulated NbzA in the presence of methanol. Open circles, soluble NbzA; solid triangles, PEI (1%) silica-encapsulated NbzA and solid squares, PEI (10%) silica-encapsulated NbzA. The silica-encapsulated and soluble NbzA preparations contained 0.05 IU/mL and were incubated at 25 °C in potassium phosphate buffer containing methanol (50%) for the indicated times prior to assays. (B) Stability of soluble and PEI silica-encapsulated NbzA in the presence of acetonitrile. Open circles, soluble NbzA; solid triangles, PEI (1%) silica-encapsulated NbzA; and solid squares, PEI (10%) silica-encapsulated NbzA. The silica-encapsulated and soluble NbzA preparations contained 0.05 IU/mL and were incubated at 25 °C in potassium phosphate buffer containing acetonitrile (15%) for the indicated times prior to assays.

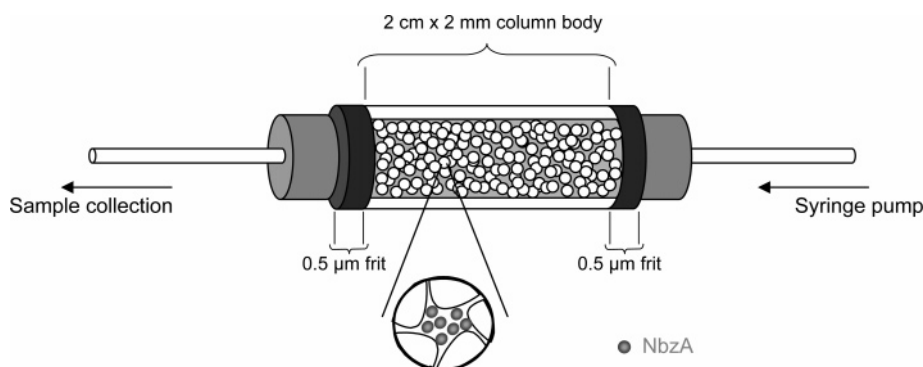


Figure 5. Scheme for immobilized-enzyme microcolumn. The stainless steel body of the microcolumn is 2 mm wide \times 2 cm long, for a total volume of 250 μ L. 6 IU of silica-encapsulated NbzA in 1% PEI (o) were packed inside the column. Two 0.5 μ m frits are placed to both extremities (dark gray). The microcolumn was linked to a syringe pump on one end and a sample collector on the other end.

subsequent wash fractions, indicating negligible loss of activity during immobilization.

The immobilized preparations expressed 60 (\pm 5) % of the theoretical entrapped activity for NbzA concentrations up to 1 mg/mL. Increases in protein concentration above 1 mg/mL resulted in a decrease in immobilization yield as the loading capacity of the silica particles reached saturation, as previously reported.¹⁵ The loading capacity of the reaction could be enhanced, however, by adding additional TMOS to the reaction mixture, thereby extending immobilization yields of higher than 80% to all of the protein concentrations studied (Figure 1).

PEI typically produces silica spheres, but the structures can be manipulated by the addition of solvents during the precipitation reaction, so that the resulting particles can be tailored to suit a specific application.¹⁹ SEM analysis revealed that here PEI mediated the formation of a matrix of interconnected silica particles of approximately 0.5–1.0 μ m diameter (Figure 2).

Kinetics Parameters of Silica-Encapsulated NbzA. Nitroreductases from a wide range of organisms differ substantially in their activity against CB1954 and nitrofurazone (Table 1). The desirable properties of potential enzyme-prodrug combinations are a high differential toxicity of the active species relative to the prodrug and a high affinity of the enzyme for the prodrug. The affinity of the soluble NbzA for nitrofurazone is low in comparison to other enzymes,^{2,27} whereas the affinity for CB1954 is very high (Table 1). The apparent K_m value for nitrobenzene of PEI silica-encapsulated NbzA was comparable to that of the soluble enzyme (Table 1), indicating that enzyme

activity was not significantly hindered by the immobilization within silica particles. For CB1954 and nitrofurazone, apparent K_m values of PEI silica-encapsulated NbzA were 3 and 5 times higher, respectively (Table 1). Diffusion limitations and steric hindrances in immobilized enzyme preparations have been shown to be responsible for higher apparent K_m values compared to the soluble forms.^{28–30}

Stability of Silica-Encapsulated NbzA. Enzymes are extremely versatile and able to catalyze a wide variety of chemical reactions, but practical applications are often hindered by the instability of enzymes.²¹ The expressed activity of silica-encapsulated NbzA remained unchanged when stored at 4 °C for several months (data not shown). The silica-encapsulated NbzA also was dramatically more thermostable than the soluble enzyme (Figure 3). The enhanced stability of immobilized enzyme preparations provides a greater versatility for their use in a wide range of applications.^{14,31–34} The higher thermal stability of the silica-encapsulated NbzA appears to be a consequence not only of the movement constraints imposed by the rigidity of the support³⁵ but also of the presence of PEI itself, which has proven in many instances to have a protective effect on the stability of enzymes.^{20,34,36,37}

A primary limitation of prodrugs such as CB1954 is their relative insolubility in aqueous solutions.^{38,39} The encapsulation of the nitroreductase enzyme within silica might protect the enzyme from solvent denaturation and provide an opportunity to screen poorly soluble prodrugs if the compounds are dissolved in cosolvents. Immobilization of NbzA in silica exerted a

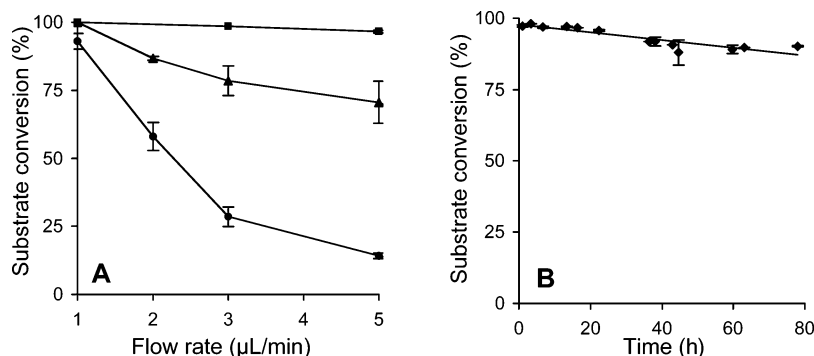


Figure 6. (A) Effect of flow rate on the NbzA column activity. Activity was determined at a range of flow rates between 1 and 5 $\mu\text{L}/\text{min}$. The reaction buffer contained 100 μM substrate (nitrobenzene, squares; CB1954, triangles; and nitrofurazone, circles) and 250 μM NADPH in phosphate buffer. The microcolumn was packed with PEI silica-encapsulated NbzA and contained 6 IU. (B) Operational stability of the NbzA microcolumn. The operational activity was tested with the microcolumn packed with PEI silica-encapsulated NbzA and containing 6 IU. The reaction buffer contained nitrobenzene 100 μM and NADPH 250 μM in potassium phosphate buffer. The continuous flow rate was 5 $\mu\text{L}/\text{min}$.

significant stabilizing effect in methanol and acetonitrile relative to the soluble enzyme (Figure 4). The solvent stability of the immobilized enzymes was even more pronounced when a high concentration of PEI was added during the immobilization process. Addition of PEI concentrations ranging from 1% to 10% to soluble NbzA preparations did not modify the enzymatic activity (data not shown) but provided a protective environment for the enzyme that resulted in complete retention of the initial activity for up to 5 h, in the presence of 50% methanol (Figure 4A). A higher PEI concentration also proved critical for improving the enzyme stability in the presence of acetonitrile (Figure 4B). PEI is a highly hydrophilic molecule; therefore, stabilization could be the result of formation of a hydrophilic shell that promotes a partitioning of the organic solvent, decreasing its concentration in the enzyme microenvironment, an effect that has been previously reported.⁴⁰ Thus, by increasing the amount of PEI in the surroundings of the enzyme, we were able to minimize the negative effect that the organic solvent molecules exert on the enzyme stability.

Continuous Flow-Through System. The size and stability of the silica-encapsulated NbzA particles obtained with our method are suitable for flow-through applications. For microfluidic purposes,¹³ for example, small particle sizes provide a high surface-to-volume ratio and a concomitant increase in mass transfer efficiency. Silica-encapsulated NbzA was packed into a stainless steel microfluidic device as shown in Figure 5. Throughout all the experiments, no enzyme activity was detected in the eluate, indicating that the NbzA was physically entrapped within the silica particles during silica formation and there was no leaching from the particles during continuous use.

Flow rates typical of microfluidic applications (1–5 $\mu\text{L}/\text{min}$) were used^{41,42} without creating back-pressure problems. The flow-through system proved suitable for continuous operation. Conversions of nitrobenzene, CB1954, and nitrofurazone were achieved at a wide range of flow rates (Figure 6A). The conversion decreased with increasing flow rates as expected as a consequence of a reduction in the residence time of the substrate within the microcolumn and the reduced contact time between the substrate and the immobilized enzyme. At 1 $\mu\text{L}/\text{min}$, the three substrates were stoichiometrically converted (Figure 6A). With increasing flow rates, the conversion correlated with the previously measured substrate specificity of NbzA. NbzA, for example, demonstrated the highest affinity for nitrobenzene, and maximum conversion efficiency (substrate conversion per time unit) was achieved at flow rates up to 5 $\mu\text{L}/\text{min}$. The mechanical properties of the immobilized enzyme provided excellent operational stability. A conversion of more

than 90% of the nitrobenzene was observed during continuous use for more than 3 days at room temperature and a flow rate of 5 $\mu\text{L}/\text{min}$ (Figure 6B).

Other nitroreductases with affinity for CB1954 that have been recently purified and characterized^{3,43} could be immobilized in PEI–silica and packed on the microcolumn, as an efficient and cost-effective way to screen for different prodrug reductions. The microreactor designed in this study could also be useful to test the reduction of nitrofurazone derivatives by NbzA or other nitroreductase enzymes immobilized inside the microcolumn.

Conclusion

Advances in the field of microreactors are limited by the availability of new support materials and immobilized enzymes or the lack of robustness of the immobilized preparations.^{12,44} On the basis of our results, PEI-mediated silica encapsulation seems to be an effective way to immobilize enzymes for use in microreactors. Moreover, the excellent stability properties of our system provided the basis for a range of potential microfluidic applications of silica-encapsulated enzymes. Further experiments on the tailoring of the physical morphology of the PEI silica for a particular application as well as optimizing the column configuration will broaden the range of applications of the system.

Acknowledgment. This work was supported by funding from the Air Force Office of Scientific Research. C. B., L.B., and H.R.L. were supported by postdoctoral fellowships from the Oak Ridge Institute for Science and Education (U.S. Department of Energy). The authors thank Jae Hyeong Seo for the SEM pictures and Rebecca Daprato for the use of the syringe pumps.

References and Notes

- (1) Denny, W. A. *Curr. Pharm. Des.* **2002**, *8*, 1349–1361.
- (2) Anlezark, G. M.; Melton, R. G.; Sherwood, R. F.; Coles, B.; Friedlos, F.; Knox, R. J. *Biochem. Pharmacol.* **1992**, *44*, 2289–2295.
- (3) Anlezark, G. M.; Vaughan, T.; Fashola-Stone, E.; Michael, N. P.; Murdoch, H.; Sims, M. A.; Stubbs, S.; Wigley, S.; Minton, N. P. *Microbiology* **2002**, *148*, 297–306.
- (4) Searle, P. F.; Chen, M. J.; Hu, L.; Race, P. R.; Lovering, A. L.; Grove, J. I.; Guise, C.; Jaberipour, M.; James, N. D.; Mautner, V.; Young, L. S.; Kerr, D. J.; Mountain, A.; White, S. A.; Hyde, E. I. *Clin. Exp. Pharmacol. Physiol.* **2004**, *31*, 811–816.
- (5) Chen, M. J.; Green, N. K.; Reynolds, G. M.; Flavell, J. R.; Mautner, V.; Kerr, D. J.; Young, L. S.; Searle, P. F. *Gene Ther.* **2004**, *11*, 1126–1136.

- (6) de Poorter, J. J.; Tolboom, T. C.; Rabelink, M. J.; Pieterman, E.; Hoebe, R. C.; Nelissen, R. G.; Huizinga, T. W. *J. Gene Med.* **2005**, 7, 1421–1428.
- (7) Whiteway, J.; Koziarz, P.; Veall, J.; Sandhu, N.; Kumar, P.; Hoecher, B.; Lambert, I. B. *J. Bacteriol.* **1998**, 180, 5529–5539.
- (8) Sisson, G.; Jeong, J. Y.; Goodwin, A.; Bryden, L.; Rossler, N.; Lim-Morrison, S.; Raudonikienė, A.; Berg, D. E.; Hoffman, P. S. *J. Bacteriol.* **2000**, 182, 5091–5096.
- (9) Jenks, P. J.; Ferrero, R. L.; Tankovic, J.; Thiberge, J. M.; Labigne, A. *Antimicrob. Agents Chemother.* **2000**, 44, 2623–2629.
- (10) Gruz, V.; Abian, O.; Mateo, C.; Batista-Viera, F.; Fernandez-Lafuente, R.; Guisan, J. M. *Biotechnol. Bioeng.* **2005**, 90, 597–605.
- (11) Cao, L. Immobilised enzymes: science or art? *Curr. Opin. Chem. Biol.* **2005**, 9, 217–226.
- (12) Urban, P. L.; Goodall, D. M.; Bruce, N. C. *Biotechnol. Adv.* **2006**, 24, 42–57.
- (13) Peterson, D. S. *Lab Chip* **2005**, 5, 132–139.
- (14) Kim, J.; Grate, J. W.; Wang, P. *Chem. Eng. Sci.* **2006**, 61, 1017–1024.
- (15) Luckarift, H. R.; Spain, J. C.; Naik, R. R.; Stone, M. O. *Nat. Biotechnol.* **2004**, 22, 211–213.
- (16) Naik, R. R.; Tomczak, M. M.; Luckarift, H. R.; Spain, J. C.; Stone, M. O. *Chem. Commun. (Cambridge, U. K.)* **2004**, 15, 1684–1685.
- (17) Shimizu, K.; Cha, J.; Stucky, G. D.; Morse, D. E. *Proc. Natl. Acad. Sci. U.S.A.* **1998**, 95, 6234–6238.
- (18) Belton, D. J.; Siddharth, V.; Patwardhan, C.; Perry, C. C. *J. Mater. Chem.* **2005**, 15, 4629–4638.
- (19) Ren-Hua, J. H.; Yuan, J. J. *Macromol. Chem. Phys.* **2005**, 206, 2160–2170.
- (20) Andersson, M. M.; Hatti-Kaul, R. *J. Biotechnol.* **1999**, 72, 21–25.
- (21) O’Fagain, C. *Enzyme Microb. Technol.* **2003**, 33, 137–139.
- (22) Somerville, C. C.; Nishino, S. F.; Spain, J. C. *J. Bacteriol.* **1995**, 177, 3837–3842.
- (23) Fiorella, P. D.; Spain, J. C. *Appl. Environ. Microbiol.* **1997**, 63, 2007–2015.
- (24) Naal, Z.; Park, J. H.; Bernhard, S.; Shapleigh, J. P.; Batt, C. A.; Abruna, H. D. *Anal. Chem.* **2002**, 74, 140–148.
- (25) Kalaji, M.; Williams, P. A.; Gwenin, C. D. WO Patent 2005/056815 A1, June 23, 2005.
- (26) Kadiyala, V.; Nadeau, L. J.; Spain, J. C. *Appl. Environ. Microbiol.* **2003**, 69, 6520–6526.
- (27) Bryant, C.; DeLuca, M. *J. Biol. Chem.* **1991**, 266, 4119–4125.
- (28) Tukel, S. S.; Alptekin, O. *Process Biochem. (Oxford, U. K.)* **2004**, 39, 2149–2455.
- (29) Ozyilmaz, G.; Tukel, S. S.; Alptekin, O. *J. Mol. Catal., B: Enzymatic* **2005**, 35, 154–160.
- (30) Blandino, A.; Macias, M.; Cantero, D. *Process Biochem. (Oxford, U. K.)* **2001**, 36, 601–606.
- (31) Betancor, L.; Lopez-Gallego, F.; Hidalgo, A.; Fuentes, M.; Podrasky, O.; Kuncova, G.; Guisan, J. M.; Fernandez-Lafuente, R. *Biomacromolecules* **2005**, 6, 1027–1030.
- (32) Palomo, J. M.; Segura, R. L.; Mateo, C.; Fernandez-Lafuente, R.; Guisan, J. M. *Biomacromolecules* **2004**, 5, 249–254.
- (33) Illanes, A.; Wilson, L. *Crit. Rev. Biotechnol.* **2003**, 23, 61–93.
- (34) Chaniotakis, N. *Anal. Bioanal. Chem.* **2004**, 378, 89–94.
- (35) Gill, I. *Chem. Mater.* **2001**, 13, 3404–3421.
- (36) Lopez-Gallego, F.; Betancor, L.; Hidalgo, A.; Alonso, N.; Fernandez-Lafuente, R.; Guisan, J. M. *Biomacromolecules* **2005**, 6, 1839–1842.
- (37) Wilson, L.; Illanes, A.; Abian, O.; Pessela, B. C. C.; Fernandez-Lafuente, R.; Guisan, J. M. *Biomacromolecules* **2004**, 5, 852–857.
- (38) Anlezark, G. M.; Melton, R. G.; Sherwood, R. F.; Wilson, W. R.; Denny, W. A.; Palmer, B. D.; Knox, R. J.; Friedlos, F.; Williams, A. *Biochem. Pharmacol.* **1995**, 50, 609–618.
- (39) Helsby, N. A.; Atwell, G. J.; Yang, S.; Palmer, B. D.; Anderson, R. F.; Pullen, S. M.; Ferry, D. M.; Hogg, A.; Wilson, W. R.; Denny, W. A. *J. Med. Chem.* **2004**, 47, 3295–3307.
- (40) Abian, O.; Wilson, L.; Mateo, C.; Fernandez-Lorente, G.; Palomo, J. M.; Fernandez-Lafuente, R.; Guisan, J. M.; Re, D.; Tam, A.; Daminatti, M. *J. Mol. Catal., B: Enzymatic* **2002**, 19, 295–303.
- (41) Nath, P.; Roy, S.; Conlisk, T.; Fleischman, A. J. *Biomed. Microdevices* **2005**, 7, 169–177.
- (42) Bilitewski, U.; Genrich, M.; Kadow, S.; Mersal, G. *Anal. Bioanal. Chem.* **2003**, 377, 556–569.
- (43) Perez-Reinado, E.; Blasco, R.; Castillo, F.; Moreno-Vivian, C.; Roldan, M. D. *Appl. Environ. Microbiol.* **2005**, 71, 7643–7649.
- (44) Girelli, A. M.; Mattei, E. *J. Chromatogr., B* **2005**, 819, 3–16.
- (45) Race, P. R.; Lovering, A. L.; Green, R. M.; Ossor, A.; White, S. A.; Searle, P. F.; Wrighton, C. J.; Hyde, E. I. *Biol. Chem.* **2005**, 280, 13256–13564.

BM060166D